MECHANICAL PROPERTIES OF THE RESPIRATORY SYSTEM

A Study in Humans and Rats by Forced Oscillations

MECHANICAL PROPERTIES OF THE RESPIRATORY SYSTEM

A STUDY IN HUMANS AND RATS BY FORCED OSCILLATIONS

Mechanische Eigenschappen van het Ademhalingssysteem

Een Studie met Geforceerde Oscillaties bij Mens en Rat

(met een samenvatting in het Nederlands)

PROEFSCHRIFT

Ter verkrijging van de graad van doctor
aan de Rijksuniversiteit te Utrecht
op gezag van de Rector Magnificus, Prof. dr. J.A. van Ginkel,
volgens het besluit van het College van Decanen
in het openbaar te verdedigen
op vrijdag 13 september 1991 des namiddags te 2.30 uur

door

TNO VOEDING
BIBLIOTHEEK
26 AUG. 1991
ZEIST

Cornelia Maria Allegonda Oostveen

geboren op 25 juni 1960 te Snelrewaard

Promotores:

Prof. dr. ir. J.J. Denier van der Gon
(Department of Medical and Physiological Physics, University of Utrecht)

Prof. dr. S.C.M. Luijendijk
(Department of Pulmonology, University of Limburg, Maastricht)

Co-promotor:

Dr. A. Zwart
(Institute for Nutrition and Food Research, TNO, Zeist)

The study described in this thesis was financially supported by the Netherlands Organization for Applied Scientific Research (TNO, Nutrition and Food Research, Zeist). The study was performed at the Department of Medical Physiology and Sports Medicine, University of Utrecht, l'Unité 14 de Physiopathologie Respiratoire, INSERM, Nancy (France), and the Institute for Nutrition and Food Research, TNO, Zeist.

Contents

List of abbreviations		7
1	**Introduction, summary, and general discussion**	9
	Introduction	9
	Summary	15
	General discussion	18
	Conclusions	21
2	**Flow and volume dependence of respiratory mechanical properties studied by forced oscillation**	27
	Introduction	28
	Methods	29
	Results	33
	Discussion	37
3	**Airway impedance during single inspirations of foreign gases**	47
	Introduction	48
	Methods	50
	Results	54
	Discussion	60
4	**Respiratory transfer impedance and derived mechanical properties of conscious rats**	71
	Introduction	72
	Material and Methods	73
	Results	77
	Discussion	83
5	**Effects of pentobarbital and halothane anesthesia on the respiratory transfer impedance of rats**	95
	Introduction	96
	Methods	96
	Results	99
	Discussion	105

Samenvatting 117

Curriculum Vitae 123

Dankwoord 125

List of abbreviations

P	pressure
$\dot{V}$	flow
V	volume
f	frequency
ω	$2 \pi f$
j	$(-1)^{½}$
Z	Impedance
Zin	input impedance
Ztr	transfer impedance
Re[Ztr]	Real part of transfer impedance
Im[Ztr]	Imaginary part of transfer impedance
f_0	resonant frequency (Im = 0)
Zaw	airway impedance
Zti	tissue impedance
Zg	impedance of the alveolar gas
R	Resistance
Rrs	resistance of the respiratory system (sum of the serial resistances)
Raw	airway resistance
Rcaw	central airway resistance
Rpaw	peripheral airway resistance
Rn	nose resistance
RL	lung resistance (airways + lung tissue)
Rti	tissue resistance (lung tissue + chest wall)
Rw	chest wall resistance
I	Inertance
Irs	respiratory inertance (sum of serial inertances)
Iaw	airway inertance
Icaw	central airway inertance
Iti	tissue inertance (lung tissue + chest wall)
Iw	chest wall inertance
Iuaw	inertance of the extrathoracic upper airway walls

C	Compliance
Crs	compliance of the respiratory system
Cti	tissue compliance (lung tissue + chest wall)
C_L	lung tissue compliance
Cb	bronchial compliance
Cg	alveolar gas compressibility
Cuaw	compliance of the extrathoracic upper airway walls
Cdyn	dynamic lung compliance ($\Delta V_L/\Delta P_{tp}$ where ΔP_{tp} is the change in transpulmonary pressure as measured during spontaneous breathing)

ρ	density
μ	viscosity

Chapter 1

Introduction, Summary, and General Discussion

Introduction

The mechanical properties of the respiratory system can be studied non-invasively by imposing sinusoidal pressure variations (forced oscillations) across the total system and by measuring the respiratory flow response. If the respiratory system behaves as a linear system, a sinusoidal pressure variation results in a sinusoidal flow response. In general, the amplitude of the pressure variations is limited to 0.1 kPa (≈1 cm H_2O) in order to ensure that the respiratory system remains within the linear range. The pressure-flow relationship, or respiratory impedance (Z), is a complex quantity which can be characterized by its modulus ($|Z|$) and argument (ϕ) (amplitude ratio and phase angle, respectively, between pressure and flow). Commonly, however, the impedance Z is expressed in terms of its real part (Re), or effective resistance, and its imaginary part (Im) or reactance, where $Re=|Z|\cos(\phi)$ and $Im=|Z|\sin(\phi)$.

Measurement of the flow response of the respiratory system to pressure oscillations at a variety of frequencies provides a means for studying the resistive, compliant and inertial properties of this system. If the respiratory system behaves as a simple R–I–C series network, the total resistance of the respiratory system (Rrs) can be obtained directly from the real part of impedance, and the total respiratory compliance (Crs) and inertance (Irs) can be obtained from the imaginary part at low frequency and high frequency, respectively (since $Z= Re + Im$ and, in this case, $Re= Rrs$ and $Im= j(-1/(\omega Crs) + \omega Irs)$, where $\omega=2\pi f$ with f=frequency of oscillation, and $j= (-1)^{1/2}$). In general, however, the behavior of Re and Im as a function of frequency tend to be less simple, and Re and Im are interpreted by fitting mathematical models to the data. The coefficients of the model, then, represent specific mechanical properties of the respiratory system.

DuBois et al. (9) introduced the technique of forced oscillations in 1956 in order to study the mechanics of breathing in humans. These authors imposed small sinusoidal pressure variations with a frequency between 2 and 15 Hz while the subject voluntarily relaxed at end-expiration. Two different conditions were measured: in the first condition sinusoidal pressure variations were applied at the airway opening and

in the second pressure oscillations were applied around the chest wall of the subject. In both cases the flow response to the pressure variations was measured at the airway opening. The following observations made by DuBois and co-workers have influenced research in this area for years. They observed that the pressure-flow relationship differed in the two conditions, which indicated that the respiratory system did not behave as a simple resistance-inertance-compliance in series. They ascribed the difference between the obtained impedances to the compressibility of the alveolar gas. An electrical analogue of the respiratory system as proposed by these authors is shown in Fig. 1.1. The airways are represented by their resistance (Raw) and inertance (Iaw). The lung and chest wall tissues are represented by their resistance (Rti), inertance (Iti), and compliance (Cti). The alveolar gas is represented by its compressibility (Cg). The impedance of the compressibility of the alveolar gas is in parallel with the airway impedance when the pressure oscillations are applied around the chest wall, but it is in parallel with the tissue impedance when the pressure oscillations are applied at the mouth. DuBois and co-workers also noted that application of pressure variations at the mouth resulted in visible motions of the soft tissues of chin and cheeks. By making surface velocity measurements of different regions of the chest wall, they observed that the chest wall did not behave homo-

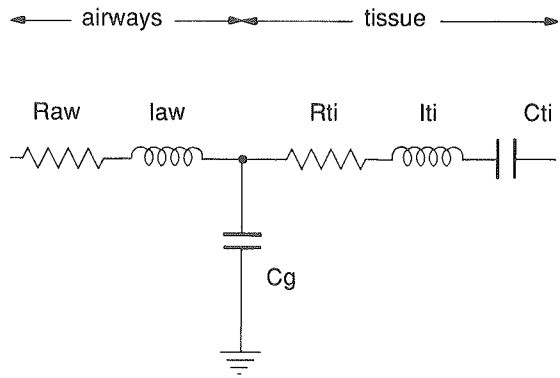

Figure 1.1. *Electrical analogue of DuBois' six-coefficient model which consists of three compartments: an airway compartment (airway resistance (Raw) and inertance (Iaw)), a tissue compartment (tissue resistance (Rti), inertance (Iti), and compliance (Cti)), and a gas compartment (alveolar gas compressibility (Cg)).*

geneously at high frequencies. Their most important observation, however, was that the estimated respiratory resistance obtained from the modulus of impedance at the frequency where pressure and flow were in phase (resonant frequency) corresponded to resistance values obtained by Otis et al. (26).

Mead (21) improved the technique by using a loudspeaker instead of a pump and by measuring the respiratory impedance while the subject breathed spontaneously. He demonstrated that the technique could also be applied to spontaneously breathing guinea pigs.

The advent of digital computers and fast Fourier transforms made it possible to explore other pressure signals, besides sinusoidal ones. Michaelson et al. (22) introduced a random noise pressure signal which contained all frequency components between 3 and 45 Hz. The frequency components of the pressure and flow signals were determined by spectral analysis and the corresponding respiratory impedance was calculated as a function of frequency. Since the peak-to-peak pressure has to be limited in order to remain within the linear range of respiratory system, the signal-to-noise ratio is reduced when different frequencies are applied simultaneously. Michaelson and co-workers used confidence intervals and the coherence function to estimate the reliability of the respiratory impedance. Shortly thereafter, Lándsér et al. (19) introduced a pressure signal composed of a number of discrete, harmonic frequencies. When the frequency components have random phases, to minimize the peak-to-peak pressure, this type of input signal is called pseudo random noise (PRN). The introduction of composite pressure signals further reduced the measurement time and eliminated the frequency dependence of impedance caused by the time-variability of respiratory parameters. Another advantage of nonsinusoidal pressure signals is that they exclude (or reduce) the synchronization of respiratory muscle activity with the excitation signal.

Recent improvements in the forced oscillation technique consist of procedures to correct for the asymmetry of pressure transducers, correction procedures to reduce the influence of spontaneous breathing on the final results for the respiratory impedance, and the development of a method to minimize the influence of chin and cheek impedance when pressure is applied at the airway opening (6, 7, 10, 25, 28). Investigation of the respiratory impedance at frequencies below, around, and above the frequency of spontaneous breathing has revealed that the forced oscillation technique can be a useful tool for studying the visco-elastic, lumped-mechanical or acoustical properties of the respiratory system. The chapter on oscillation mechanics in the Handbook of Physiology (31) reviews most of the results obtained in this field.

In this thesis, the impedance measurements described are those where the frequency of oscillation was restricted to a range above the natural breathing frequency. Linear, lumped models of the respiratory system were used to analyze the data.

The forced oscillation technique offers great advantages over other lung function tests since it permits respiratory mechanics to be studied non-invasively during spontaneous breathing. Pressure oscillations have to be applied at frequencies higher (or lower) than the natural breathing frequency in order to avoid the breathing signal from interfering with the excitation signal. Since the forced oscillation technique allows the respiratory mechanics to be measured during spontaneous breathing, it does not depend on close cooperation on the part of the subject. Therefore, it can also be used with small children and animals.

As mentioned before, there are two different measuring conditions: 1) application of pressure variations and measurement of flow at the same site of the respiratory system, which yields the respiratory input impedance (Zin), and 2) application of pressure variations and measurement of flow at different sites of the respiratory system, pressure being usually applied around the chest and flow measured at the mouth, which yields the respiratory transfer impedance (Ztr). The measurement of Ztr has advantages as compared to the measurement of Zin. Since the upper airway walls (chin, cheeks) are parallel to the pneumotachograph (low impedance), the upper airway walls hardly influence the measurement of Ztr. During the measurement of Zin with pressure oscillations applied at the airway opening, a technique commonly used due to the applicability in clinical practice, the upper airway walls are parallel to the respiratory system. This may lead to an underestimation of the respiratory impedance especially when the respiratory impedance is large (patients). A second advantage is that Ztr data provide more information on the properties of the respiratory system than do Zin data, at least in healthy subjects (4–30 Hz). In healthy subjects, Zin roughly describes the response of a three-coefficient model (Rrs–Irs–Crs model with Rrs=Raw+Rti, Irs=Iaw+Iti, and Crs=Cti, Fig. 1.1). Ztr data, on the other hand, have been interpreted successfully using DuBois' six-coefficient model. Since the model response is of the fourth order and there are six coefficients, one coefficient must be known in order to estimate the other five coefficients by model analysis. In general, the value of gas compressibility (Cg) derived from lung volume that is determined with an independent method (body plethysmography) is entered into the model analysis. Thus, Ztr data allow airway properties and properties of the tissues to be estimated provided the lung volume at which the measurements were performed is known.

The appropriateness of the interpretation of the coefficients of the DuBois model for analysis of Ztr data of healthy humans was partly validated in experiments where a load was added to the airways or where the chest wall was strapped. This resulted in an increased airway impedance and a decreased tissue compliance, respectively (30). Analysis with DuBois' model, however, also showed some shortcomings in studies where input and transfer impedance data were obtained in the same subjects (29, 35).

Airway resistance, as obtained from DuBois' model, is an estimate of the overall resistance to gas flow in the airways from the mouth up to the alveoli. The resistance is located at the level of the glottis and the bifurcations, but the conducting tubes of airways also resist gas flow. The resistance of a tube depends on its length and diameter, and on the physical properties and flow profile of the gas. Airway inertance is mainly determined by airway geometry (length and diameter of the conduits) and by the density of the gas. One can show that Iaw is mainly located in the large airways by calculating Iaw per airway generation from morphological data of the airways. DuBois' tissue impedance represents the overall impedance of the lung in series with that of the chest wall. Although the contributions of the two subsystems cannot be separated (except when the pressure variations in the esophagus are also measured), the chest wall probably contributes most to the tissue impedance as the chest wall is less compliant than the lung and contains more mass.

Respiratory impedance is commonly obtained by averaging data over a number of breathing cycles. It is known, however, that the respiratory impedance may vary considerably during the breathing cycle (22, 23), as a function of respiratory flow (33) and lung volume (22, 24). The influence of lung volume or the phase of breathing on the respiratory impedance has been studied in the past by measurement of Zin (22, 23, 24) or by measurement of Ztr at a single frequency (33). These variations cannot be ascribed to specific respiratory properties except when esophageal pressure is measured as well (24). Moreover, the changes in Zin are probably affected by the upper airway shunt. Since the mechanical properties of the respiratory system can be estimated from the DuBois model, our first study was designed to investigate the effects of flow, lung volume and lung volume history on Ztr obtained in the frequency range 4 to 30 Hz. This study also (partly) allowed the physiological interpretation of the DuBois coefficients to be validated since the flow and volume dependence of Raw had been studied previously with other methods (1, 3, 4, 11).

To improve the sensitivity of the forced oscillation technique for peripheral airway abnormalities, measurements were performed in the past while the subject breathed a

gas mixture with a lower density than that of air [80%He–20%O_2 (2, 37)]. Since the central airways have a density-dependent resistance, their contribution to the total airway resistance is reduced when the lungs are filled with a lower-density mixture. Data have also been obtained on the density dependence of airway impedance by combining Zin and Ztr data obtained in healthy subjects both when they were breathing air and when breathing He–O_2 (35).

Another way of using a gas with different physical properties than those of air consists of measuring the respiratory impedance as a function of time during a single inspiration of the gas. Then, the change in impedance that is measured results from the change in the local Raw and Iaw of those airways where the foreign gas replaces the air. In a preliminary study (32), it has been shown that the results may provide information on the distribution of density- and viscosity-dependent resistance along the airways. Exploration of such applications of the forced oscillation technique is important since the main interest of this method is to detect airway abnormalities non-invasively. Measurement of the serial distribution of the airway resistance would be a big step forward. The potential of the method to locate resistance and inertance in the bronchial tree by Ztr measurements during a single inspiration of foreign gas is further investigated in chapter 3.

As mentioned above, the forced oscillation technique can also be applied in animals. Both Zin and Ztr have been measured in a variety of species. Small laboratory animals are particularly interesting since they are widely used as models for investigating the effects of pharmacological or toxic agents on respiratory function. In conscious guinea pigs Ztr was measured at a single frequency (the resonant frequency) in order to obtain the respiratory resistance (14, 21). In tracheotomized rats Zin was measured in a broad frequency range (20–90 Hz) and the data were interpreted by model analysis in order to obtain information on specific respiratory properties (15). The potential of the method was further investigated by the measurement of Zin in ozone-exposed rats. The results of the estimated respiratory parameters roughly correlated with the histologic findings (18).

Development of non-invasive respiratory function tests for small animals is important for the following reasons. First, repeated measurements in the same animal can be performed which allows longitudinal studies to be done. Fewer animals are therefore needed to investigate the effects of experimental intervention on pulmonary function: the animal is not killed and, moreover, serves as its own control. In general, a sensitive test is obtained by making paired observations. A reduction in the required number of animals may be an important reason for using non-invasive techniques, particularly when animals are part of long-term and expensive studies.

Second, from the point of view of animal care, the lung function test should cause minimum discomfort to the animal. Third, non-invasive tests causes minimal disturbance to the normal respiratory function. In this respect, it may be important to use tests that do not require anesthesia, since anesthesia probably affects the respiratory function. Moreover, anesthesia may interfere with the effects of pharmacological or toxicological agents, and, therefore, should be avoided. To our knowledge, up till now there was no method for measuring the mechanical properties of the respiratory system of unanesthetized rats at a variety of frequencies.

We modified the forced oscillation technique used for humans in order to measure the respiratory transfer impedance of conscious rats (chapter 4). As a first step in evaluating the usefulness of such measurements, we studied the effects of anesthesia on the respiratory impedance of normal rats (chapter 5). Measurement in intact rats includes the nose and upper airways which are the primary target organs when rats are exposed to irritating or toxic gases. Because repeated measurements are possible, impedance measurements in conscious rats provide a promising lung function test.

Summary

The aim of our first study (chapter 2) was to investigate the influences of respiratory flow ($\dot{V}$), lung volume (VL) and lung volume history on the mechanical properties of the respiratory system. To this end, healthy subjects performed several constant inspiratory and expiratory flow maneuvers within a predetermined lung volume range with standardized lung volume history. During the maneuvers, Ztr was measured in the frequency range 4–30 Hz and airway and tissue properties were estimated by model analysis. The results showed that Ztr, especially Re[Ztr], varied considerably with the maneuver performed. Model analysis showed that airway resistance (Raw) and airway inertance (Iaw) did not show concomitant changes with the different maneuvers performed. Increasing $\dot{V}$ significantly increased Raw but decreased Iaw. During expiration Raw was larger than during inspiration whereas Iaw did not vary with the phase of breathing. In agreement with previous studies (1, 3, 4), a linear relationship was found between the reciprocal of Raw and VL. Iaw, on the other hand, did not change with VL. Significant differences in tissue properties were found only between inspiration and expiration and when the maneuvers were performed at different VL. This indicated that changes in the mechanical properties of the tissue probably reflect the level of respiratory muscle activity and that the tissue coefficients mainly represent the mechanical properties of the chest wall and not those of the lung tissue.

In chapter 3 the potential of impedance measurements to obtain information on the distribution of Raw and Iaw in the bronchial tree was investigated. In this study healthy subjects were asked to inspire at a constant low flow rate (0.1 l/s). During the maneuver, the inspiratory gas was changed from room air to a foreign gas with a different viscosity and/or density than air. The foreign gas will affect the local Raw and Iaw since it replaces the air in successive airways during the inspiration. During the entire maneuver, Ztr was measured at a single frequency (20 Hz) and Re[Ztr] and Im[Ztr] were calculated on a cycle-per-cycle basis. As a result of the changes in Raw and Iaw with progressive substitution of air by the foreign gas, Re[Ztr] and Im[Ztr] changed as a function of time. Correcting the Ztr data for tissue impedance, which is not affected by the type of gas in the airways, and Cg, resulted in information of the changes in Raw and Iaw as a function of time. Since time is related to volume, the changes in Raw and Iaw as a function of the inhaled volume of foreign gas could be determined. In other words, the results provided information on the distribution of Raw and Iaw in the bronchial tree.

The results showed that when the airways were washed with 500 ml of foreign gas, the total change in Iaw was close to the predicted change based on the ratio of density of the foreign gas and that of air, confirming the validity of the model. The total change in Raw cannot be predicted since the contribution of density-dependent and viscosity-dependent resistance to Raw is not known. The total change in Raw, after 500 ml inhalation of foreign gas, varied between subjects; in some subjects Raw tended to be more density-dependent, whereas in other subjects Raw tended to be more viscosity-dependent. By calculating the derivative of Raw and Iaw as a function of the inhaled volume of foreign gas, information was obtained on the distribution of Raw and Iaw in the airways. Unfortunately the distribution profiles of Raw were very noisy. The less noisy data showed that the density-dependent part of Raw was located proximal to the viscosity-dependent part of Raw. Comparison of the distribution profiles obtained for Raw and Iaw showed that resistance is distributed more peripherally than inertance.

In chapter 4 the setup developed to measure Ztr of conscious rats is described. The main problem with small animals is a correct measurement of the flow. Since small animals have large respiratory impedances, the flow is very small. Rats, as other rodents, are obligatory nose breathers. Mead (21) used a face mask to measure the flow response in guinea pigs when applying pressure variations around the chest wall. Face masks are not accepted by conscious rats, so an indirect method was developed to measure flow. In our setup, the rat was restrained in a tube which was placed in a chamber where PRN pressure variations (16–208 Hz) were applied. After

the rat had been placed in the body chamber, it respired from a small box. The nose flow (spontaneous breathing plus response to the applied PRN pressure variations) resulted in pressure variations in the small box. The (nose) flow could be calculated by relating the measured pressure variations in the small box to the impedance of this box. The above method depends on a good separation of the head and the body of the rat in the restraining tube, which was achieved by the application of a dough collar around the neck.

Repeated measurements in the same animal showed that the reproducibility was satisfactory (coefficient of variation of |Ztr| of about 10%). Consequently, longitudinal studies can be performed for pharmacological or toxicological purposes. The Ztr data of conscious rats were incompatible with DuBois' model at low frequency. Therefore the DuBois six-coefficient model was modified to include nose resistance (Rn) shunted by the upper airway wall impedance. Interpretation of the data with this model showed that total airway resistance (Raw+Rn) and inertance (Iaw) were about 85% of the total respiratory resistance (Rrs=Raw+Rn+Rti) and total respiratory inertance (Irs=Iaw+Iti). In contrast to Cti of humans, which reflects chest wall compliance, Cti of rats probably mainly reflects lung compliance.

To our knowledge, we are the first to report on mechanical properties of conscious rats. Therefore, we compared Ztr of conscious rats to that of anesthetized rats (chapter 5). Normal rats were anesthetized with either pentobarbital sodium or halothane. In this study, it was shown that anesthesia significantly increased respiratory impedance. During pentobarbital anesthesia, Re[Ztr] was increased over the entire frequency range and Im[Ztr] was lower at low frequencies. Twenty minutes after injection of pentobarbital, the average increase in Re[Ztr] at 16 Hz amounted to 140% of the values found during consciousness, but there were large interindividual variations. Halothane anesthesia induced smaller changes in Ztr than did pentobarbital anesthesia, and the changes were independent of time, in contrast to those seen during pentobarbital anesthesia. The shape of Ztr during anesthesia completely differed from that found during consciousness. A frequency-dependent fall in Re[Ztr] in the low frequency range was found during anesthesia, similar to the frequency dependence found in obstructive human patients. Therefore, models including parallel pathways in the lung were fitted to the data. Analysis showed that a model that included a shunt pathway (bronchial compliance) to the peripheral airways best explained the data. Compared to consciousness, anesthesia with pentobarbital or halothane induced an increase in both the total airway resistance (180% and 100%, respectively) and the total airway inertance (70% and 50%, respectively).

General Discussion

Impedance measurements by forced oscillations provide a way to study the mechanical properties of the respiratory system non-invasively. When the impedance is measured at a number of frequencies, more detailed information on the mechanical properties of the airways and tissues can be obtained by fitting mathematical models to the impedance data. The model must provide an adequate description of the experimental data and the model coefficients must be physiologically meaningful and the estimated values reliable. Peslin et al. (34) showed that the six-coefficient model proposed by DuBois et al. [Fig. 1.1 (9)] adequately described Ztr data in the frequency range 4–50 Hz, obtained in healthy human subjects. The appropriateness of the physiological interpretation of the coefficients was validated to some extent in a previous study (30) and is further confirmed by the flow and volume dependence of resistance (chapter 2), which is in agreement with the results of other studies, and by the close relationship between predicted and observed changes in airway inertance when the airways were washed with foreign gases (chapter 3).

From a sensitivity analysis of dog impedance data Lutchen and Jackson (20) predicted that the respiratory parameters of DuBois' model can be extracted more accurately from Zin data than from Ztr data when the data are obtained in a limited frequency range (4–64 Hz). Moreover, these authors concluded that the coefficients of DuBois' model are poorly determined in the limited frequency range 4–32 Hz. It was expected that these conclusions could not be extrapolated to human Ztr data but, until recently, this had not been proved. Rotger et al. (36) showed unequivocally that the estimated values of DuBois' six-coefficient model are reliable. In their study the variation in the estimated coefficients of DuBois' model was obtained from repeated Ztr measurements in healthy subjects (4–32 Hz). The coefficients of variation (CV) for Raw and Iaw were 6.3% and 4.9%, respectively. Those of the tissue coefficients were larger; mean CVs for Rti, Iti, and Cti were 10.9%, 20.3% and 6.5%, respectively.

Separating the mechanical properties of the airways from those of the tissue by means of DuBois' model enabled us to study the flow, lung volume and gas-dependent characteristics of the respiratory system. The studies were performed in healthy subjects since special respiratory maneuvers were required.

The influences of the phase of breathing, the magnitude of the respiratory flow, lung volume and lung volume history on the respiratory mechanical properties were studied while the subjects performed constant flow maneuvers. The maneuver may have altered the mechanical properties, since respiration had to be actively controlled.

This is contrary to normal impedance measurements where the measurement is performed during quiet, spontaneous breathing. In general, however, the results obtained during constant flow maneuvers corresponded to results obtained by other authors using different methods. Our results indicate that knowledge about the magnitude of the respiratory flow, the duration of inspiration and expiration, and the lung volume at which the measurements are performed, is important for the interpretation and comparison of data obtained in different subjects, or under different experimental conditions. The sensitivity of impedance measurements to detect and diagnose respiratory disfunction may be improved by measuring impedance data separately at different points in time during inspiration and expiration (5).

The usefulness of impedance measurements would certainly improve if the measurements were to provide information on the distribution of airway impedance (chapter 3). Our study showed that some information can be obtained on the serial distribution of Raw and Iaw from impedance measurements during single inspirations of foreign gases. The Raw values, however, were noisy in most subjects. There are several explanations for this finding. First, glottis control probably helped to perform the constant flow maneuver. Since the glottis contributes substantially to Raw and cannot be excluded in non-invasive measurements, variability in glottis aperture is a source of variability in Raw. Imposing the desired flow on a relaxed subject might reduce this source of error and this may be the first step in adapting the method to clinical practice. Second, all the noise in the measurement resulted in changes in Raw and Iaw. We implicitly assumed constant tissue properties in the computation of Raw and Iaw. An incorrect estimation of the tissue contribution or lung volume affected the computed Raw value to a larger extent than the computed Iaw value. Measurement at a lower frequency (e.g. 10 Hz) should improve the reliability of the Raw estimate. Nevertheless, the study revealed systematic differences in the distribution of Raw between subjects and the results confirmed the localization of density- and viscosity-dependent resistance based on predictions of flow-regimes in the airways. The study shows that impedance measurements made during inspiration of foreign gases might be useful for physiological or diagnostic purposes.

The fact that DuBois' model adequately describes Ztr data of healthy subjects does not imply that it describes Ztr of patients. Recently, Ying et al. (38) measured Ztr (4–30 Hz) in patients with severe chronic obstructive pulmonary disease and found that analyzing the data with DuBois' model yielded unrealistic values for one or more coefficients. The data were best described with a model incorporating intrathoracic airway wall compliance and peripheral airway resistance. This is the same model as the one that best described our Ztr data of anesthetized rats.

Small laboratory animals are used as a model for human respiratory disease, and to evaluate potentially harmful inhalatory agents and pharmacological drugs. Most of the lung function tests developed for humans have been adapted for use in small animals. However, since most of the tests require cooperation (determination of total lung capacity, vital capacity, forced maximum expiratory flow etc), lung function tests in small animals usually require some form of invasion and anesthesia. Irrespective of the technique, the major problem with measurements in small animals is the occurrence of leaks between measuring devices and the animal. In previously described adaptations of the forced oscillation technique for measuring the impedance of rats use was made of a tracheal cannula to obtain an airtight fit between airway opening and flow measuring device (12, 15).

The experimental setup and method for measuring non-invasively Ztr of conscious rats is described in chapter 4. The validity of the Ztr data depends on several factors. To obtain the flow response to the pressure oscillations, the impedance of the front chamber needs to be known as a function of frequency. This was achieved by constructing a calibration unit with a known impedance. Further, the connection between the two chambers should be leak-free, since every leak results in underestimation of the respiratory impedance. The solution was to use a neck collar which limited the leakage to a negligible amount. Compression of the animal's back should be avoided, since this changes the impedance of the rat.

The reproducibility of the respiratory transfer impedance measured in conscious rats was satisfactory: the coefficient of variation of $|Ztr|$ was about 10%. This is in the same range as or better than the results obtained with other methods (14, 27). Model analysis revealed that total airway resistance (Rn+Raw) and Iaw made the largest contributions ($\approx$ 85%) to the total respiratory resistance and inertance, respectively, and estimated tissue compliance was close to the previously reported value of pulmonary compliance (8, 13, 16, 17, 27). These results make Ztr measurements a promising tool in pharmacological and toxicological research since the main interest in these research areas is to detect changes in the mechanical properties of the lung and its airways.

To our knowledge we are the first to have measured respiratory mechanical properties of conscious rats. To evaluate the usefulness of such measurements and to explain the discrepancy between our results and previously reported results for anesthetized rats, we compared Ztr of rats in the conscious state to Ztr in the anesthetized state. The results showed that Ztr during anesthesia was quite different from Ztr during consciousness. The respiratory impedance obtained during anesthesia

depended on the type of anesthetic used. During pentobarbital anesthesia, which is commonly used for small animals, large differences were found between animals both in the magnitude of the increase in |Ztr| compared to consciousness and in the changes in |Ztr| as a function of time during the period of anesthesia. Halothane anesthesia, on the other hand, induced a smaller change in |Ztr| than pentobarbital anesthesia, and the changes were time-independent. Nevertheless, the average increase in |Ztr| at 16 Hz during halothane anesthesia amounted to 80% of the values found during consciousness, and a considerable range of increases was found between the rats (20–150%). These results indicate that it will be difficult to standardize measurements during anesthesia.

The extended DuBois model that was used to describe Ztr of conscious rats provided physiologically meaningful values for the different coefficients. The variations in the estimated coefficients obtained from repeated measurements were small; thus, reliable estimates were obtained. The model, however, has not yet been validated. As discussed in chapter 4 a different model, in which mechanical inhomogeneity of the tissue compartments was assumed, described the measured data equally well. Validation of the model requires measurements in a variety of conditions which result in predictable changes of the respiratory properties. Such experiments are not within easy reach. Fortunately, comparison of the results of the two models showed that the estimated values of the properties of the airways and of those of the tissue compliance did not substantially differ. Thus, it is likely that transfer impedance measurements in conscious rats provide a reliable method for estimating the mechanical properties of their respiratory system.

Conclusions

- In healthy human subjects, transfer impedance data from 4–30 Hz can be analyzed by DuBois' six-coefficient model. The estimated values of the coefficients provide physiologically meaningful values of specific mechanical properties of the respiratory system.
- During targeted flow maneuvers, airway resistance and airway inertance show significant and opposite changes with respiratory flow. Airway resistance, and tissue resistance, inertance, and compliance differ significantly between inspiration and expiration. A linear relationship exists between the reciprocal of airway resistance and lung volume; lung volume further significantly affects the tissue properties.
- The determinants of airway resistance and airway inertance are not identical.

- The level of respiratory activity influences the tissue properties.
- Information on the distribution of airway resistance and inertance in the bronchial tree can be obtained from non-invasive impedance measurements during single inspirations of foreign gases.
- The partitioning between density- and viscosity-dependent resistance varies among healthy subjects.
- Airway resistance is located more peripherally than airway inertance.
- The developed method for measuring conscious rats was found to provide reproducible transfer impedance data.
- Reliable estimates of the airway resistance and airway inertance of conscious rats can be obtained by model analysis of transfer impedance data (16–208 Hz).
- In normal rats, both pentobarbital anesthesia and halothane anesthesia induce a large increase in the real part of Ztr and a decrease in the imaginary part at low frequency.
- Pentobarbital anesthesia and halothane anesthesia induce an increase in airway resistance and airway inertance in normal rats.
- Pentobarbital and halothane anesthesia result in an increased interindividual variability of the respiratory impedance of normal rats.

References

1. BLIDE, R. W., H.D. KERR, AND W.S. SPICER, JR. Measurement of upper and lower airway resistance and conductance in man. J. Appl. Physiol. 19: 1059–1069, 1964.
2. BROCHARD, L., G. PELLE, J. DE PALMAS, P. BROCHARD, A. CARRE, H. LORINO, AND A. HARF. Density and frequency dependence of resistance in early airway obstruction. Am. Rev. Respir. Dis. 135: 579–584, 1987.
3. BRISCOE, W.A., AND A.B. DUBOIS. The relationship between airway resistance, airway conductance and lung volume in subjects of different age and body size. J. Clin. Invest. 37: 1279–1285, 1958.
4. BUTLER, J., C.G. CARO, R. ALCALA, AND A.B. DUBOIS. Physiological factors affecting airway resistance in normal subjects and in patients with obstructive respiratory disease. J. Clin. Invest. 39: 584–591, 1960.
5. CAUBERGHS, M., AND K.P. VAN DE WOESTIJNE. "Instantaneous" measurements of total respiratory impedance. Eur. Respir. Reviews, 1991 (in press)
6. DARÓCZY, B., AND Z. HANTOS. An improved forced oscillatory estimation of respiratory impedance. Int. J. Bio–Medical Computing 13: 221–235, 1982

7. DELAVAULT, E., G. SAUMON, AND R. GEORGES. Identification of transducer defect in respiratory impedance measurements by forced random noise. Correction of experimental data. Resp. Physiol. 40: 107–117, 1980.
8. DIAMOND, L., AND M. O'DONNELL. Pulmonary mechanics in normal rats. J. Appl. Physiol.: Respirat. Environ. Exercise Physiol.: 43: 942–948, 1977.
9. DUBOIS, A.B., A.W. BRODY, D.H. LEWIS, AND B.F. BURGESS, JR. Oscillation mechanics of lungs and chest in man. J. Appl. Physiol. 8: 587–594, 1956.
10. FARRÉ, R., D. NAVAJAS, R. PESLIN, M. ROTGER, AND C. DUVIVIER. A correction procedure for the asymmetry of differential pressure transducers in respiratory impedance measurements. IEEE Trans. Biomed. Eng. 36: 1137–1140, 1989.
11. FERRIS, JR., B.G., J. MEAD, AND L.H. OPIE. Partitioning of respiratory flow resistance in man. J. Appl. Physiol. 19: 653–658, 1964.
12. HANTOS, Z., B. DARÓCZY, B. SUKI, AND S. NAGY. Low-frequency respiratory mechanical impedance in the rat. J. Appl. Physiol. 63: 36–43, 1987.
13. HARKEMA, J.R., J.L. MAUDERLY, AND F.F. HAHN. The effects of emphysema on oxygen toxicity in rats. Am. Rev. Respir. Dis. 126: 1058–1065, 1982.
14. HIETT, D.M. Tests of ventilatory function for use in long-term animal studies. Br. J. Industr. Med. 31: 53–58, 1974.
15. JACKSON, A.C., AND J.W. WATSON. Oscillatory mechanics of the respiratory system in normal rats. Resp. Physiol. 48: 309–322, 1982.
16. JOHANSON, JR., W.G., AND A.K. PIERCE. A noninvasive technique for measurement of airway conductance in small animals. J. Appl. Physiol. 30: 146–150, 1971.
17. KING, T.K.C. Mechanical properties of the lungs in the rat. J. Appl. Physiol. 21: 259–264, 1966.
18. KOTLIKOFF, M.I., A.C. JACKSON, AND J.W. WATSON. Oscillatory mechanics of the respiratory system in ozone-exposed rats. J. Appl. Physiol. 56: 182–186, 1984.
19. LÁNDSÉR, F.J., J. NAGELS, M. DEMEDTS, L. BILLIET, AND K.P. VAN DE WOESTIJNE. A new method to determine frequency characteristics of the respiratory system. J. Appl. Physiol. 41: 101–106, 1976
20. LUTCHEN, K.R., AND A.C. JACKSON. Reliability of parameter estimates from models applied to respiratory impedance data. J. Appl. Physiol. 62: 403–413, 1987.
21. MEAD, J. Control of respiratory frequency. J. Appl. Physiol. 15: 325–336, 1960.
22. MICHAELSON, E.D., E.D. GRASSMAN, AND W.R. PETERS. Pulmonary mechanics by spectral analysis of forced random noise. J. Clin. Invest. 56: 1210–1230, 1975.

23. MILLER, T.K., AND R.L. PIMMEL. Forced noise mechanical parameters during inspiration and expiration. J. Appl. Physiol.: Respirat. Environ. Exercise Physiol.: 52: 1530–1534, 1982.
24. NAGELS, J., F.J. LÁNDSÉR, L. VAN DER LINDEN, J. CLÉMENT, AND K.P. VAN DE WOESTIJNE. Mechanical properties of lungs and chest wall during spontaneous breathing. J. Appl. Physiol.: Respirat. Environ. Exercise Physiol. 49: 408–416, 1980.
25. NAVAJAS, D., R. FARRÉ, M. ROTGER, AND R. PESLIN. A new estimator to minimize the error due to breathing in the measurement of respiratory impedance. IEEE Trans. Biomed. Eng. 35: 1001–1005, 1988.
26. OTIS, A.B., C.B. MCKERROW, R.A. BARTLETT, J. MEAD, M.B. MCILROY, N.J. SILVERSTONE, AND E.P. RADFORD. Mechanical factors in distribution of pulmonary ventilation. J. Appl. Physiol. 8: 427–443, 1956.
27. PALEČEK, F. Measurement of ventilatory mechanics in the rat. J. Appl. Physiol.: 27: 149–156, 1969.
28. PESLIN, R, C. DUVIVIER, J. DIDELON, AND C. GALLINA. Respiratory impedance measured with head generator to minimize upper airway shunt. J. Appl. Physiol. 59: 1790–1795, 1985.
29. PESLIN, R., C. DUVIVIER, AND C. GALLINA. Total respiratory input and transfer impedances in humans. J. Appl. Physiol. 59: 492–501, 1985.
30. PESLIN, R., C. DUVIVIER, AND B. HANNHART. Respiratory mechanical impedances. – Methodology and interpretation. Biorheology, Suppl. I; 183–191, 1984.
31. PESLIN, R., AND J.J. FREDBERG. Oscillation mechanics of the respiratory system. In: *Handbook of Physiology. The Respiratory System. Mechanics of Breathing.* Bethesda, MD: Am. Physiol. Soc., 1986, sect. 3, vol. III, pt. 1, chapt. 11, p. 145–177.
32. PESLIN, R., B. HANNHART, AND C. DUVIVIER. Airway impedance studied during airway washing with foreign gases. Bull. Eur. Physiopathol. Respir. 14: 70p–72p, 1978.
33. PESLIN, R., T. HIXON, AND J. MEAD. Variations des résistances thoracopulmonaires au cours du cycle ventilatoire étudiées par méthode d'oscillation. Bull. Physiopathol. Respir. 7: 173–186, 1971.
34. PESLIN, R., J. PAPON, C. DUVIVIER, AND J. RICHALET. Frequency response of the chest: modeling and parameter estimation. J. Appl. Physiol. 39: 523–534, 1975.
35. ROTGER, M., R. PESLIN, C. DUVIVIER, D. NAVAJAS, AND C. GALLINA. Density dependence of respiratory input and transfer impedances in humans. J. Appl. Physiol. 65: 928–933, 1988.
36. ROTGER, M, R. PESLIN, E. OOSTVEEN, AND C. GALLINA. Confidence intervals of

respiratory mechanical properties derived from transfer impedance. J. Appl. Physiol. 70: 2432–2438, 1991.

37. WOUTERS, E.F.M. Impedance measurement during air and He–O_2 breathing before and after salbutamol in normal subjects. J. Appl. Physiol. 69: 1665–1669, 1990.
38. YING, Y., R. PESLIN, C. DUVIVIER, G. GALLINA, AND J. FELICIO DA SILVA. Respiratory input and transfer mechanical impedances in patients with chronic obstructive pulmonary disease. Eur. Respir. J. 3: 1186–1192, 1990.

Chapter 2

Flow and Volume Dependence of Respiratory Mechanical Properties Studied by Forced Oscillation

E. Oostveen, R. Peslin, C. Gallina, and A. Zwart

Published in the Journal of Applied Physiology: Vol. 67: 2212–2218, 1989.

Abstract

The influence of inspiratory and expiratory flow magnitude, lung volume, and lung volume history on respiratory system properties was studied by measuring transfer impedances (4–30 Hz) in seven healthy subjects during various constant flow maneuvers. The measured impedances were analyzed with a six-coefficient model including airway resistance (Raw) and inertance (Iaw), tissue resistance (Rti), inertance (Iti), and compliance (Cti), and alveolar gas compressibility. Increasing respiratory flow from 0.1 to 0.4 l/s was found to increase inspiratory and expiratory Raw by 63% and 32%, respectively, and to decrease Iaw, but did not change tissue properties. Raw, Iti, and Cti were larger and Rti was lower during expiration than during inspiration. Decreasing lung volume from 70 to 30% of vital capacity increased Raw by 80%. Cti was larger at functional residual capacity than at the volume extremes. Preceding the measurement by a full expiration rather than by a full inspiration increased Iaw by 15%. The data suggest that the determinants of Raw and Iaw are not identical, that airway hysteresis is larger than lung hysteresis, and that respiratory muscle activity influences tissue properties.

Introduction

Since its measurement was first proposed by DuBois et al. (8), respiratory mechanical impedance (Zrs) is commonly obtained by applying pressure variations at the airway opening and assessing the relationship between the applied pressure and the resulting gas flow in the airways (input impedance, Zin). An alternative, proposed by Mead (16), is to make the same measurements when pressure is varied around the chest rather than at the mouth, which provides respiratory transfer impedance (Ztr). Peslin et al. (24) have shown that transfer impedance data obtained in the frequency range from 4 to 50 Hz may be interpreted with DuBois' six-coefficient model (8) (Fig. 2.1), and, provided alveolar gas compressibility (Cg) is known, may be used to estimate tissue compliance (Cti), resistance (Rti) and inertance (Iti) as well as airway resistance (Raw) and inertance (Iaw).

Both Zin and Ztr are usually measured during quiet breathing, and the data averaged over several breathing cycles. It has been shown, however, that Zrs changes as a function of the phase of breathing (17, 18), and is influenced by the magnitude of respiratory flow (9, 23). An inverse relationship has also been reported between the resistive component of Zrs and lung volume (17, 19, 25). These variations are likely to be related, in part, to the volume and flow dependences of Raw observed with other methods (2–5, 9, 12). The objective of this study was to assess more precisely the effects of varying lung volume, volume history, and respiratory flow ($\dot{V}$)

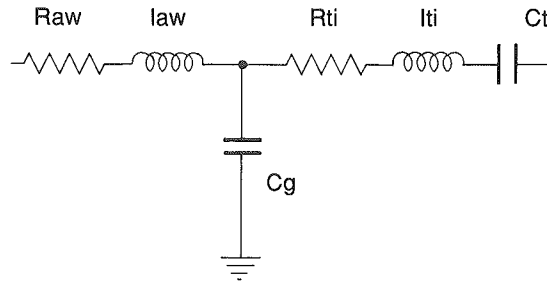

Figure 2.1. Electrical analogue of DuBois' six-coefficient model featuring airway resistance (Raw) and inertance (Iaw), alveolar gas compressibility (Cg), and tissue resistance (Rti), inertance (Iti), and compliance (Cti).

on the specific airway and tissue properties that may be derived from Ztr by using DuBois' model. For this, we measured Ztr in normal subjects from 4 to 30 Hz during constant flow maneuvers performed at different lung volumes [30–70% of vital capacity (VC)] and with different inspiratory and expiratory flows (0.1–0.4 l/s). We also compared the data obtained with a lung volume history of a full inflation and of a full deflation.

Methods

The study was made in seven healthy subjects (3 females), aged 26–50 yr, trained to respiratory maneuvers. Their biometric characteristics, smoking habits, plethysmographic Raw, and lung volumes are shown in Table 2.1.

To measure respiratory transfer impedance, the subject was seated up to his neck in a 350-liter body chamber equipped with two 90-W loudspeakers. A relatively good seal at the neck without compression of the upper airways was obtained with a collar made of soft synthetic foam. The loudspeakers were supplied through a power amplifier with a composite signal containing all harmonics of 2 Hz from 4 to 30 Hz.

Table 2.1. *Biometric characteristics, smoking habits and lung volumes of subjects.*

Subject no.	Sex	Age yr	Height cm	Weight kg	Smoking Habit	Raw,pl kPa.l^{-1}.s	FRC liters	VC liters	ERV liters
1	M	50	178	55	ES	0.090	5.62	5.20	2.61
2	F	26	171	66	NS	0.159	2.80	4.62	1.80
3	F	32	160	54	NS	0.203	2.88	3.41	1.49
4	F	28	170	55	S	0.043	3.53	4.36	2.00
5	M	30	171	65	NS	0.169	2.99	4.01	1.88
6	M	49	169	89	NS	0.155	3.09	5.53	1.18
7	M	50	168	64	NS	0.065	3.36	4.32	1.89

Raw,pl, airway resistance measured by plethysmography; FRC, functional residual capacity; VC, vital capacity; ERV, expiratory reserve volume; NS, nonsmoker; ES, exsmoker; S, smoker.

Table 2.2. Measuring conditions.

Condition	Flow Direction	Flow Rate l/s	Initial Volume	Volume History	Sampling Periods
I-0.1	Inspiration	0.1	FRC	TLC	8
I-0.2	Inspiration	0.2	FRC	TLC	4
I-0.4	Inspiration	0.4	FRC	TLC	2
E-0.1	Expiration	0.1	FRC +800 ml	TLC	8
E-0.2	Expiration	0.2	FRC +800 ml	TLC	4
E-0.4	Expiration	0.4	FRC +800 ml	TLC	2
I-30	Inspiration	0.2	30% VC	TLC	4
I-70	Inspiration	0.2	70% VC	TLC	4
I-RV	Inspiration	0.2	FRC	RV	4

FRC, functional residual capacity; TLC, total lung capacity; RV, residual volume; VC, vital capacity.

The amplitude of the resulting pressure oscillations in the chamber (Pbs) was limited to 0.1 kPa peak-to-peak. $\dot{V}$ was measured with a Fleisch no. 2 pneumotachograph connected to a MP-45 Validyne transducer (± 0.2 kPa). Pbs was obtained with an identical transducer, matched to the first within 1% of amplitude and 1° of phase up to 30 Hz. $\dot{V}$ and Pbs were digitized on-line with a sampling rate of 128 Hz by an Apple IIe system. The sampling period varied from 2 to 8 s according to the imposed $\dot{V}$ (Table 2.2), so that the change in lung volume from the beginning to the end of the period was reasonably small (0.8 liter) and constant. The signals were processed by Fourier analysis according to Michaelson et al. (17) to obtain at each frequency the real part of impedance or effective resistance (Re[Ztr]), and its imaginary part or reactance (Im[Ztr]). The analysis was made on blocks of 64 data points when the sampling period was 2 s, and on blocks of 256 points when it was larger, with 50% overlap between blocks. The analysis also provided the coherence function (γ^2), which is an index of the signal-to-noise ratio (17). The data were rejected when γ^2

was less than 0.95. In each of the conditions described below the measurements were repeated until the total sampling period was at least 30 s, and the data were averaged.

The subjects wore a noseclip and breathed through a mouthpiece. The measurements were performed in nine different conditions defined in Table 2.2. All were made during constant flow, inspiratory, or expiratory maneuvers, initiated at a specific lung volume, and preceded by either a full inspiration to total lung capacity (TLC) or by a complete expiration to residual volume (RV). To help the subject to achieve the desired maneuver, the integrated flow signal was shown on an oscilloscope, to which was added a voltage proportional to the volume the subject had to expire from TLC or inspire from RV to reach the proper lung volume. Slanted lines were also drawn on the oscilloscope with a slope corresponding to the desired flow. In practice, the subject slightly hyperventilated for a few seconds and, then, inspired to TLC or expired to RV, at which point the integrator was reset. He then went to the target lung volume, as indicated on the oscilloscope, and, finally, inspired or expired while trying to keep the spot parallel to one of the slanted flow lines. The target volume was fixed 200 ml below (for inspiratory maneuvers) or above (for expiratory maneuvers) the required level, so that the subject had a little time to adjust his flow before data acquisition was triggered. The maneuver was discarded when the flow was irregular or when the average flow departed by more than 10% from the desired value. In all subjects satisfactory maneuvers were reproducibly obtained after one or two training sessions.

The impedance data were analyzed by using the model proposed by DuBois et al. (8) (Fig. 2.1). The analysis required entering the value of Cg (24). This value was derived from functional residual capacity (FRC) measured by body plethysmography (Table 2.1) corrected for the difference between FRC and the mean thoracic gas volume (TGV) at which the measurements were made ($Cg = TGV/(P_B - P_{H_2O})$). The set of model coefficients giving the best fit to the impedance data was obtained by using a parameter estimation algorithm (6) to minimize the mean relative difference (D, Eq. 1) between the response of the model and that of the subject. The residual value of D (Dr) is a measure of the quality of the fit

$$D = \frac{1}{n} \sum_{i=1}^{n} \frac{[(\mathrm{Re},m - \mathrm{Re},s)^2 + (\mathrm{Im},m - \mathrm{Im},s)^2]^{1/2}}{(\mathrm{Re},s^2 + \mathrm{Im},s^2)^{1/2}} \qquad (1)$$

where n is the number of data points, Re and Im the real and imaginary parts of the impedance of the model (index m) and of the subject (index s).

Table 2.3. Coefficients derived from impedance data by using DuBois' six-coefficient model.

Condition	Raw $kPa.l^{-1}.s$	Iaw $Pa.l^{-1}.s^2$	Rti $kPa.l^{-1}.s$	Iti $Pa.l^{-1}.s^2$	Cti $l.kPa^{-1}$	Dr %
I-0.1	0.111 ± 0.057	2.12 ± 0.45	0.089 ± 0.029	0.10 ± 0.12	0.232 ± 0.055	4.5 ± 1.4
I-0.2	0.143 ± 0.069	2.00 ± 0.45	0.090 ± 0.022	0.13 ± 0.15	0.229 ± 0.066	5.0 ± 1.0
I-0.4	0.181 ± 0.074	1.79 ± 0.32	0.093 ± 0.039	0.08 ± 0.08	0.235 ± 0.041	5.2 ± 1.5
E-0.1	0.165 ± 0.083	2.15 ± 0.58	0.069 ± 0.014	0.17 ± 0.10	0.294 ± 0.071	4.7 ± 0.7
E-0.2	0.213 ± 0.101	2.10 ± 0.66	0.061 ± 0.032	0.18 ± 0.10	0.406 ± 0.233	4.4 ± 0.7
E-0.4	0.218 ± 0.119	1.91 ± 0.78	0.069 ± 0.056	0.18 ± 0.09	0.345 ± 0.158	4.8 ± 2.2
I-30	0.176 ± 0.043	2.06 ± 0.44	0.096 ± 0.036	0.14 ± 0.13	0.204 ± 0.044	4.9 ± 1.8
I-0.2	0.143 ± 0.069	2.00 ± 0.45	0.090 ± 0.022	0.13 ± 0.15	0.229 ± 0.066	5.0 ± 1.0
I-70	0.098 ± 0.046	2.03 ± 0.44	0.087 ± 0.030	0.05 ± 0.08	0.197 ± 0.064	5.4 ± 1.7
I-0.2	0.143 ± 0.069	2.00 ± 0.45	0.090 ± 0.022	0.13 ± 0.15	0.229 ± 0.066	5.0 ± 1.0
I-RV	0.149 ± 0.052	2.29 ± 0.52	0.097 ± 0.025	0.09 ± 0.09	0.195 ± 0.053	5.3 ± 1.4

Values are means ± SD for seven subjects. Raw, airway resistance; Iaw, airway inertance; Rti, tissue resistance; Iti, tissue inertance; Cti, tissue compliance; Dr, residual value of difference. Conditions are as defined in Table 2.2. Condition I-0.2 is shown three times to facilitate comparison. Raw and Iaw are corrected for the resistance and inertance of the pneumotachograph.

The statistical significance of the differences between conditions was assessed by using paired t test (denoted p) and two- and three-way variance analysis (denoted P).

Results

Average transfer impedances obtained during inspiratory $\dot{V}$ maneuvers initiated at FRC and preceded by a full inspiration to TLC are shown in Fig. 2.2. Re[Ztr] increased substantially with increasing flow and the differences were statistically

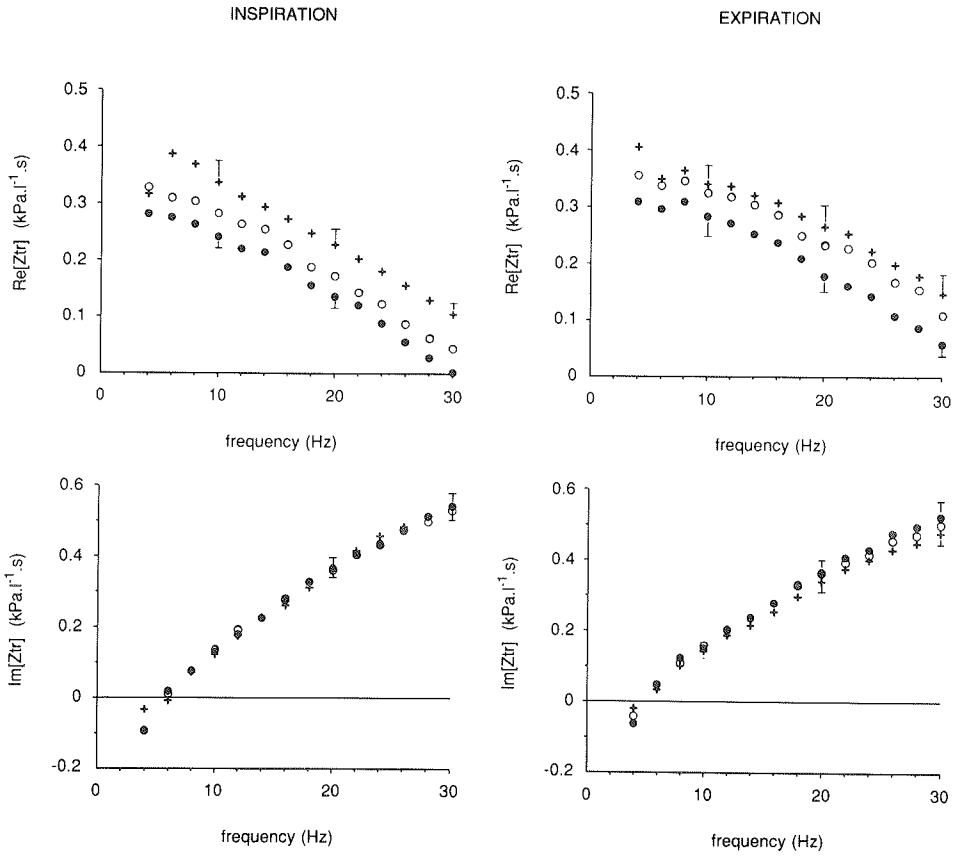

Figure 2.2. *Real (Re, top) and imaginary (Im, bottom) parts of respiratory transfer impedance measured from 4 to 30 Hz during constant inspiratory (left) or expiratory (right) flows of 0.1 l/s (●), 0.2 l/s (○), and 0.4 l/s (+). Means of seven subjects are given. Some standard errors are shown (vertical bars).*

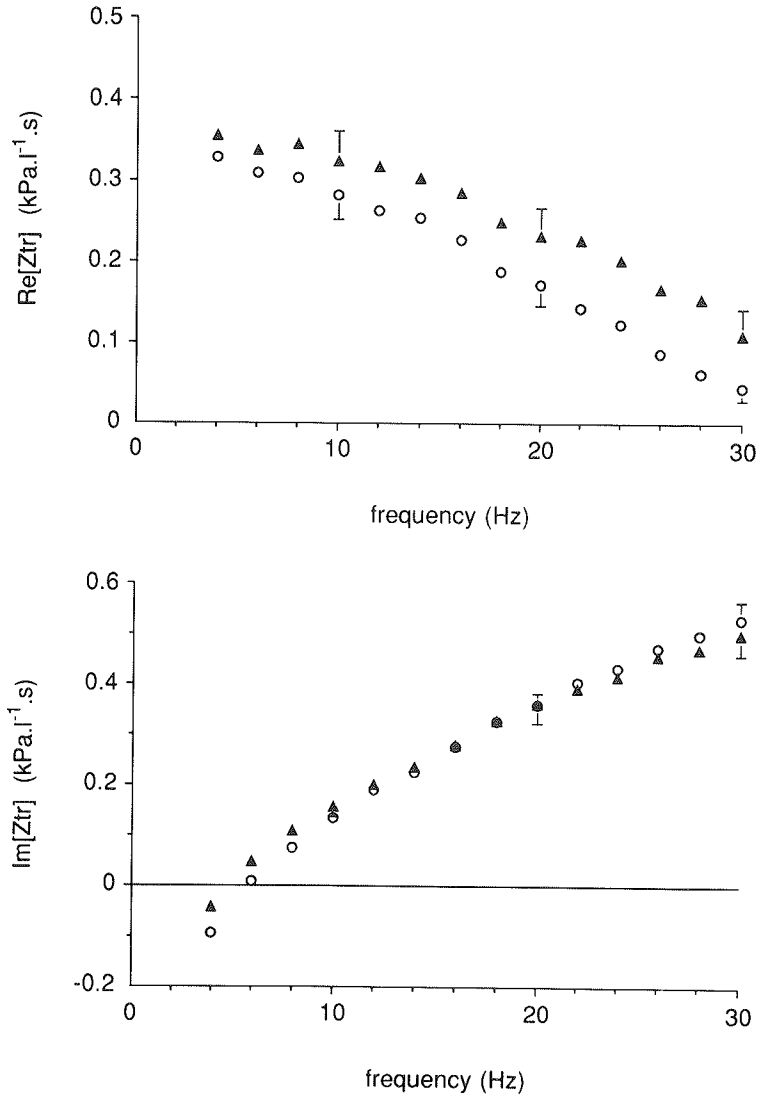

Figure 2.3. *Real (Re, top) and imaginary (Im, bottom) parts of respiratory transfer impedance measured during constant inspiratory (○) and expiratory (▲) flows of 0.2 l/s. Means of seven subjects are given. Some standard errors are shown.*

significant from 0.1 to 0.4 l/s and from 0.2 to 0.4 l/s ($p < 0.05$ by paired t test) at all frequencies. In contrast, the reactances obtained at different flows were remarkably superimposed. Data analysis with DuBois' six-coefficient model demonstrated significant changes in the airway but not in the tissue coefficients (Table 2.3). Raw increased by 29% from 0.1 l/s to 0.2 l/s, and further increased by 27% from 0.2 to 0.4 l/s ($P < 0.01$ by variance analysis). Iaw decreased by 16% from 0.1 to 0.4 l/s ($P < 0.05$).

Re[Ztr] also exhibited some flow dependence during expiratory maneuvers, but to a lesser extent than during inspiratory maneuvers on the same volume range (Fig. 2.2). At almost all frequencies, significant differences were only found between 0.1 and 0.4 l/s ($p < 0.05$). Increasing expiratory flow, on the other hand, tended to increase reactance values at low frequencies and to decrease them at high frequencies ($p < 0.05$ above 24 Hz between 0.1 and 0.4 l/s). As for inspiration, model analysis indicated that these changes could be explained by an increased Raw and decreased Iaw. It was also found that Cti was higher in all subjects at 0.2 l/s than at 0.1 l/s. Because of interindividual variability, however, none of these differences was statistically significant.

At all flows, Re[Ztr] tended to be higher during expiratory than during inspiratory maneuvers, particularly at the highest frequencies (Fig. 2.3), but the differences were only significant at 0.2 l/s ($p < 0.05$ at most frequencies above 8 Hz). There was also a trend towards higher reactances at low frequencies and lower reactances at higher frequencies during expiratory maneuvers. Expiratory Raw was 49, 49 and 20% larger than inspiratory Raw at 0.1, 0.2, and 0.4 l/s, respectively ($P < 0.01$ by three-way variance analysis), whereas Iaw was independent of flow direction. Expiratory flow also resulted in lower Rti ($P < 0.05$), higher Iti ($P < 0.01$), and higher Cti ($P < 0.001$) as compared to inspiratory flow (Table 2.3).

The influence of lung volume was studied by comparing the data obtained during inspiratory maneuvers at a flow of 0.2 l/s initiated at 30% VC, FRC, (42 ± 9% VC), and 70% VC. In all instances the maneuvers were preceded by a full inspiration to TLC and an expiration to the desired volume. In all subjects and at all frequencies Re[Ztr] increased with decreasing lung volume (Fig. 2.4). The differences were significant at all frequencies from 8 to 30 Hz between 30 and 70% VC ($p < 0.01$). At low frequencies the reactances were not influenced by lung volume, but at the highest frequencies they tended to be larger at the volume extremes than at FRC ($p < 0.05$ between 70% VC and FRC at 28 and 30 Hz). Lung volume changes significantly influenced Raw ($p < 0.01$), which increased by 80% from 70 to 30% VC, but

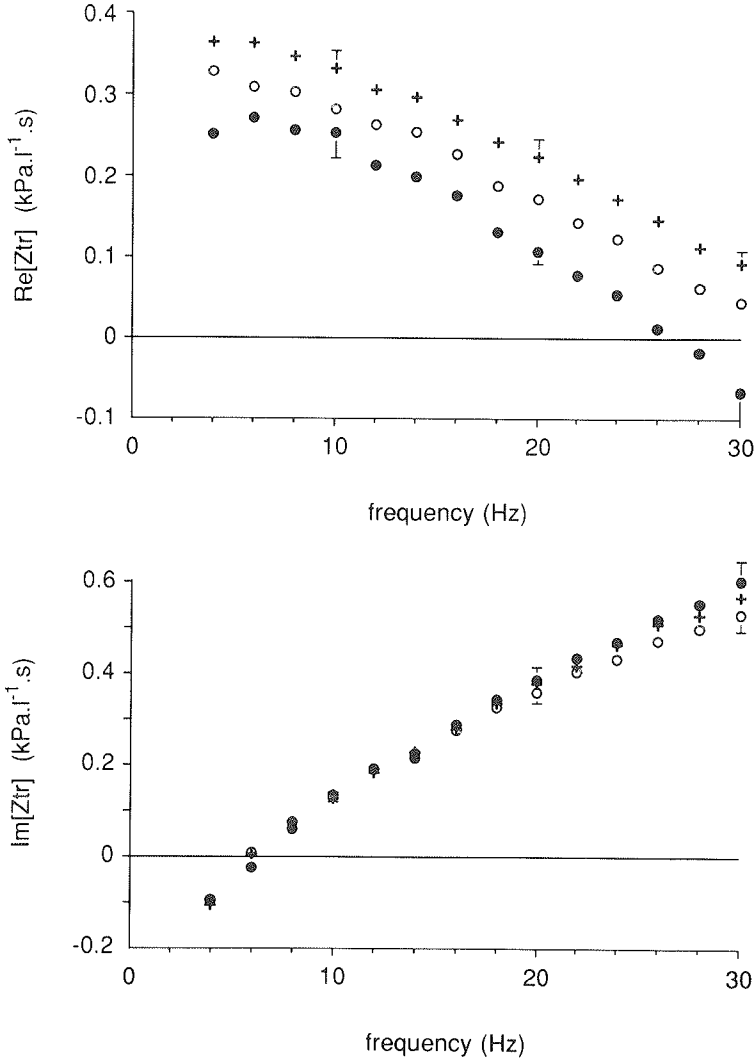

Figure 2.4. *Real (Re, top) and imaginary (Im, bottom) parts of respiratory transfer impedance measured during constant inspiratory flow of 0.2 l/s at different lung volumes; 30% of vital capacity (+), functional residual capacity (○), and 70% of vital capacity (●). Means of the group are given. Some standard errors are shown.*

did not modify Iaw. Cti was lower at the volume extremes than at FRC, but the difference was only significant at 70% VC ($p < 0.01$ by paired t-test). Increasing lung volume from FRC to 70% VC also resulted in decreased Iti ($p < 0.05$).

Finally, the influence of lung volume history was studied by comparing measurements during inspiratory maneuvers at FRC (0.2 l/s) preceded by a full inflation to TLC and a full deflation to RV. Re[Ztr] was similar in the two conditions at all frequencies, but the reactance increased more with increasing frequency and was significantly larger at frequencies above 12 Hz when the maneuver was preceded by a full deflation. These differences appeared to be related to a 15% larger Iaw ($p < 0.05$). Tissue compliance also appeared to be slightly decreased, but not significantly so.

Discussion

This study revealed systematic and, sometimes, unexpected changes of airway or tissue properties when varying $\dot{V}$, lung volume, and volume history. Before discussing these data, it is appropriate to question the validity of our model analysis to accurately recognize such changes.

Although a little more sophisticated than the resistance-inertance-compliance model generally used to interpret input impedance data (22), DuBois' six-coefficient model is still a very crude representation of the respiratory system. The main assumptions are that the system is homogeneous (monoalveolar), that the properties are independent of frequency, and that the airways are uncompliant structures. In spite of these shortcomings, there is evidence that the model is adequate to interpret transfer impedance data from 4 to 30 Hz in healthy subjects: 1) a good fit is generally obtained between model impedance and observed impedances with residual distances (Eq. 1) of 3-5% on average (20, 24); 2) the values of Raw, Iaw, and Iti are in good agreement with those found with other methods (24); in this study Raw was significantly correlated to the values obtained by body plethysmography ($r=0.78$); 3) except for tissue inertance, the coefficients are almost unchanged when the upper limit of the frequency range is increased from 20 to 50 Hz (24); 4) the analysis permits recognition of induced changes in airway and tissue properties (added Raw and Iaw, elastic loading of the chest wall) (24). A recent study where Zin and Ztr were measured both when breathing air and a lighter gas mixture has revealed minor errors in the estimation of airway inertance, but generally confirmed the adequacy of the model analysis to partition airway and tissue properties (26). All of the above evidence has been obtained in healthy subjects. To our knowledge, the validity of the

analysis has not been evaluated in patients with pulmonary disease. It is unlikely that the monoalveolar assumption will prove acceptable in such patients.

If we take for granted the fact that the model provides unbiased estimates of respiratory mechanical properties in healthy subjects, another important issue is how precise are those estimates. This will depend on how much the impedance is influenced by the properties in question on the considered frequency range (15). This has been evaluated by computing the relative change in the impedance modulus ($|Ztr| = (Re[Ztr]^2 + Im[Ztr]^2)^{½}$) when the value of each coefficient is separately increased by a fixed amount (20%) with respect to the mean value obtained during inspiratory maneuvers at 0.2 l/s. As shown in Fig. 2.5, transfer impedance is little influenced by Cti, except at the lowest frequencies; it is very sensitive to Raw, Iaw, and Rti on most of the frequency range, and almost insensitive to Iti, except at the largest frequencies. One may, therefore, expect to obtain reliable estimates of Raw, Iaw, and Rti on our frequency range, but rather imprecise values of Cti and Iti. On the basis of these results one may even wonder about the usefulness of including Iti in the model. This was investigated by analyzing some of the data by the simpler

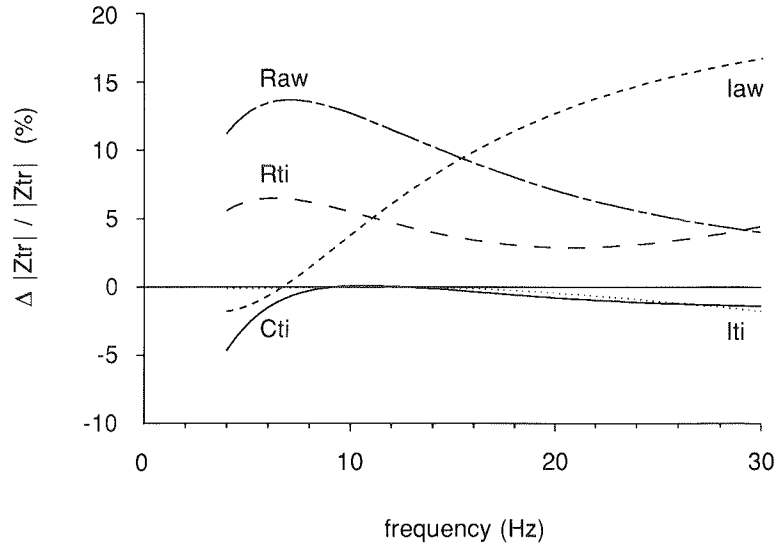

Figure 2.5. Relative change in impedance modulus (|Ztr|) as a function of frequency computed for a 20% increase in the value of each coefficient separately.

five-coefficient model. It was found that neglecting Iti was responsible for small but systematic errors on the other coefficient (underestimation of Raw, and overestimation of Rti and Cti) and, therefore, it was preferable to use the six- rather than the five-coefficient model.

Raw. In this study we found that Raw increased with increasing inspiratory and expiratory flow, was larger during expiration than during inspiration, and decreased with increasing lung volume.

Flow dependence of Raw, pulmonary, and respiratory resistance was studied in the past by using a variety of techniques and during various respiratory maneuvers: direct recording of the pressure drop across the upper airway during tidal breathing and hyperventilation (9, 12, 13, 27), measurement of transpulmonary pressure during breathing (9) and during constant flow maneuvers (14), plethysmographic determination of alveolar pressure during panting (9) and various degrees of hyperventilation (3), and finally measurement of total respiratory impedance at a single frequency during spontaneous breathing (23). Ferris et al. (9) demonstrated that the resistance of lower airways and that of the tissues was approximately constant up to 2 l/s, and that, as already observed by Hyatt and Wilcox (12), upper Raw increased with increasing flow both during inspiration and expiration. As expressed by Rohrer's constant K_2, the reported flow dependence of respiratory resistance varies largely among studies, ranging from about 0.01 (9) to 0.1 $kPa.l^{-2}.s^2$ (23). This seems to be the result both of a large interindividual variability and of the different measuring conditions. Indeed, it has been shown that K_2 varies systematically with the breathing pattern, probably in relation with the glottis aperture (9, 11, 28). This study is the first study where Raw and Rti were derived from transfer impedance measurements during constant flow maneuvers. A peculiarity of resistance measurements by forced oscillations is that small flow changes are superimposed upon the subject's flow. Then, what is measured is not the chord of the pressure flow relationship ($P/\dot{V}$), but its slope ($\Delta P/\Delta \dot{V}$) in the vicinity of the subject's flow. Starting from Rohrer's equation it may be shown that for small amplitudes

$$\Delta P/\Delta \dot{V} = K_1 + 2\,K_2 \cdot \dot{V} \qquad (2)$$

so that the flow dependence of the differential resistance should be twice that of the chord resistance. Actually, the validity of that prediction has been questioned by Dorkin et al. (7) on the basis of observations concerning the interaction of unidirectional and oscillatory flows in straight tubes. There is, therefore, some uncertainty on

how K_2 should be computed from forced oscillation data. Applying Eq. 2, inspiratory K_2 was found to be 0.114 ± 0.08 kPa.l^{-2}.s^2 in our subjects; it could be twice as large if Dorkin's conclusions may be applied to the upper airway. These values are much larger than observed with other techniques (3, 9, 12), and even slightly above those derived from impedance measurements during tidal breathing (23). This may be the result of a narrowing of the glottis during voluntary constant flow maneuvers and also of the range of flows considered in this study. Indeed, most previous observations have been made at much larger flows, when the glottis aperture tends to be larger (28).

Phasic variations of respiratory resistance have been reported in many previous studies, with a larger resistance and a larger flow dependence of resistance during expiration than during inspiration (9, 11, 14, 18, 23). Such differences are usually attributed to a smaller glottis opening during expiration, as demonstrated by Stanescu (28), and, when large flows are involved, to dynamic compression of intrathoracic airways (9). In this study, we also observed larger Raw during expiratory maneuvers, but the flow dependence of resistance was rather smaller than during inspiratory maneuvers. Again this discrepancy may be related to the fact that the measurements were made during targeted constant flow maneuvers. Our interpretation is that the glottis opening is narrower at very low flows but enlarges more with increasing flow during expiratory than during inspiratory maneuvers. This would be the case if the glottis contributed more to the regulation of flow during expiration.

Because of our experimental conditions the volume dependence of respiratory parameters could only be studied over a volume range of 1.7 liters on average (FRC −0.5 liter to FRC +1.2 liters). In agreement with previous studies (2, 4, 5), we observed an approximately linear relationship between airway conductance (Gaw) and lung volume. On average Gaw increased by 2.66 l.s^{-1}.kPa^{-1} per liter, which is in close agreement with the findings of Briscoe and DuBois (4), Butler et al. (5), and Blide et al. (2) (e.g., 2.20–2.80 s^{-1}.kPa^{-1}). Finally, we did not observe any change in Raw when the measurements made at FRC were preceded by a full deflation to RV, rather than by a full inflation to TLC. This will be discussed together with the changes in Iaw.

Iaw. Most of Iaw is expected to be located in the large airways, where the total cross-section area is small and gas acceleration is large. To our knowledge, flow dependence of respiratory inertance or Iaw has not been investigated in the past. Contrary to Raw, Iaw was seen to decrease with increasing $\dot{V}$, both during inspiratory and expiratory maneuvers. This strongly suggest that Iaw is little influenced by

the factors responsible for the flow dependence of Raw, particularly the glottis. On the other hand, the decrease in Iaw with increasing flow is consistent with a blunter velocity profile in the large airways at 0.4 than at 0.1 l/s. Indeed, inertance is expected to be 33% lower when the velocity profile is blunt than when it is parabolic (22). While Miller and Pimmel (18) observed 25% lower values of the total respiratory inertance (Irs) during expiration, we did not find any difference between inspiratory and expiratory Iaw. The contribution of tissue inertance to Irs may explain some of the discrepancy, but not all of it because Iti represents less than 10% of Irs (Table 2.3). It may also be the result of the difference in techniques because Miller and Pimmel (18) measured input rather than transfer impedance. It is noteworthy that Irs values are commonly lower when derived from Zin, probably because of the upper airway shunt impedance (21). The underestimation of Irs by that mechanism could be more important during expiration when respiratory impedance is larger. Similarly, we did not observe any volume dependence of Iaw. Because Iaw is proportional to airway length and to the reciprocal of airway cross section (22), this suggests that the airways contributing to Iaw either did not change their axial and radial dimensions with increasing lung volume (which might be the case for some of the extrathoracic airways) or increased their length and diameter similarly. In the latter instance some decrease in Raw is to be expected because resistance is proportional to length but is a power function of the cross-sectional area. Our observations are completely at variance with those of Nagels et al. (19), who measured Zin and reported a considerable decrease of Irs from 70 to 25% VC. Again we think that those data reflect a larger effect of the upper airway shunt at low lung volume when the overall impedance is larger. Their unrealistic value found at 25% VC (0.5 $Pa.l^{-1}.s^2$) supports that interpretation.

Iaw was the only coefficient to vary significantly when the volume history was modified. The increased Iaw when the measurement was preceded by a full expiration rather than by a full inspiration confirms that the degree of hysteresis of the large airways is in general more important than that of the lung (10). The absence of a concomitant increase in Raw again demonstrates that the determinants of these two properties are different. As most of Raw is also located in the large airways, our data suggest that Raw depends more on singular losses at the level of the glottis and of the bifurcations than on the diameter of the trachea and the main bronchi.

Rti. Ferris et al. (9) demonstrated that most of tissue resistance is located within the chest wall and that it is independent of flow up to 2 l/s. In agreement with that study, we did not observe any flow dependence of Rti. On the other hand, we found

that Rti was on average 37% larger during inspiratory than during expiratory maneuvers. This may represent the effect of a larger level of muscle activity during inspiration. Indeed, it has been shown by Barnas et al. (1) that respiratory effort increases chest wall resistance (Rw). One should point out that the pattern of respiratory muscle activity may be substantially different during targeted inspiratory or expiratory flow maneuvers from what it is during spontaneous breathing. One may speculate that a constant flow rate is achieved by varying glottis aperture, as suggested above, and by using both agonist and antagonist muscles. The values of Rti found in this study during inspiration, however, are very similar to those derived from impedance data during spontaneous breathing (0.093 $kPa.l^{-1}.s$ (20)). Rti was found to be slightly higher at 30% than at 70% VC, but not significantly so. A larger increase in Rw when lung volume decreased from 40 to 25% VC was seen by Nagels et al. (19) in healthy subjects but not in patients with chronic obstructive lung disease.

Iti. As mentioned earlier, Iti cannot be obtained with much precision on the frequency range explored in this study. The data should, therefore, be interpreted cautiously. Iti was found to be independent of flow but significantly larger during expiratory than during inspiratory maneuvers. This coefficient is related to the mass of the tissues and to the acceleration to which they are submitted. The acceleration will depend on the distribution of motion among parallel pathways which, itself, is a function of their respective impedance. The larger Iti during expiratory maneuvers could therefore indicate an increased contribution of a pathway with a larger mass-to-area ratio. The same mechanism could also contribute to the decrease of Iti with increasing lung volume. Another but minor factor could be the decreased acceleration of the tissues as a result of their larger external surface area at high lung volume.

Cti. Again, as indicated by the sensitivity function in Fig. 2.5, our frequency range did not permit a very precise determination of Cti. Cti was found to be significantly larger during expiratory than during inspiratory maneuvers. A similar observation was made by Miller and Pimmel (18), who compared inspiratory and expiratory phases of spontaneous breathing. They suggested that the difference could reflect phasic variations in the level of activity of respiratory muscles and also, for a part, the hysteresis of lung elastic properties. The hysteresis of lung elastic properties could also explain the trend to have lower values of Cti when the measurement was preceded by a full expiration. Cti was also seen to be smaller at 70 and 30% VC than at FRC, which is in agreement with the observation Nagels et al. (19), and is consistent with the sigmoid shape of the static pressure-volume curve. It may also

reflect for a part the increased level of muscle activity required to maintain lung volume above or below FRC.

Conclusion

This study confirms the flow, volume, and phase dependence of Raw and demonstrates that the determinants of Raw and Iaw are not identical. In addition, it supports the notion that airway hysteresis is larger than lung hysteresis and that the level of respiratory muscle activity influences tissue properties. It also confirms that the measurement of respiratory transfer impedance combined with the use of DuBois' six-coefficient model is a valuable tool to explore a number of specific airway and tissue properties in healthy subjects. The potential of the method would be further increased by extending the frequency range to frequencies below 4 Hz and above 30 Hz.

References

1. BARNAS, G.M., N.C. HEGLUND, D. YAGER, K. YOSHINO, S.H. LORING, AND J. MEAD. Impedance of the chest wall during sustained respiratory muscle contraction. J. Appl. Physiol. 66: 360–369, 1989.
2. BLIDE, R. W., H.D. KERR, AND W.S. SPICER, JR. Measurement of upper and lower airway resistance and conductance in man. J. Appl. Physiol. 19: 1059–1069, 1964.
3. BOUHUYS, A., AND B. JONSON. Alveolar pressure, airflow rate, and lung inflation in man. J. Appl. Physiol. 22: 1086–1100, 1967.
4. BRISCOE, W.A., AND A.B. DUBOIS. The relationship between airway resistance, airway conductance and lung volume in subjects of different age and body size. J. Clin. Invest. 37: 1279–1285, 1958.
5. BUTLER, J., C.G. CARO, R. ALCALA, AND A.B. DUBOIS. Physiological factors affecting airway resistance in normal subjects and in patients with obstructive respiratory disease. J. Clin. Invest. 39: 584–591, 1960.
6. CSENDES, T., B. DARÓCZY, AND Z. HANTOS. Nonlinear parameter estimation by global optimisation: comparison of local search methods in respiratory system modelling. In: *System Modelling and Optimisation. Proceeding of the 12th IFIP Conference*. Berlin: Springer Verlag, 1986, p. 188–192.
7. DORKIN, H.L., A.C. JACKSON, D.J. STRIEDER, AND S.V. DAWSON. Interaction of

oscillatory and unidirectional flows in straight tubes and an airway cast. J. Appl. Physiol.: Respirat. Environ. Exercise Physiol. 52: 1097–1105, 1982.
8. DuBois, A.B., A.W. Brody, D.H. Lewis, and B.F. Burgess, Jr. Oscillation mechanics of lungs and chest in man. J. Appl. Physiol. 8: 587–594, 1956.
9. Ferris, Jr., B.G., J. Mead, and L.H. Opie. Partitioning of respiratory flow resistance in man. J. Appl. Physiol. 19: 653–658, 1964.
10. Froeb, H.F., and J. Mead. Relative hysteresis of the dead space and lung in vivo. J. Appl. Physiol. 25: 244–248, 1968.
11. Goldstein, D., and J. Mead. Total respiratory impedance immediately after panting. J. Appl. Physiol.: Respirat. Environ. Exercise Physiol. 48: 1024–1028, 1980.
12. Hyatt, R.E., and R.E. Wilcox. Extrathoracic airway resistance in man. J. Appl. Physiol. 16: 326–330, 1961.
13. Jaeger, M.J., and H. Matthys. The pattern of flow in the upper human airways. Respir. Physiol. 6: 113–127, 1968/1969.
14. Jonson, B. Pulmonary mechanics in normal men, studied with the flow regulator method. Scand. J. Clin. Lab. Invest. 25: 363–373, 1970.
15. Lutchen, K.R., and A.C. Jackson. Reliability of parameter estimates from models applied to respiratory impedance data. J. Appl. Physiol. 62: 403–413, 1987.
16. Mead, J. Control of respiratory frequency. J. Appl. Physiol. 15: 325–336, 1960.
17. Michaelson, E.D., E.D. Grassman, and W.R. Peters. Pulmonary mechanics by spectral analysis of forced random noise. J. Clin. Invest. 56: 1210–1230, 1975.
18. Miller, T.K., and R.L. Pimmel. Forced noise mechanical parameters during inspiration and expiration. J. Appl. Physiol.: Respirat. Environ. Exercise Physiol.: 52: 1530–1534, 1982.
19. Nagels, J., F.J. Landsér, L. van der Linden, J. Clément, and K.P. van de Woestijne. Mechanical properties of lungs and chest wall during spontaneous breathing. J. Appl. Physiol.: Respirat. Environ. Exercise Physiol. 49: 408–416, 1980.
20. Peslin, R., C. Duvivier, and C. Gallina. Total respiratory input and transfer impedances in humans. J. Appl. Physiol. 59: 492–501, 1985.
21. Peslin, R., C. Duvivier, C. Gallina, and P. Cervantes. Upper airway artifact in respiratory impedance measurements. Am. Rev. Respir. Dis. 132: 712–714, 1985.
22. Peslin, R., and J.J. Fredberg. Oscillation mechanics of the respiratory system. In: *Handbook of Physiology. The Respiratory System. Mechanics of Breathing.*

Bethesda, MD: Am. Physiol. Soc., 1986, sect. 3, vol. III, pt. 1, chapt. 11, p. 145–177.

23. PESLIN, R., T. HIXON, AND J. MEAD. Variations des résistances thoraco-pulmonaires au cours du cycle ventilatoire étudiées par méthode d'oscillation. Bull. Physiopathol. Respir. 7: 173–186, 1971.
24. PESLIN, R., J. PAPON, C. DUVIVIER, AND J. RICHALET. Frequency response of the chest: modeling and parameter estimation. J. Appl. Physiol. 39: 523–534, 1975.
25. PETRO, W., G. V. NIEDING, W. BÖLL, AND U. SCHMIDT. Determination of respiratory resistance by an oscillation method. Respiration 42: 243–251, 1981.
26. ROTGER, M., R. PESLIN, C. DUVIVIER, D. NAVAJAS, AND C. GALLINA. Density dependence of respiratory input and transfer impedances in humans. J. Appl. Physiol. 65: 928–933, 1988.
27. SPANN, R.W., AND R.E. HYATT. Factors affecting upper airway resistance in conscious man. J. Appl. Physiol. 31: 708–712, 1971.
28. STĂNESCU, D.C., J. PATTIJN, J. CLÉMENT, AND K.P. VAN DE WOESTIJNE. Glottis opening and airway resistance. J. Appl. Physiol. 32: 460–466, 1972.

Chapter 3

Airway Impedance during Single Inspirations of Foreign Gases

E. Oostveen, R. Peslin, C. Duvivier, M. Rotger, and J. Mead

Abstract

The changes in airway resistance (Raw) and inertance (Iaw) during single inspirations of pure methane, helium, neon, and ethane at a flow of 0.1 l/s were measured in six healthy subjects using the forced oscillation technique. Raw and Iaw were computed from respiratory transfer impedance obtained at a frequency of 20 Hz by applying pressure oscillations at the chest and measuring flow at the mouth with a bag-in-box system. Compared to the control data, the changes of Iaw after inhaling 500 ml of gas averaged −41.1% with methane, −82.8% with helium, −25.8% with neon, and +4.8% with ethane. These changes were slightly less than the changes in density of the foreign gases as compared to air (−44%, −86%, −30%, and +5%, respectively). The inhaled volumes at which 50% of the changes had occurred (V50) did not differ significantly among gases and were about 100 ml. For Raw the data were more noisy than for Iaw, and were discarded in two subjects because of a strong and non reproducible volume dependence in air. Consistent differences were seen between the remaining subjects, one of whom exhibited a predominant viscosity dependence of Raw, one a predominant density dependence, and two an intermediate type. V50s were larger for Raw than for Iaw, indicating a more peripheral distribution of Raw. For Raw, V50s were lower with helium than with methane, in agreement with the notion that density-dependent resistance is mainly located in the large airways. The results suggest that some information on the serial distribution of Raw and Iaw may be derived from impedance measurements with foreign gases.

Introduction

While common pulmonary function tests may give some information on the site of airway obstruction (15), assessing more directly the longitudinal distribution of airway properties by a non-invasive method is of much interest for a number of physiological and clinical applications. Such a method has been described by Jackson et al. (12) and by Sidell et al. (23) who developed a technique to measure cross-sectional areas of the large airways by acoustic reflection. Another interesting method is the inference of airway geometry from aerosol deposition (9, 10).

A quite different approach consists of measuring the changes in airway properties during the flushing of the airways by a gas having a different viscosity (μ) and/or density (ρ) than air. In a preliminary study (21), we have followed the changes in airway resistance (Raw) and inertance (Iaw), measured 10 times per second by a forced oscillation technique, during slow inspirations of methane, neon and a mixture of neon and sulfur hexafluoride. Although noisy, the data were in agreement with theoretical predictions and experimental evidence concerning the flow regime in the airways (4, 14, 16): For instance, when taking a single breath of neon, which has a lower density (0.70) and a larger viscosity (1.70) than air, Raw decreased at the beginning of the breath when the gas progressed along the proximal airways, and subsequently increased when the gas reached more peripheral bronchi. This is consistent with the notion that resistance is density-dependent in the large airways and viscosity-dependent in the peripheral airways. The aim of this study was to further investigate the potential of that approach.

Principle

The principles of our approach are illustrated with a simple mechanical analog (Fig. 3.1). It is made of a tube with negligible resistance of its own, but containing two discrete resistive elements placed at some distance from the entrance and from each other. The first is a purely viscosity-dependent resistance, e.g. a wire-mesh screen, and the second a purely density-dependent resistance, e.g. an orifice. The tube is flushed by a constant flow of air for which the resistances of the two elements are respectively R1 and R2 and the total resistance Rair = R1 + R2. Keeping the flow constant but switching from air to some foreign gas, resistance will stay constant until the concentration front, which for simplicity is assumed to be blunt (flat velocity profile and negligible axial diffusion), reaches the first resistive element. Then a step change in resistance dR1 may occur, followed by a plateau and by a

second step change dR2 when the foreign gas reaches the orifice. The magnitude and direction of dR1 and dR2 will depend on R1 and R2 and on the viscosity and density of the gas compared to those of air (specific μ and ρ, μ_s and ρ_s).

A particularly interesting case (Fig. 3.1) is that of a gas with a higher or lower density and viscosity than air, but a similar kinematic viscosity ($\mu_s / \rho_s = 1$), which is almost the case for pure methane ($\mu_s = 0.59$, $\rho_s = 0.56$). Then the change in local resistance is in the same direction and has the same relative amplitude whatever the type of resistive element: $dR = (K-1)R$ with $K = \mu_s = \rho_s$. Knowing K one may therefore recover the initial resistance distribution along the tube. Other interesting cases are gases or gas mixtures which differ from air by their density only or their viscosity only and, therefore, will only reveal specific types of resistance. With ethane for instance ($\mu_s = 0.49$, $\rho_s = 1.05$), the orifice would be practically ignored, while with helium ($\mu_s = 1.06$, $\rho_s = 0.14$), the screen would be barely perceptible. So, it is theoretically possible to obtain separately the distribution of viscosity-dependent

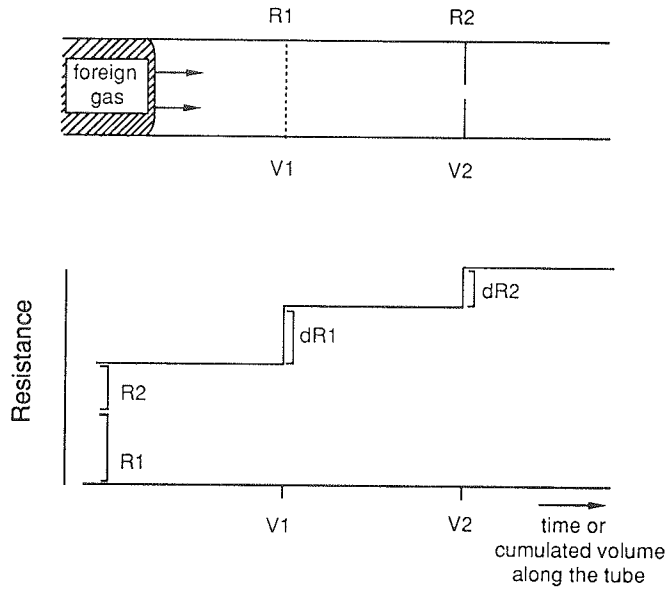

Figure 3.1. *Illustration on a simple mechanical analog of the approach used in this study. R1 and R2, viscosity-dependent and density-dependent resistances placed at volume V1 and V2 along the tube, respectively; dR1 and dR2, changes in total resistance when gas with a viscosity and density 80% larger than air reaches R1 and R2.*

and of density-dependent resistances.

Many simplifying assumptions have been used in the above description. Except for the glottis and for singular losses at the bifurcations, the airways are not made of discrete purely viscosity-dependent or density-dependent resistive elements. Rather, Raw is distributed along tubes and the resistance of a tube varies with the Reynolds number. Therefore, Raw is not only a function of gas flow and of the airway cross-sectional area, but also of the gas kinematic viscosity. Except when the gas kinematic viscosity is kept constant, switching from one gas species to another will, to some extent, change the very distribution of resistance that one is trying to assess, as well as its dependence upon gas physical properties. Of still greater importance may be the fact that the front of foreign gas does not progress along the airways like a piston in a cylinder. Unless the velocity profile is flat, the outer layers will be washed more slowly than the central core of the airway, a phenomenon which, combined with axial diffusion, will blur and distort the measured resistance profile. In spite of these obvious complicating features, it was hoped that measuring the airway resistance (or inertance) when the airways were rinsed with different foreign gases would provide distribution profiles of physiological interest.

Methods

Even at the lowest inspiratory flow that a trained subject may reproducible sustain (about 0.1 l/s), the airways are washed in just a few seconds. Thus, the forced oscillation technique is the only available method having the time resolution required to follow the changes in resistance expected during a single inspiration of a foreign gas. In this study Raw and Iaw were derived from respiratory transfer impedance (Ztr) measured by applying pressure oscillations around the chest and measuring flow at the airway opening. That variant of the forced oscillation technique was preferred to the more common input impedance because, using a model proposed by DuBois et al. (5), the airway components of total respiratory resistance and inertance may be computed from Ztr data (22).

Equipment

The subjects were enclosed up to the neck in a 350 l body chamber (Fig. 3.2) equipped with two 90 watt loudspeakers. The latter were supplied with a 20 Hz sinusoidal signal and delivered pressure oscillations around the body (Pbs) with an amplitude of about 0.1 kPa peak-to-peak. During the measurements the subject was

connected by a short mouthpiece to a bag-in-box system. The box was open to atmosphere through a screen-type pneumotachograph, so that box pressure (Pb), once corrected for the time constant of the box, was proportional to the gas flow entering or leaving the bag ($\dot{V}b$). The gas under study, contained in a tank, was decompressed by a regulating valve and injected into the mouthpiece through a solenoid valve, by a number of lateral holes. The flow of foreign gas ($\dot{V}g$) was always largely in excess of the inspiratory flow required from the subject so as to reduce the time necessary to wash the mouthpiece and avoid contamination of inspired gas by diffusion of air from the bag. As $\dot{V}g$ was not strictly constant but exhibited a slight transient at the beginning of the injection, it was measured with a small capillary type pneumotachograph placed on the injection line, close to the mouthpiece. Then, the amount of foreign gas inhaled by the subject could be obtained at any time by integrating flow at the airway opening ($\dot{V}ao$) as given by the difference of $\dot{V}g$ and $\dot{V}b$.

Pbs, Pb, mouth pressure (Pm) and the pressure drop across the pneumotachograph were measured with identical transducers (Validyne MP-45 ± 0.2 kPa). The transducers for Pbs and Pm were statically calibrated with a slanted water manometer, cross-calibrated and matched for phase within 2° at 20 Hz. The bag-in-box system was calibrated by the integral method using a 1 liter syringe. Its time constant was assessed by reference with a Fleisch pneumotachograph placed in series with it. As gas adiabatic compressibility depends on the gas species, the time constant varied

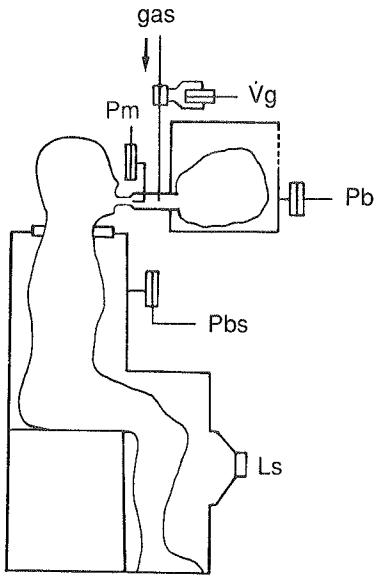

Figure 3.2. *Experimental setup. Pbs, Pm, and Pb, pressures at the body surface, at the mouth and in bag-in-box system, respectively; $\dot{V}g$, flow of foreign gas injected into mouthpiece; Ls, loudspeaker.*

slightly with the gas in the bag, and with its amount. It was verified that these variations influenced the data negligibly. The small pneumotachograph used for measuring $\dot{V}g$ was calibrated statically for each gas species by reference to the bag-in-box system.

The two pressure signals and the difference of the two flow signals ($\dot{V}ao$) were digitized on-line with a sampling rate of 160 Hz by an Apple 2e microcomputer system. The volume of gas inhaled by the subject was obtained by numerical integration of $\dot{V}ao$. After filtering out the low-frequency components of the signals, their relative amplitude and phase angle for the 20 Hz component were obtained on a cycle-per-cycle basis by computing their Fourier coefficients for that frequency. This provided 20 estimates per second of the total transfer impedance ($Ztr = Pbs/\dot{V}ao$) and of the impedance of the equipment placed at the mouth ($Ze = Pm/\dot{V}ao$). These impedances were corrected for the time-constant of the bag-in-box system. They were used to compute Raw and Iaw as described below.

Model analysis

The computation of airway impedance (Zaw) was based on the classical T-network model (19) which, besides Zaw, includes tissue impedance (Zti) and alveolar gas shunt impedance (Zg). Ztr is related to the above impedances and to Ze by:

$$Ztr = Zti + Zaw + Ze + \frac{Zti.(Zaw+Ze)}{Zg} \quad (1)$$

Then, Zaw is given by:

$$Zaw = Zg.\frac{(Ztr - Zti)}{(Zti + Zg)} - Ze \quad (2)$$

and may be computed provided Zg and Zti are known. Zg is related to alveolar gas compressibility ($Zg = -j/(\omega.Cg)$ where j is the unit imaginary number and $\omega = 2\pi f$) which is proportional to thoracic gas volume ($Cg = TGV/PB$ where PB is barometric minus alveolar water vapor pressure). It was computed from plethysmographic estimates of functional residual capacity (FRC), corrected for the volume inspired by the subject. Zti is related to tissue resistance (Rti), inertance (Iti) and compliance (Cti):

$$Zti = Rti + j.(\omega.Iti - 1/(\omega.Cti)) \quad (3)$$

To obtain these coefficients, Ztr was separately measured from 4 to 30 Hz as previously described (17), using the same pressure generator, and in the same inspiratory flow conditions as during the foreign gas measurements. These impedance

data were analyzed with DuBois' six-coefficient model (5) which includes the above tissue coefficients as well as Cg, and the airway coefficients Raw and Iaw:

$$Zaw = Raw + j.\omega.Iaw \quad (4)$$

The analysis requires entering the value of Cg, and provides the values of the other five coefficients (22). The values of TGV, Rti, Iti and Cti used to compute Raw and Iaw from Ztr and Ze with equations 2 and 4 are listed in Table 3.1.

Protocol

The study was conducted in six healthy subjects whose biometric characteristics are shown in Table 3.1. In each of them measurements were performed on different days with helium, methane, neon, and ethane. As a reference, data were also collected when switching from ambient air to the gas from a tank of compressed air.

All measurements were made during inspiratory maneuvers at a flow of about 0.1 l/s starting from FRC. To help him achieve the proper volume and flow, the subject was shown his integrated $\dot{V}ao$ signal (Vao) as a function of time on an oscilloscope, with slanted lines representing a flow of 0.1 l/s drawn on the screen. The sequence of

Table 3.1. *Biometric characteristics, lung volume and tissue coefficients of the subjects.*

Subject	Sex	Age yr	Height cm	TGV liters	Rti $kPa.l^{-1}.s$	Iti $Pa.l^{-1}.s^2$	Cti $l.kPa^{-1}$
1	M	50	178	5.85	0.067	0.02	0.318
2	F	26	171	2.80	0.119	0.06	0.166
3	M	50	168	3.37	0.116	0.12	0.258
4	F	28	170	3.50	0.039	0.11	0.248
5	M	30	171	3.00	0.121	0.02	0.238
6	M	49	169	3.09	0.095	0.15	0.247
mean		38.8	171.2	3.77	0.093	0.08	0.246
S.D.		11.9	3.5	1.16	0.033	0.05	0.049

TGV, thoracic gas volume; Rti, Iti, Cti, tissue resistance, inertance and compliance.

maneuvers was as follows: after a short period of hyperventilation the subject took the mouthpiece and inspired to total lung capacity. He expired a preset volume corresponding to his inspiratory capacity plus an additional 200 ml and, then, inspired at the requested flow. Data acquisition was started when the subject passed his FRC, after which the solenoid valve was activated within one second, delivering the test gas to the subject. The subject kept inspiring at the same flow for six seconds. The data were immediately processed and the maneuver was rejected when the mean inspired flow was not between 80 and 120 ml/s, or when the impedance data showed irregular variations suggesting airway closure. This was rarely the case after one or two training sessions. However, the impedance-time curves exhibited a substantial intraindividual variability. Therefore, 8 to 16 acceptable curves were obtained in each subject for each test gas and the corresponding Raw and Iaw data were averaged.

Results

Fig. 3.3 shows the average Raw and Iaw data obtained in a one subject (#6) with three of the gases. The data have been plotted as a function of the volume of gas inhaled by the subject since the beginning of injection. As a first approximation, larger volumes therefore correspond to deeper airways. This figure illustrates several features of the data which were present, to some extent, in all the subjects. First, the variability of Raw at any given inspired volume was much larger than that of Iaw. This is reflected both in the three times larger coefficient of variations and in the irregularities of the Raw curves. Second, for Iaw, the values observed immediately after the beginning of the injection differed in most instances very little from the values seen immediately before. In contrast, irrespective of the gas, Raw was transiently a little larger than the previous air value in about 50% of the cases. This is illustrated by the helium curve in Fig. 3.3 where Raw averaged 0.106 $kPa.l^{-1}.s$ before injection and reached 0.119 $kPa.l^{-1}.s$ after inhaling 50 ml of helium. Third, Iaw almost did not vary with the inspired volume during the injection of compressed air: in the six subjects the mean Iaw during the last 50 ml of the breath did not differ from the value before injection by more than 4% and the difference was not significant. In contrast, except in one subject, substantial variations of Raw with increasing lung volume were observed in air. In two subjects these variations exceeded 20% between the beginning and the end of the breath; moreover, they were not reproducible which precluded any correction of the data. In the other four subjects they ranged from 3 to 17% and were fairly reproducible. In those cases, the data obtained with the other gases were corrected for the volume dependence observed with air.

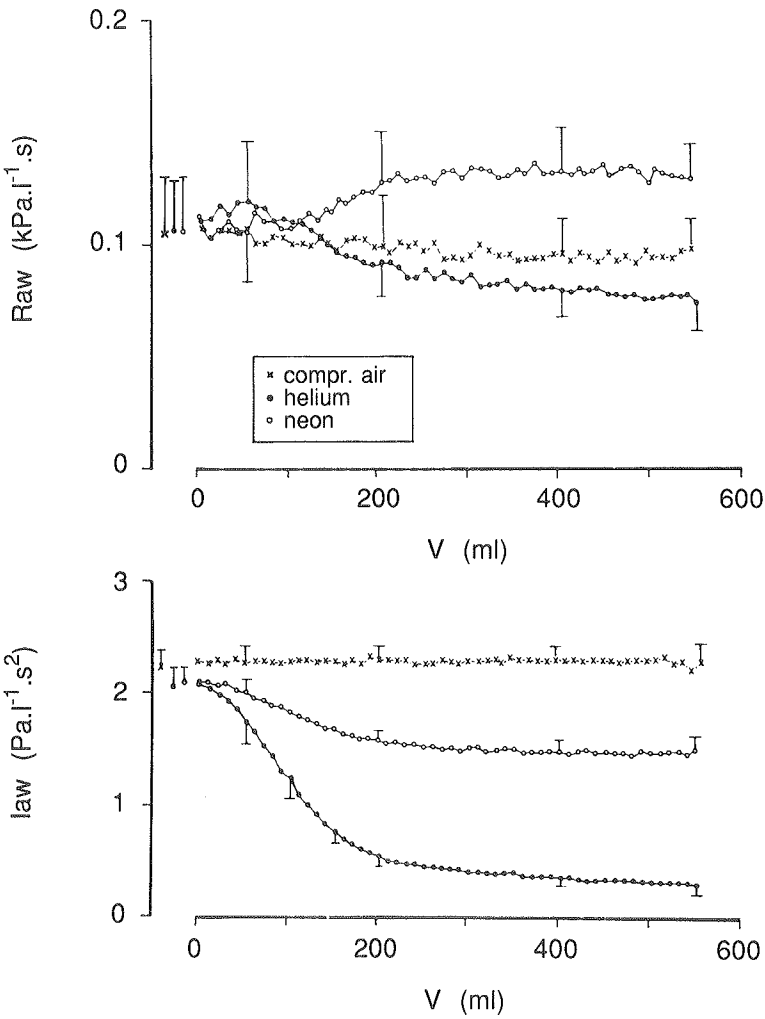

Figure 3.3. *Average values of airway resistance (Raw, top) and inertance (Iaw, bottom) obtained with three gases in subject 6. Raw and Iaw are expressed as a function of the volume of gas inhaled by the subject. Some of the standard deviations are also shown.*

Final to initial Iaw and Raw ratios

Most of the resistance and inertance changes occurred before the subjects had inhaled 300 ml of the foreign gas and very little variations were seen after 500 ml.

The average Raw and Iaw between 500 ml inspiration of the gas up to the end of the inspiration were computed and are referred to below as the final values for the gas in question. They were related to the initial Raw or Iaw, defined as the mean values observed just before the injection. When the injection was followed by an increase in Raw as mentioned above, the initial Raw was taken as the mean value over the first 50 ml following the injection.

The ratios of the final to initial inertance values for the four foreign gases are

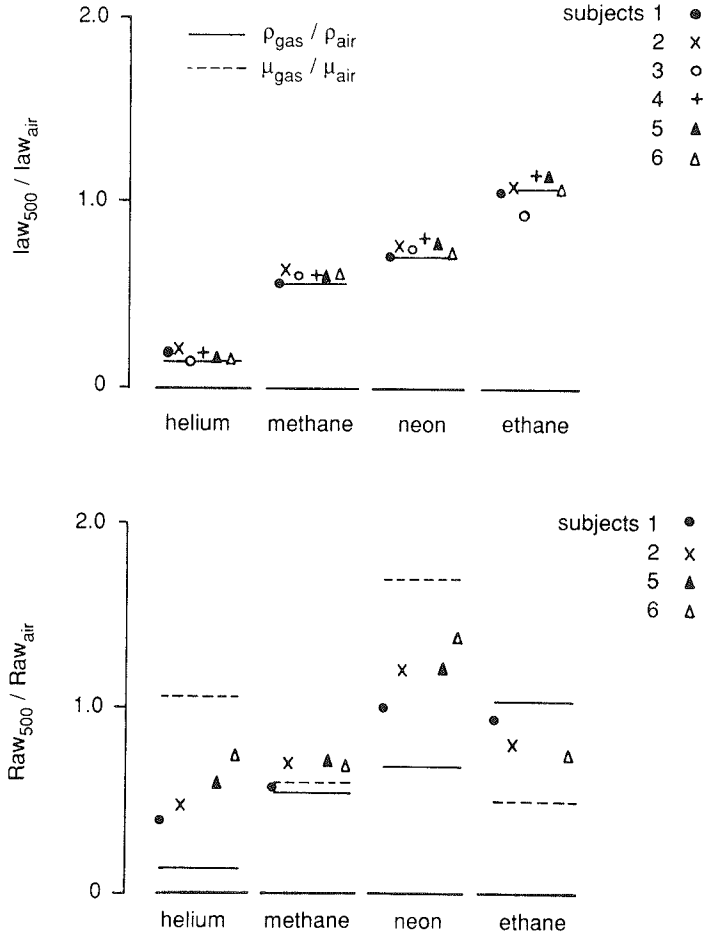

Figure 3.4. *Iaw (top) and Raw (bottom) after inhalation of 500 ml of gas related to air values. Continuous and broken horizontal lines indicate specific densities and viscosities, respectively.*

shown in Fig. 3.4 (top). Since Iaw should be strictly density-dependent, the data were compared to the specific densities of the gases. It may be seen that the observed ratios were close to the expected values but tended to be slightly larger than expected for helium, methane, and neon, suggesting that the airways were not completely washed after inhaling 500 ml of the gas.

The ratios of the final to initial Raw values in the four subjects for whom the volume dependence in air could be corrected for, are shown in Fig. 3.4 (bottom). In one of them the ethane data were excessively noisy and were discarded. Since resistance may depend on both factors, the data were compared to specific densities and viscosities. With methane, which has almost the same kinematic viscosity as air ($\mu_s = \rho_s$), the decrease in resistance was a little less than expected. This, again, points to incomplete washin. Helium, neon, and ethane have very different μ_s and ρ_s which permits quantifying the relative influence of the two factors. In this respect the data revealed consistent differences among subjects, best illustrated by subjects 1 and 6. In subject 1 the resistance ratio was always much closer to the specific densities than to the specific viscosities, while the opposite was true for subject 6.

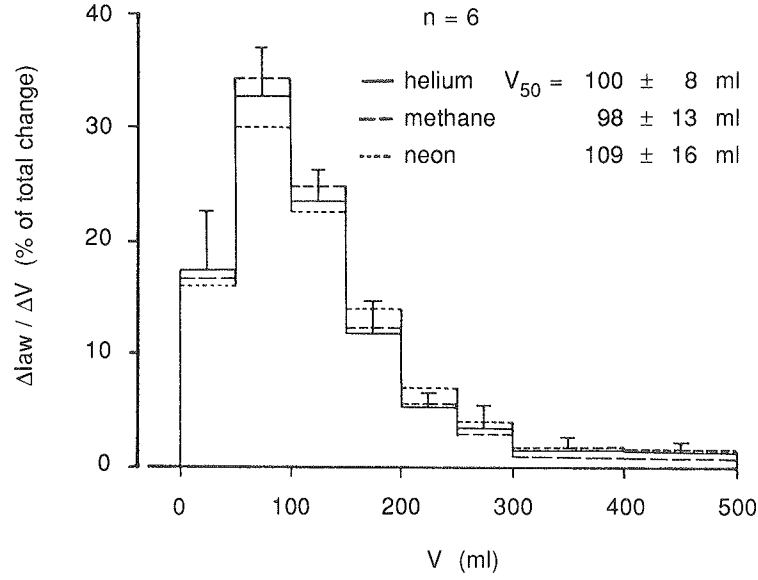

Figure 3.5. *Average distribution profiles of Iaw for all subjects for three gases. Standard deviations with helium are also shown.* V_{50}*: median of the distribution.*

Distribution profiles

If the concentration front in the airways was perfectly blunt and the data noise free, the slope of the inertance–volume curve at any volume would be proportional to that part of Iaw which is located at a volumetric depth corresponding to the volume in question. Thus, the derivative of the curve (dIaw/dV) would indicate the distribution of Iaw along the airways. To reduce the influence of the noise we obtained

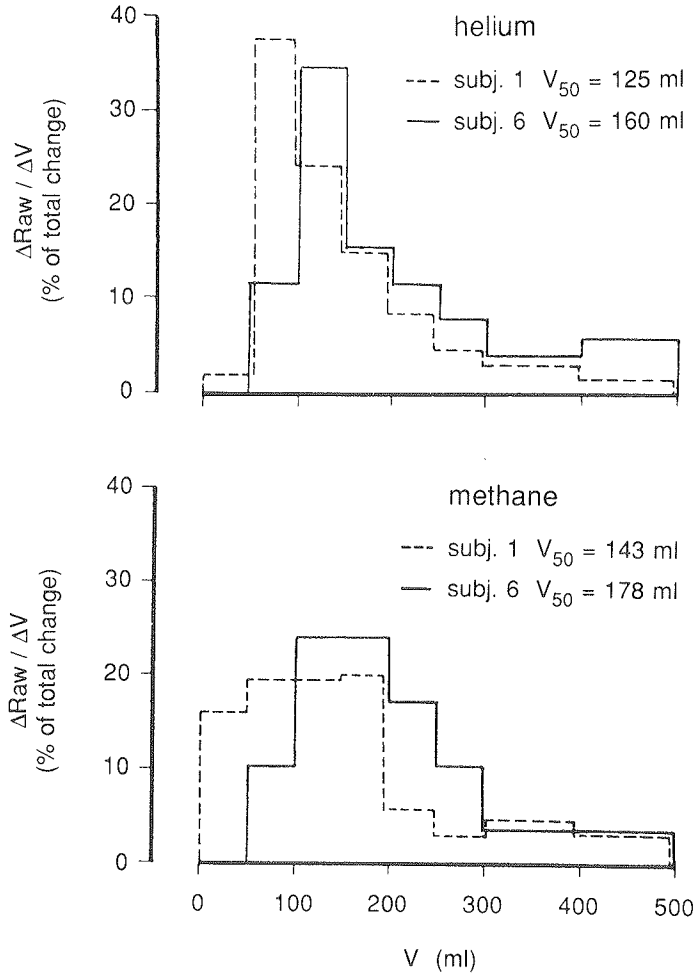

Figure 3.6. *Distribution profiles of Raw with helium (top) and methane (bottom) in subjects 1 and 6.*

distribution profiles by computing a filtered derivative of the curves. This was done by taking the slope of successive 50 ml segments (0–50, 50–100, ..., 450–500 ml); the data were normalized for the total change in Iaw. The analysis could not be done for ethane which had almost the same density as air, and modified Iaw very little (Fig. 3.4). The mean distribution profiles in the six subjects with the three other gases are shown in Fig. 3.5. Variance analysis did not reveal any significant difference between the profiles obtained with helium, methane, and neon. With all three gases the profiles were skewed with a mode located between 50 and 100 ml of inspired volume. The volumes at which 50% of the total Iaw change was achieved (V50) did not differ significantly and averaged 100 ± 8 ml for helium, 98 ± 13 ml for methane and 109 ± 16 ml for neon.

For Raw, besides the problem of volume dependence in air, the changes were in many instances too small and/or too noisy to allow computation of distribution profiles or even of V50s. Approximate profiles for methane and helium were computed in subjects 1 and 6 who had the most striking differences in terms of viscosity and density dependence of Raw. They are shown in Fig. 3.6 and the corresponding V50s are compared in Table 3.2 to those obtained for Iaw. In both subjects and for both gases V50s were substantially larger for Raw than for Iaw, suggesting that resistance is less centrally located than inertance. Also in both subjects, V50s for Raw were smaller for helium, which almost exclusively detects density-dependent resistance, than for methane, which should reveal any type of resistance. Finally, for both gases, V50s were smaller for subject 1, who had a predominantly density-dependent Raw (Fig. 3.4, bottom), than for subject 6, whose Raw depended much more on viscosity.

Table 3.2. *Medians (V_{50}) of distribution profiles.*

	Iaw		Raw	
Subject	Helium	Methane	Helium	Methane
1	102	100	125	143
6	102	102	160	178

Values are in ml.

Discussion

In this study we tried to follow Raw and Iaw changes taking place within a few seconds and which, in most cases, did not reach 50% of the initial air values. Considering the short-term variability of Raw (20), probably originating in the glottis, it is not surprising that the signal-to-noise ratio of our measurements was not very high and that the study provided at best approximate results. Still, the data were consistent with theoretical predictions and experimental findings concerning the physics of gas within the airways. Before discussing the data several methodological issues should be addressed.

Computation of Raw and Iaw

Airway impedance at 20 Hz was derived from total respiratory impedance using DuBois' monoalveolar six-coefficient model (Eq. 2) and previously determined values of TGV and tissue properties. The tissue coefficients were computed from Ztr data obtained in the frequency range 4–30 Hz, using the same model and the same value of TGV. Previous studies have shown that in normal subjects the model gives a good fit to the data in that frequency range and that the coefficients supplied by the analysis are physiologically meaningful (22). It was also shown that some of these coefficients vary systematically with lung volume, volume history and respiratory flow (17). This is why, in this study, we have computed Rti, Iti, and Cti from Ztr data collected in exactly the same conditions as the foreign gas measurements, i.e. inspiratory maneuvers at a flow of 0.1 l/s initiated at FRC and preceded by a full inspiration to TLC.

There were no significant differences between the mean values of Raw and Iaw derived from impedance data in the frequency range 4 to 30 Hz and Raw and Iaw computed from the 20 Hz measurements when taking a breath of air. There were some individual differences for Raw, but Iaw values were highly correlated (r=0.90) which suggests that the coefficients entered into the computation were adequate. Still, we wondered to what extend a slight misestimation of the tissue coefficients or of TGV would impair our estimates of Raw and Iaw. This was investigated by computing the influence on our data of a 20% error in any of the coefficients. It appeared that, whatever the foreign gas, the final-to-initial Raw and Iaw ratios would be little affected by errors on Iti and Cti, changing the original values for Raw and Iaw by less than 5% in most cases. With regard to Rti and TGV the errors would in general be larger, particularly for Raw, and depend on whether Raw increases or decreases. The worst case is that of helium where a 20% error in Rti could cause an error of the

same order in the Raw ratio when resistance is viscosity-dependent, and an almost 100% error when it is density-dependent because the final value of Raw is very small. Similarly, errors on TGV could be responsible for substantial errors in the Raw ratio with helium, ethane, and neon when resistance is viscosity-dependent. An important point is that the directions of these errors are such that, with all gases, an overestimation of Rti and/or TGV would tend to exaggerate the apparent density dependence, and an underestimation of these coefficients would have the opposite effect. We therefore wondered whether the differences between subject 1 and 6 (Fig. 3.4, bottom) could have been induced by errors in the coefficients. Recomputing their data with a 20% lower Rti and TGV for subject 1 and a 20% larger Rti and TGV for subject 6 indeed erased most of the difference between their Raw ratios with helium. However, their neon and ethane ratios remained markedly different. Computer simulation also revealed that 20% errors in any of the coefficients would negligibly affect the distribution profiles.

Correction for Raw volume dependence

In the approach developed in this study, an implicit assumption is that the observed changes in Raw or Iaw are entirely due to the progression of the foreign gas along the airways. This implies that airway geometry does not change during the 600 ml inspiratory maneuver. That this was not actually the case is demonstrated by the substantial Raw variations observed during the inhalation of air in all but one subject. These variations ranged from −15% to +38%. So, they are not always explained by the well-documented decrease of Raw with increasing lung volume [about 15% over the volume range considered (1, 17)]. An increasing Raw during inspiration could be due to a progressive closure of the glottis, a phenomenon which may have been elicited by the low-flow maneuver required from the subjects (17, 24). In three of them the variations were fairly reproducible so that a correction could be applied to the final-to-initial Raw ratios. It was achieved by relating the ratio obtained with the foreign gas to that seen with air. This provides the ratio of the gas and air values at the end of the maneuver, so the results in Fig. 3.4b pertain to the state of the airways at that time. For the distribution profiles there is no solution to the problem. Indeed, no accurate correction can be applied without knowing whether the change seen in air over any given volume increment takes place in a part of the airways proximal or distal to the foreign gas front, and how this change may be affected by the gas density and viscosity. Fortunately, since Raw varied almost linearly during inspiration of compressed air, these variations had a nearly negligible effect on the distribution profiles.

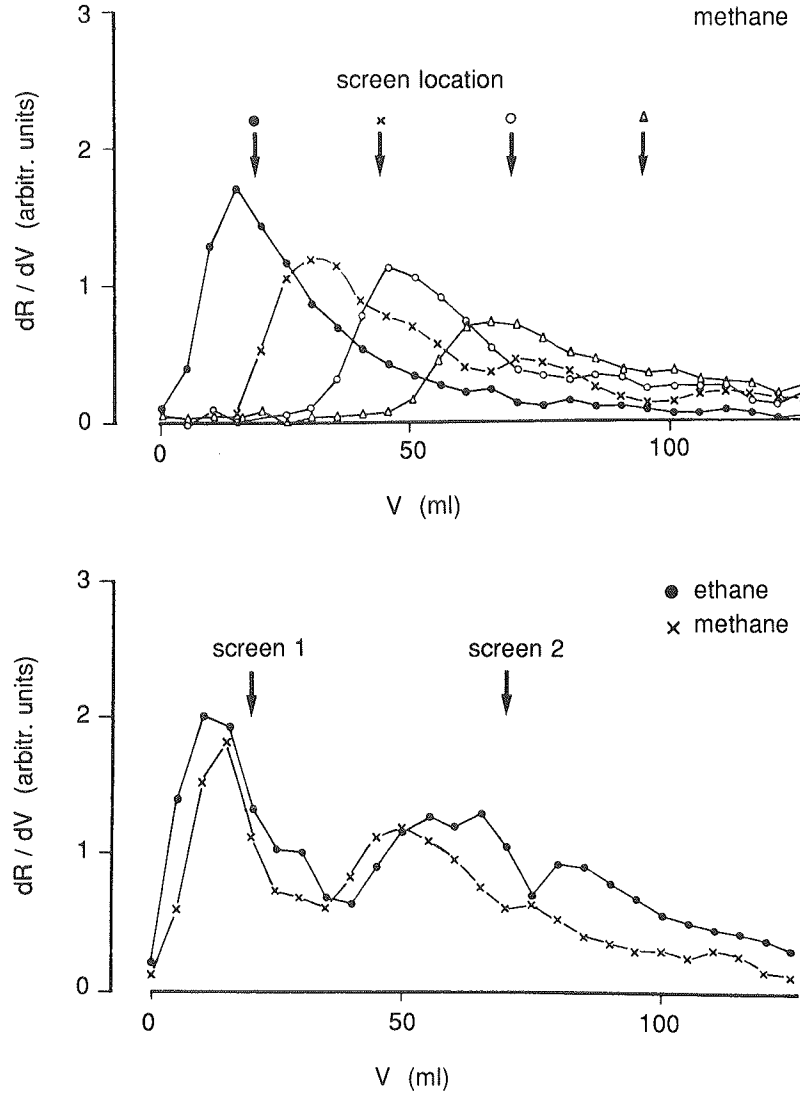

Figure 3.7. *Resistance distribution profiles obtained with mechanical analog made of a tube with a wire-mesh screen placed at various locations (top) and with two screens placed 50 ml apart (bottom). Locations of screens are indicated by arrows.*

Influence of gas diffusion and velocity profiles

The interpretation of the derivatives of the Raw- and Iaw-volume curves in terms of distribution of these properties along the airways is based upon the assumption that the front of foreign gas is blunt, i.e. progresses like a piston in a cylinder. This, in turn, implies that diffusion is negligible and that the gas velocity profile itself is blunt. This is most unlikely, particularly at the low inspiratory flows considered in this study. A complicating feature is the superimposed forced oscillation (volume amplitude of about 2 ml) which would favor gas mixing (3) and modify the velocity profiles (8). We have not attempted a rigorous theoretical analysis of the physics of gas diffusion and convection within the airways in our experimental conditions. Such an analysis requires a number of simplifying assumptions and is probably not justified in view of the qualitative nature of our findings. Rather, the overall influence of these factors on our estimates of Raw and Iaw distribution profiles was investigated by performing the same measurements on a simple analog. The latter was made of a tube (cross-sectional area 5 cm^2, length 24 cm) with one or several wire-mesh screen(s) having a resistance of 0.1 $kPa.l^{-1}.s$ placed at various locations along the tube. One extremity of the tube was connected to the usual injection and bag-in-box system, and the other to a small drum covered with a rubber membrane exposed to the pressure input. That same end was also connected to a high impedance vacuum line by which a constant gas flow could be drawn through the tube. The system closely mimicked the experimental situation, with the membrane representing lung and chest wall tissues. The resistance and inertance of the analog were computed as usual from Eq. 2, entering the resistance (0.01 $kPa.l^{-1}.s$), inertance (0.27 $Pa.l^{-1}.s^2$) and compliance (42 $ml.kPa^{-1}$) of the membrane, as well as the compressibility of the gas in the drum (1.5 $ml.kPa^{-1}$). The data are illustrated in Fig. 3.7 which shows the distribution profiles obtained with methane for a single screen placed at different locations, and with both methane and ethane for two screens placed 10 cm (i.e. 50 ml) apart. In both cases the flow of foreign gas through the tube was 0.05 l/s. In what follows, the position of the screen with respect to the injection point is expressed in terms of volume (distance times the 5 cm^2 cross-section) and referred to as the screen distance.

From the upper panel of Fig. 3.7 it may be seen that the distribution profile corresponding to a unique discrete resistance is skewed and exhibits a substantial dispersion. The dispersion is more important when the screen is further away. As a consequence, since the area under the curve (the total resistance change) is constant, the peak value decreases as the screen distance increases. It may also be seen that the

mode is located before the screen, which indicates that a sizable amount of foreign gas has reached the screen at a time when the injected volume could not have filled all of the tube upstream from it. The ratio of the mode to the screen distance was almost constant (0.65–0.75). These features are consistent with the expected effect of diffusion and/or departure from a flat velocity profile. If, for instance, the flow pattern was laminar, gas velocity in the center of the tube would be twice the mean velocity; the corresponding distribution profile would be asymmetrical and the mode/screen distance ratio would be 0.50. Axial diffusion would further diminish that ratio and increase the spread. Its effects, as well as the distance between molecules having different velocities, increases with time, which explains the larger dispersion when the screen is further downstream. Assessing the relative influence of gas diffusion and velocity profiles is difficult since controllable parameters tend in general to modify both factors. For instance, increasing the flow of foreign gas through the system should decrease the diffusion and flatten the velocity profile, both of which should decrease the spread of the gas molecules. Indeed, repetition of the measurements illustrated in Fig. 3.7 (top) with a flow of 0.1 l/s substantially decreased the dispersion and increased the mode/screen distance ratio (0.78–0.89). A few measurements were also performed with two amplitudes of the input pressure swings corresponding to volume oscillations of about 1.6 and 4.8 ml; we did not observe any consistent change in the mode/screen distance ratio, which suggests that the role of increased dispersion by oscillatory mixing was not important.

Comparing gas mixtures with different densities but similar kinematic viscosities provides theoretically a way to investigate separately the effects of diffusion since the velocity profiles should be unchanged. However, it is not easily achieved with available foreign gases. All those used in this study differed both by their density and kinematic viscosity. The data shown in the bottom of Fig. 3.7 illustrate the difference between ethane and methane. The area under the curve is smaller for methane because the change in viscosity is 18% less than for ethane. V50 is slightly smaller with methane (47.6 vs 53.1 ml), which is consistent with the larger kinematic viscosity (lower Reynolds number, more parabolic velocity profile) compared to ethane. In both respects still larger differences exist between methane and helium, which certainly contributes to the differences between the profiles obtained with the two gases in subjects 1 and 6 (Fig. 3.6). Fig. 3.7 (bottom) also illustrates the fact that discrete resistances located 50 ml apart are well separated. Such is still the case when they are 25 ml apart, but this is about the limit to see a bimodal distribution. Finally, comparing the methane curve in Fig. 3.7 (bottom) to the 1st and 3rd curves in the top of Fig. 3.7, it may be seen that the distribution profile obtained with two screens

resembles very much the sum of the profiles of the corresponding single screens. In other words, there does not seem to be much interference between serially located resistances, at least when they are 50 ml apart. From this study of simple analogues, we conclude that diffusion and/or axial differences in gas velocities may substantially distort distribution profiles. However, comparing the volume scales in Fig. 3.6 and Fig. 3.7, it appears that these factors should not completely obscure the actual resistance or inertance distribution along the airways. This conclusion is also supported by the great similarity of the inertance distribution profiles obtained with three gases (Fig. 3.5), the densities of which differed by a factor 5 and the kinematic viscosities by a factor 7.

The main observations in this study were that the distribution of inertance was more proximal than that of resistance, that the resistance distribution profiles varied according to the tracer gas, and that the density and viscosity dependence of Raw as well as their distribution profiles varied systematically among subjects. The remainder of the discussion will focus on these three points.

Gas inertance in a tube depends little upon the flow regime (19) and the glottic orifice is not expected to contribute to the inertance. The serial distribution of Iaw may, therefore, be predicted from airway geometry with a good approximation. Using the area-distance functions obtained by acoustic reflection (11), one may compute that about 50% of Iaw should be located in the upper airway, from the mouth to the larynx, and a third in the trachea. While longitudinal distribution of lower airway resistance has been predicted by Pedley et al. (18) for various inspiratory flows, distribution of total Raw is largely unpredictable because the contribution of the glottis may vary considerably between subjects and according to the respiratory maneuver (6, 24). To our knowledge, the relative importance of upper and lower Raw has not been measured in humans during inspiratory maneuvers at the very low flows used in this study. According to Ferris et al. (6) the upper airway would account for 28% of Raw during the inspiratory phases of quiet breathing while the data of Finucane and Mead (7) suggest it may be much larger during voluntary breathholding. The results observed in this study (Table 3.2) indicate that the distribution of Raw is more peripheral than that of Iaw. Indeed, the change in Raw with methane is only 36% and 10% in subjects 1 and 6 respectively (Fig. 3.6, bottom) when the change in Iaw is already 50%. This suggests that the contribution of the upper airway to Raw in our measuring conditions is closer to that seen during quiet breathing than during breathholding.

As already mentioned, methane has almost the same kinematic viscosity as air and should decrease viscosity-dependent and density-dependent resistances similarly. Also, it should not influence the flow regime and the distribution of resistance. On the contrary, helium would markedly and almost exclusively modify density-dependent resistances. Our findings of a more centrally distribution of Raw with helium than with methane does not mean that the resistance is more centrally located when the airways are completely filled with air; it only means than the change in resistance induced by helium is confined to more central airways than that induced by methane. It is in agreement with experimental evidence suggesting that, even at low flows, resistance is predominantly density-dependent in the upper airways (13), in the trachea (2) and in the upper part of the bronchial tree (4, 25), while peripheral airway resistance depends little upon density (4). Another effect of helium, which has a much higher kinematic viscosity than air or methane is to decrease Reynolds numbers and, hence, promote a more laminar flow regime. This should move the transition between predominantly viscosity-dependent and density-dependent resistances towards larger airways, and shift further mouthward the helium distribution profiles.

Perhaps the most interesting finding in this study was the observation of important and consistent differences in the density and viscosity dependences of Raw in two subjects, as well as their Raw distribution profiles (Fig. 3.4 and 3.6): the more central distribution of Raw in subject 1 was associated with a predominant density dependence, which, again, is in agreement with the notion that the influence of density is mainly in the central airways. The subjects also differed by the absolute values of their Raw and Iaw in air, subject 1 having both a lower Raw (0.06 $kPa.l^{-1}.s$) and Iaw (1.4 $Pa.l^{-1}.s^2$) than subject 6 (0.11 $kPa.l^{-1}.s$ and 2.1 $Pa.l^{-1}.s^2$, respectively). A potentially important source of interindividual differences is the contribution of the glottis to Raw. A smaller glottic aperture is, however, an unlikely explanation for the larger density dependence in subject 1 in view of his low Raw. Also, as the two subjects had about the same sitting height, there is no reason to suspect that they have large differences in airway lengths. Our tentative explanation is, therefore, that subject 6 had narrower peripheral airways and, to a lesser extent, narrower central airways than subject 1. The narrower peripheral airways would account for a part of the 83% larger Raw, its predominant viscosity dependence and more peripheral distribution profile. The narrower central airways would be responsible for some of the larger Raw and for the 50% larger Iaw. These differences in airway dimensions could in part be related to the fact that subject 1 had a large TGV while subject 6, who was slightly overweight, had a small one.

In the presentation of our approach and in the above discussion, we have postulated that early changes in Raw and Iaw correspond to proximal airways and late changes to peripheral airways. This interpretation in terms of serial distribution of airway properties will lose its meaning in the presence of parallel inhomogeneity. Then, late changes would represent the contribution of poorly ventilated lung regions. As Reynolds numbers would be low in such regions, one may expect the corresponding resistance to be viscosity-dependent. This mechanism may offer an alternative explanation for the findings in subject 6. Inasmuch as gas distribution is flow-dependent, making measurements at different inspiratory flows would provide a way to distinguish between the contribution of peripheral airways and that of slower regions.

The above results indicate that respiratory impedance measurements during inhalation of foreign gases may provide information of physiological and diagnostic value. Indeed, it would be of interest to study the serial (or parallel) distribution of airway properties in disease, and how it is modified by bronchomotor drugs and therapeutic agents. The method used in this study, however, does not lend itself to routine applications. It requires some training and a high degree of cooperation from the subject. Moreover, the resistance data are often too noisy for the purpose. We believe that these difficulties are due in part to the fact that we asked the subjects to voluntarily achieve and sustain a low inspiratory flow. Hopefully, a more natural respiratory pattern or the use of external device to control the flow would both facilitate the measurements in untrained subjects and reduce the variability.

References

1. BRISCOE, W.A., AND A.B. DUBOIS. The relationship between airway resistance, airway conductance and lung volume in subjects of different age and body size. J. Clin. Invest. 37: 1279–1285, 1958.
2. DEKKER, E. Transition between laminar and turbulent flow in human trachea. J. Appl. Physiol. 16: 1060–1064, 1961.
3. DRAZEN, J.M., R.D. KAMM, AND A.S. SLUTSKY. High-frequency ventilation. Physiological Reviews 64: 505–543, 1984.
4. DRAZEN, J.M., S.H. LORING, AND R.H. INGRAM, JR. Distribution of pulmonary resistance: effects of gas density, viscosity, and flow rate. J. Appl. Physiol. 41: 388–395, 1976.
5. DUBOIS, A.B., A.W. BRODY, D.H. LEWIS, AND B.F. BURGESS, JR. Oscillation

mechanics of lungs and chest in man. J. Appl. Physiol. 8: 587–594, 1956.
6. FERRIS, JR., B.G., J. MEAD, AND L.H. OPIE. Partitioning of respiratory flow resistance in man. J. Appl. Physiol. 19: 653–658, 1964.
7. FINUCANE, K.E., AND J. MEAD. Estimation of alveolar pressure during forced oscillation of the respiratory system. J. Appl. Physiol. 38: 531–537, 1975.
8. FRANKEN H., J. CLÉMENT, M. CAUBERGHS, AND K.P. VAN DE WOESTIJNE. Oscillating flow of a viscous compressible fluid through a rigid tube: a theoretical model. IEEE Trans. Biomed. Eng. 28: 416–420, 1981.
9. HEYDER, J. Charting human thoracic airways by aerosols. Clin. Phys. Physiol. Meas. 4: 29–37, 1983.
10. HEYDER, J., J. GEBHART, AND G. SCHEUCH. Influence of human lung morphology on particle deposition. J. Aerosol Med. 1: 81–88, 1988.
11. HOFFSTEIN, V., AND J.J. FREDBERG. The acoustic technique for non-invasive assessment of upper airway area. Eur. Respir. J. under press.
12. JACKSON, A.C., J.P. BUTLER, E.J. MILLET, F.G. HOPPIN, JR., AND S.V. DAWSON. Airway geometry by analysis of acoustic pulse response measurements. J. Appl. Physiol.: Respirat. Environ. Exercise Physiol. 43: 523–536, 1977.
13. JAEGER, M.J., AND H. MATTHYS. The pattern of flow in the upper human airways. Respir. Physiol. 6: 113–127, 1968/1969.
14. JAFFRIN, M.Y., AND P. KESIC. Airway resistance: a fluid mechanical approach. J. Appl. Physiol. 36: 354–361, 1974.
15. MEAD, J. Analysis of the configuration of maximum expiratory flow-volume curves. J. Appl. Physiol.: Respirat. Environ. Exercise Physiol. 44: 156–165, 1978.
16. OLSON, D.E., G.A. DART, AND G.F. FILLEY. Pressure drop and fluid flow regime of air inspired into the human lung. J. Appl. Physiol. 28: 482–494, 1970.
17. OOSTVEEN, E., R. PESLIN, C. GALLINA, AND A. ZWART. Flow and volume dependence of respiratory mechanical properties studied by forced oscillation. J. Appl. Physiol. 67: 2212–2218, 1989.
18. PEDLEY, T.J., R.C. SCHROTER, AND M.F. SUDLOW. The prediction of pressure drop and variation of resistance within the human bronchial airways. Respir. Physiol. 9: 387–405, 1970.
19. PESLIN, R., AND J.J. FREDBERG. Oscillation mechanics of the respiratory system. In: *Handbook of Physiology. The Respiratory System. Mechanics of Breathing.* Bethesda, MD: Am. Physiol. Soc., 1986, sect. 3, vol. III, pt. 1, chapt. 11, p. 145–177.
20. PESLIN, R., C. GALLINA, AND M. ROTGER. Methodological factors in the variability of lung volume and specific airway resistance measured by body

plethysmography. Bull. Eur. Physiopathol. Respir. 23: 323–327, 1987.

21. PESLIN, R., B. HANNHART, AND C. DUVIVIER. Airway impedance studied during airway washing with foreign gases. Bull. Eur. Physiopathol. Respir. 14: 70p–72p, 1978.
22. PESLIN, R., J. PAPON, C. DUVIVIER, AND J. RICHALET. Frequency response of the chest: modeling and parameter estimation. J. Appl. Physiol. 39: 523–534, 1975.
23. SIDELL, R.S., AND J.J. FREDBERG. Noninvasive inference of airway network geometry from broadband lung reflection data. ASME J. Biomed. Eng. 100: 131–138, 1978.
24. STĂNESCU, D.C., J. PATTIJN, J. CLÉMENT, AND K.P. VAN DE WOESTIJNE. Glottis opening and airway resistance. J. Appl. Physiol. 32: 460–466, 1972.
25. WEST, J.B., AND P. HUGH-JONES. Patterns of gas flow in the upper bronchial tree. J. Appl. Physiol. 14: 753–759, 1959.

Chapter 4

Respiratory Transfer Impedance and Derived Mechanical Properties of Conscious Rats

E. Oostveen, A. Zwart, R. Peslin, and C. Duvivier

Abstract

A setup is described for measuring the respiratory transfer impedance of conscious rats in the frequency range 16 to 208 Hz. The rats were placed in a restraining tube wherein head and body were separated by means of a dough neck collar. The restraining tube was placed in a body chamber allowing the application of pseudo-random noise pressure variations to the chest and abdomen. The flow at the airway opening was measured in a small chamber connected to the body chamber. The short-term reproducibility of the transfer impedance was tested by repeated measurements in nine normal Wistar rats. The mean coefficient of variation for the impedance did not exceed 10%. The impedance data were analyzed using a modification of DuBois' model. This model consists of a tissue compartment (resistance Rti, inertance Iti, and compliance Cti), an airway compartment (resistance Raw and inertance Iaw) and an alveolar gas compartment (compressibility Cg). The airway compartment was extended with a nose resistance (Rn), shunted by the upper airways (Iuaw and Cuaw). By using an approximate value for Cg, the other coefficients of the model could then be obtained by parameter estimation. This resulted in a total respiratory resistance (Rrs= Rn+Raw+Rti) of 13.6 ± 1.0 (SD) $kPa.l^{-1}.s$, a total respiratory inertance (Irs= Iaw+Iti) of 14.5 ± 1.3 $Pa.l^{-1}.s^2$, and a tissue compliance (Cti) of 2.5 ± 0.5 $ml.kPa^{-1}$. The intraindividual coefficient of variation for Rrs and Irs was 11% and 18%, respectively. Rrs, Irs, and Cti were independent of the value used for Cg. With Cg fixed at 0.05 $ml.kPa^{-1}$, the total airway resistance and inertance accounted for 85% and 81% of Rrs and Irs, respectively. Our values for Rrs and Irs of conscious rats were much lower and our values for Cti were larger than previously reported values for anesthetized rats.

Introduction

The rat is one of the small laboratory animals commonly used in toxicological and physiological studies. Numerous techniques developed for determination of lung function in man have been adapted for use in small animals. Although the original methods are essentially noninvasive most of the techniques for measuring respiratory mechanics in noncooperative animals require some form of invasion, i.e. tracheotomy or intubation and measurement of esophageal or pleural pressure (3, 5, 11, 15, 22). Besides the apparent disadvantage that some techniques exclude interesting parts of the respiratory system such as the upper respiratory tract in intubated or tracheotomized animals, invasive techniques usually necessitate anesthetized subjects. Anesthesia, however, may seriously affect the respiratory mechanical properties. Anesthesia was reported to strongly decrease end expiratory lung volume, tidal volume, and breathing frequency in mice (26) and has been found to induce major changes in pulmonary resistance and compliance in hamsters (25). Moreover, the effects of anesthesia on pulmonary mechanics are probably time- and dose-dependent (25). Another disadvantage of invasive techniques is that they do not always allow for repeated measurements in the same animal, thus requiring large numbers of animals to study the time course of changes induced by inhaled irritant or toxic gases and drugs.

We developed a noninvasive technique to measure the respiratory impedance of spontaneously breathing conscious rats based on the forced oscillation technique. This technique, which does not require any form of cooperation, was chosen because it enables a fast measurement of the respiratory impedance over a broad frequency range. The oscillation technique was first described by DuBois et al. (6) to measure respiratory impedance in man. It consists of applying sinusoidal pressure variations across the respiratory system at a frequency higher than the normal breathing frequency and measurement of the flow response. Mead (18) described a setup for measurement of transfer impedance (Ztr) in unanesthetized guinea pigs, where pressure variations were applied around the thorax and flow was measured at the airway opening with the use of a face mask. Because face masks are not accepted by conscious rats we modified his setup by using a two compartment whole body box. In this paper a description of the method is presented together with the short-term intraindividual variability in normal rats. The impedance data were interpreted using a T-network electrical model.

Material and Methods

Respiratory transfer impedance in the frequency range 16 to 208 Hz was measured with the setup schematized in Fig. 4.1. The rats were placed in a restraining tube (a modified Battelle tube) which enabled an airtight seal around the neck. For this purpose two latex membranes with a central opening were glued in the tube at the expected position of the neck. A dough was put between these two sleeves to obtain a neck seal without the need of compressing the rat in the tube. After the restraining tube had been placed in the body chamber (5 liters), the rat respired from the small front chamber (100 ml) which was flushed with an air flow of 25 $ml.s^{-1}$ to prevent CO_2 buildup. This constant bias flow, obtained with a critical orifice, was led over a wire screen (resistance 5.5 $kPa.l^{-1}.s$, linear within 2% up to 60 $ml.s^{-1}$).

With a 25–W loudspeaker, mounted in the body chamber, pressure variations were applied to the rat's body. Holes in the top of the restraining tube allowed for homogeneity of the pressure around the chest and abdomen. The pressure variations in body and front chamber (Pbs and Pao, respectively) were measured with identical pressure transducers [Validyne MP15-20 (± 0.8 kPa)]. Both transducers matched

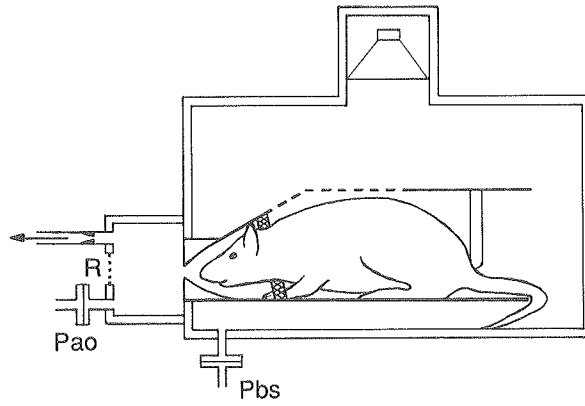

Figure 4.1. Experimental setup. The conscious rat, placed in the Battelle tube in the body box, respires from the front chamber. To prevent rebreathing the front chamber is flushed with a bias flow. R, wire-mesh screen; Pbs and Pao, pressures in the body box and the front chamber, respectively.

within 1% of amplitude and 1° of phase up to 208 Hz. With the front chamber sealed from the body chamber, Pao was less than 0.1% of the applied pressure amplitude. Hence, the effects of vibrations or sound transmission to the reference side of the Pao-transducer were negligible during the measurements. The homogeneity of the applied pressure in the body chamber was tested by measuring the differences between the pressures at several locations in the body chamber, and the pressure at a fixed position. The differences in amplitude did not exceed 5% throughout the frequency range (16–208 Hz).

The pressure in the front chamber is related to the flow at the airway opening ($\dot{V}ao$) by the impedance of the front chamber (Ze):

$$Pao = Ze . \dot{V}ao \quad (1)$$

Respiratory transfer impedance, Ztr, is defined as the pressure difference across the respiratory system divided by the flow at the airway opening:

$$Ztr = (Pbs - Pao)/\dot{V}ao = ((Pbs/Pao) - 1) . Ze \quad (2)$$

Calibration of the setup

The impedance of the front chamber, Ze, was determined using a variant of the calibration technique described by Hantos et al. (10). A calibration impedance consisting of a cylindrical tube (length 5.5 cm, ID 0.40 cm) with a screen added to one of its ends (resistance 4.4 $kPa.l^{-1}.s$) was placed between the body chamber and the front chamber. The impedance of this tube was calculated using the large tube approximation of Keefe (14). With the front chamber in the same condition as during a transfer impedance measurement the Pbs/Pao relationship was determined in the frequency range 16 to 208 Hz. From this pressure ratio the impedance Ze of the front chamber was calculated using Eq. 2. The complex impedance Ze is illustrated in Fig. 4.2. The real part of Ze decreases with frequency as a result of the compressibility of the gas in the front chamber (shunt effect).

Measurements

The excitation pressure was a variant of the pseudo-random noise pressure input (PRN) as introduced by Lándsér et al. (16). Our PRN signal consisted of all harmonics of 16 Hz from 16 to 208 Hz with a colored amplitude spectrum and optimized random phases (4). The amplitude spectrum favored the lowest six frequencies that had a relative amplitude of 1/i for the i-th harmonic of 16 Hz; the higher frequencies had a relative amplitude of 1/7. The PRN signal was generated by a

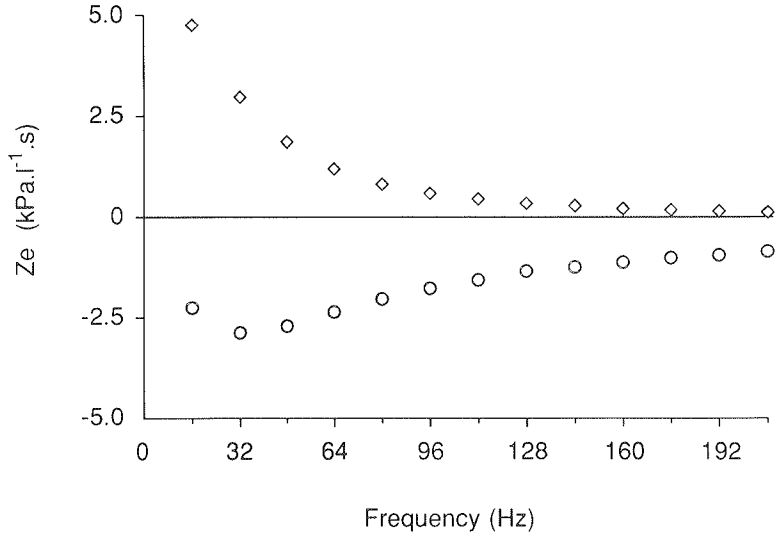

Figure 4.2. *Real (◇) and imaginary (○) part of the impedance of the front chamber (Ze).*

microcomputer (Victor V286C) with a frequency of 1024 Hz of the D/A converter. After amplification and low-pass filtering (4th order; cutoff frequency 250 Hz) this signal activated the loudspeaker. The peak-to-peak excitation pressure was limited to 0.2 kPa. The pressure signals were sampled for 4 s and digitized at a frequency of 1024 Hz by the same microcomputer. After digital high-pass filtering (Butterworth, 4 poles, cutoff frequency 10 Hz), the data were processed according to Michaelson et al. (19). Fourier transform was performed on 15 blocks of 512 data points (with 50% overlapping) using a Hanning time window. The data were corrected for the time delay between the two A/D channels (56 μs). The result at a particular frequency was discarded when the coherence value was below 0.88. The transfer impedance of a rat was the average of the results obtained for three to five measuring periods. During the periods of 4 s for data acquisition the bias flow through the front chamber was interrupted to remain within the linear range of the screen. Due to the short measuring time this results in a negligible change in air composition of the front chamber.

Nine conventional male Wistar rats, weighing 214 – 257 g (mean 239 ± 9 g) were measured using the method described above. The rats were naive, i.e. they had not been handled before the day of the first impedance measurement when they were

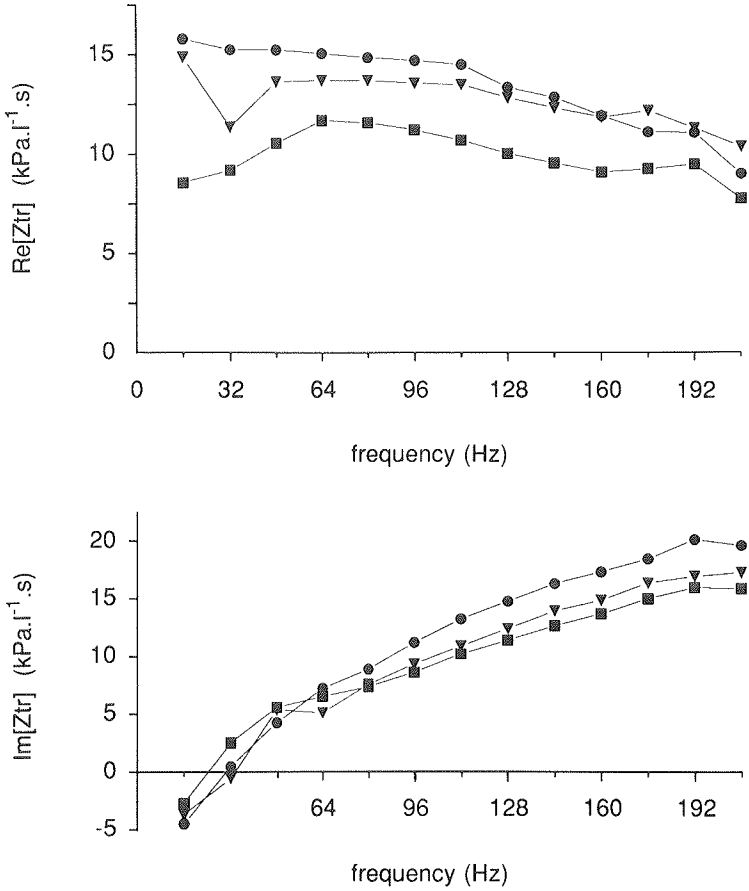

Figure 4.4. *Three examples of the real (Re, top) and imaginary (Im, bottom) part of the respiratory transfer impedance (see text).*

between 16 and 64 Hz (15 curves) were also measured in seven rats.

There were no significant differences in Re[Ztr] or Im[Ztr] between the first and last transfer impedance data measured in each rat (any frequency). This indicated that there was no measurable short-term training effect. The coefficient of variation (CV) of the modulus of the transfer impedance ($|Ztr| = (Re[Ztr]^2 + Im[Ztr]^2)^{½}$) at each frequency was calculated from the four results obtained in each rat. The impedance data for normal rats were highly reproducible: mean CV never exceeded 10%

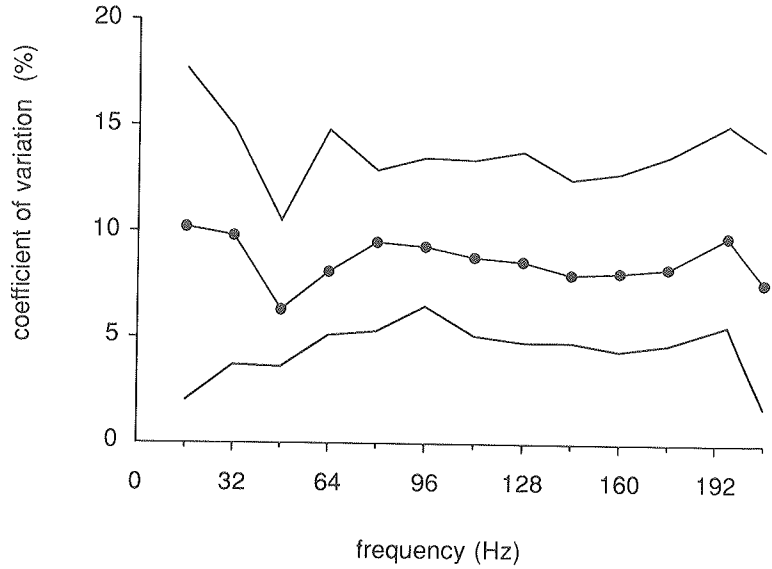

Figure 4.5. *Mean (●), minimum and maximum (——) values of the coefficient of variation of the modulus of Ztr of nine normal rats.*

(Fig. 4.5). Even at the lowest frequency the highest individual value for CV did not exceed 18%.

The optimization process for the modified DuBois' model provided two sets of coefficients with exactly the same residual sum. One solution showed a high resistance and inertance of the airway compartment and a low tissue resistance and inertance; the other solution showed high Rti and Iti values accompanied with low values for Raw and Iaw. Because only one solution corresponded with an acceptable value for Iaw (see Discussion) we only present the coefficients corresponding to the solution with the highest value of Iaw (Table 4.1). In four curves a plateau of Re[Ztr] at low frequencies was found, in contrast to the general local minimum. In these cases the shunt effect of the upper airways was negligible and, as a consequence, the nose resistance could not be separated from Raw in the model analysis. Therefore, the total airway resistance (Raw+Rn) is presented in Table 4.1. On average the nose resistance accounted for 32% (± 14%) of the total airway resistance. The estimated upper airway shunt was highly variable: the upper airway compliance (Cuaw) ranged

Table 4.1. Optimized coefficients of the modified DuBois' model.

Rat	Raw+Rn $kPa.l^{-1}.s$	Rti $kPa.l^{-1}.s$	Rrs (Raw+Rn+Rti) $kPa.l^{-1}.s$	Iaw $Pa.l^{-1}.s^2$	Iti $Pa.l^{-1}.s^2$	Irs (Iaw+Iti) $Pa.l^{-1}.s^2$	Cti * $ml.kPa^{-1}$	$\sqrt{\chi^2}$ $kPa.l^{-1}.s$
R20	12.7 ± 1.6	2.4 ± 1.7	15.1 ± 1.8	13.3 ± 2.1	3.5 ± 0.7	16.8 ± 2.7	1.5 – 2.4 [4]	0.38 ± 0.08
R21	12.8 ± 1.0	2.1 ± 1.3	14.9 ± 1.7	11.2 ± 1.5	2.6 ± 0.5	13.8 ± 1.7	1.6 – 3.5 [3]	0.44 ± 0.06
R22	12.0 ± 1.6	1.5 ± 1.3	13.5 ± 1.3	12.1 ± 2.7	1.9 ± 1.4	14.0 ± 3.9	1.8 – 4.5 [3]	0.55 ± 0.11
R23	12.6 ± 1.6	1.1 ± 1.3	13.8 ± 1.3	10.5 ± 1.3	2.7 ± 0.4	13.2 ± 1.7	1.8 – 1.9 [2]	0.49 ± 0.22
R24	11.7 ± 0.4	1.6 ± 1.9	13.2 ± 2.2	11.8 ± 1.8	2.4 ± 0.3	14.1 ± 1.9	2.3 – 4.2 [2]	0.68 ± 0.55
R25	9.5 ± 1.7	3.1 ± 1.6	12.6 ± 1.1	11.2 ± 2.8	2.6 ± 0.7	13.8 ± 3.4	1.5 – 2.9 [4]	0.44 ± 0.08
R26	10.4 ± 1.8	2.7 ± 1.6	13.1 ± 1.1	11.9 ± 1.8	2.5 ± 1.0	14.3 ± 2.9	2.4 – 3.4 [2]	0.48 ± 0.14
R27	10.8 ± 1.3	1.2 ± 1.0	12.0 ± 0.8	11.2 ± 2.1	2.7 ± 0.8	13.8 ± 2.8	1.7 – 3.0 [4]	0.44 ± 0.09
R28	12.0 ± 1.4	2.1 ± 3.2	14.0 ± 2.3	13.4 ± 3.1	3.1 ± 0.3	16.5 ± 2.9	1.7 – 3.0 [2]	0.84 ± 0.81
mean (n=9)	11.6 ± 1.1	2.0 ± 0.7	13.6 ± 1.0	11.8 ± 1.0	2.7 ± 0.4	14.5 ± 1.3	2.5 ± 0.5	0.53 ± 0.15

Mean values ± SD for repeated measurements in each rat. Raw, Iaw, airway resistance and inertance, respectively; Rn, nose resistance; Rti, Iti, Cti, tissue resistance, inertance, and compliance, respectively; $\sqrt{\chi^2}$, minimum residual distance between model and data (see text).

**: Range of Cti values for the data showing a resonant frequency (in brackets the actual number of curves).*

from 0.3 to 7.4 ml.kPa^{-1} and Iuaw ranged from 10 up to 94 Pa.l^{-1}.s^2. The resonance frequency of the upper airway shunt ($f_0 = 1/(2\pi(\text{Iuaw.Cuaw})^{½})$) was 31 ± 8 Hz. The total airway resistance (Raw+Rn) accounted for 85% of the total respiratory resistance (Rrs= Raw+Rn+Rti; Table 4.1). Airway inertance was 81% of the total respiratory inertance (Irs= Iaw+It). The mean individual CV for the total airway resistance was 11.9%, slightly higher than the value for Rrs (10.9%). Since Rrs should roughly account for the intraindividual variation in Re[Ztr], higher variation coefficients for the estimated partial resistances are to be expected. The larger CV for Raw+Rn and Rti further reflects the ability of the model to separate the tissue compartment from the airway compartment and the correctness of the value substituted for Cg (see Discussion). The individual variation in estimated inertance showed the same pattern: CV for the total respiratory inertance (Iaw+Iti) was 18.3%, compared to 17.9% and 27.4% for Iaw and Iti, respectively. The tissue compliance was 2.5 ± 0.5 ml.kPa^{-1}. This parameter only converged when the impedance data included data below the resonant frequency (Im[Ztr] below zero).

We investigated the effects of compression of the rat in the restraining tube on the obtained transfer impedance (Fig. 4.6). Five rats (231 ± 11 g) were measured successively in the normal measuring situation and when compressed at the back. Compression was such that there remained no space between the back of the rat and the tube. The measured leak resistance did not differ between the two conditions. Re[Ztr] was higher from 16 to 144 Hz (significantly at 96 and 112 Hz; $p < 0.05$) and all animals showed a steeper decrease at high frequency in the compressed situation compared to the normal condition. No differences were observed in the imaginary part at low frequencies, but Im[Ztr] was higher in compressed animals in the frequency range from 64 to 208 Hz ($p < 0.01$). Analyzing the data with the modified DuBois' model showed that in compressed rats Rrs had increased by 35% ($p < 0.01$; paired t-test) and Irs by 46% ($p < 0.05$) compared to the normal measuring situation. Assuming Cg was the same in both conditions, Rti and Raw+Rn were significantly increased (118% and 18%, respectively; $p < 0.05$) when the rats were compressed, and Iti increased by 80% ($p < 0.01$). Of course, one may wonder whether the alveolar gas volume remains unchanged when the rat is compressed. Reduction of Cg by 30% for the compressed state gave, however, similar systematic increases in Rti and Iti. Compression of the animal seems therefore to result in a large increase in resistance and inertance mainly located in the tissues. Another possible explanation for the increased impedance for the compressed state is that in this situation the excitation pressure is very inhomogeneously applied to the chest and abdomen of the rat, which results in an apparently increased respiratory impedance.

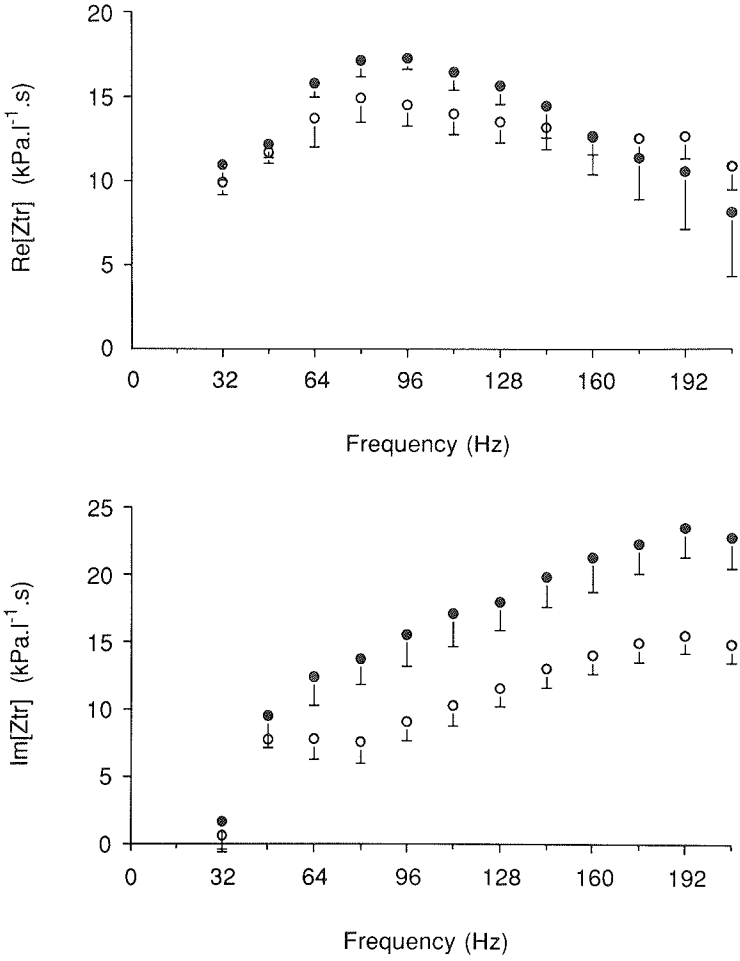

Figure 4.6. *Real (Re, top) and imaginary (Im, bottom) part of the transfer impedance of five rats measured in the normal condition (○) and compressed at the back (●). Means and SD of the group are shown.*

Discussion

Before discussing the results in detail it is appropriate to discuss the possible sources of errors associated with our measurement technique, especially the flow measurement. As can be seen from Eq. 2, calibration of the impedance of the front chamber Ze is of crucial importance to obtain the correct transfer impedance. The calibration method did not necessitate any assumptions on the nature of Ze. Moreover, Ze represents the impedance of the front chamber together with that of the pressure transducer connected to it. In this way systematic errors associated with a low impedance of the pressure transducer, as described in previous reports (8, 10), are avoided. Since impedance Ze is complex, i.e. containing real and imaginary components, we chose a complex impedance as a reference. To obtain a good estimate of Ze, the impedance of the calibration device was in the same range of magnitude as Ze. We verified the Ze values obtained by measuring the transfer impedance of a second calibration device with an impedance comparable to the rat (tube length 10.3 cm, ID 0.49 cm, added screen resistance 16.0 $kPa.l^{-1}.s$). The measured impedance modulus of this second device was within 4% of the expected value over the entire frequency range. The close agreement between the measured and the theoretical transfer impedance of this second device indicates that the transfer impedance of rats can be measured with sufficient accuracy.

The volume of the front chamber is relatively large (100 ml). As a result of the compressibility of the gas in this chamber the impedance Ze decreases with increasing frequency. Although this large volume is unfavorable for measuring high frequencies it was chosen because the Battelle tube containing the rat adds a small volume to the volume of the front chamber (the air surrounding the head of the rat). This variable volume is normally less than 10 ml. We added a volume of 5 ml to the front chamber during the calibration measurements to compensate for this otherwise systematic error. The error on Ztr due to the variability of the volume of the front chamber will thus be 5 ml at the most, i.e. less than 5%.

In our setup every leak along the animal to the front chamber will inevitably lead to an underestimation of Ztr. A leak along the neck of the animal must be considered as a parallel impedance with respect to Ztr. We know of no method to measure the exact values of this impedance. However, we can estimate the resistance of this compartment by causing a step change in pressure of the body box (by injecting a small volume of air) and measuring the time constant by which it returns to atmospheric pressure. This time constant is the RC-product of the compressibility of the gas in the body chamber ($C \approx 0.05$ $l.kPa^{-1}$) and the resistance associated with the

leak (the sealed body chamber had a time constant larger than 30 s). With a time constant of 10 s, i.e. a parallel resistance of 200 $kPa.l^{-1}.s$, the measured transfer impedance will be underestimated by 10% at the most. The parallel leak compartment probably also has an inertance, that further increases its impedance.

One of the most difficult problems to solve was to avoid leak without compressing the animal. Compression of the rat in the Battelle tube has dramatic effects on respiratory impedance (Fig. 4.6). Our results with the dough neck collar indicate that it is not necessary to compress the animal to obtain a good separation between body and head, and the measured impedances with the neck collar were reproducible. Further advantages of the elastic, viscous dough collar are that the rat may move a little without creating a leak, and that the dough can easily be removed from the fur.

The rat has a relatively high respiratory rate, about 2 to 3 Hz. The flow pattern is square wave-like, so at relatively high frequencies the harmonics of the spontaneous breathing frequency are found. An estimate of the amount of noise contaminating the pressure signals is given by the coherence function (γ^2). To test whether respiration interferes with the excitation pressure, the frequency contents of the thoracic spontaneous breathing signal was determined without exciting the animal. The signal was processed as described before, i.e. with a frequency resolution of 2 Hz. The amplitude of the 16 Hz component of spontaneous breathing was less than 1% of the amplitude of the corresponding frequency in the PRN signal. Hence, spontaneous breathing is not contaminating both input and output pressure with a correlated noise as is the case during input impedance measurements (9). In this study we used a rejection threshold for γ^2 of 0.88 because in our case of 15 blocks a standard error less than 10% of the modulus of Ztr is expected when γ^2 exceeds 0.88 (20). Although the lowest values for γ^2 were found at 16 Hz, the coefficient of variation of repeated measurements was not larger at this frequency than at high frequencies where γ^2 values close to one were found. This indicates that CV reflects intra-individual variations instead of measurements errors.

The transfer impedance data obtained in repeated measurements showed little variability, indicating that effects of repositioning in the Battelle tube and habituation were small. The information on repeated measurements of respiratory mechanics in small animals is scarce. Paleçek (22) measured lung resistance and dynamic compliance (Cdyn) in spontaneously breathing anesthetized rats at weekly intervals. His results of repeated measurements in the same animal showed a large variability which he ascribed to variations in the level of anesthesia and instrumental errors.

Hiett (11) measured resistance and compliance in unanesthetized guinea pigs and reported coefficients of variation of repeated measurements which are comparable to our results in rats.

Transfer impedance of normal rats show some features in common with transfer impedance obtained in healthy humans from 4 to 32 Hz. After an initial plateau the real part of Ztr of healthy humans decreases with increasing frequency. The imaginary part normally crosses zero between 5 and 9 Hz and increases curvilinearly with increasing frequency. In a first attempt to describe our data we estimated the coefficients of the DuBois' model which is normally used to interpret human transfer impedance data (24). In 24 out of 36 transfer impedance curves, estimation of the coefficients resulted in unrealistic, negative values for Rti. Moreover, the model cannot describe the low frequency behavior of Ztr as illustrated in Fig. 4.7. To describe the typical differences between human and rat impedance, i.e. the local minimum of Re[Ztr] at low frequencies and the steep change in slope of Im[Ztr] near 48 Hz, we extended the DuBois' model with a nose resistance and upper airway shunt. In contrast to human transfer impedance measurements where the subject is connected to a pneumotachograph via a mouth piece, our measurements include the nose impedance. Hence, in our experimental setup the impedance of the extrathoracic airway walls may present a shunt pathway to the impedance of the nose, whereas this shunt is considered negligible in man because it is in parallel with the low impedance of the mouth. An additional indication for such a shunt was found when measuring a rat that was breathing through its mouth as a result of exposure to an inhaled irritant. The local minimum in Re[Ztr], found before exposure, disappeared after the rat had switched to mouth breathing after exposure (29).

We compared the optimum response of the DuBois' model to the experimental data with that of our modified DuBois' model by using the F-test (7): in all cases the extended DuBois' model provided a significantly better fit than the six-coefficient model except for the four measurements where Re[Ztr] at low frequencies showed a plateau ($P < 0.05$). The high values of Re[Ztr] at 176 and 192 Hz found in almost all curves, however, are not described by the response of the extended DuBois' model and remain unexplained.

In order to obtain a better understanding of our model and to evaluate the reliability of the estimates of the respiratory coefficients (17), we calculated the relative change in the modulus of Ztr of our model response, when increasing, one by one, the value of each coefficient by 20% (21). The reference value of the impedance was calculated using the mean values of the coefficients found in this

study (Raw 8.3, Rti 2.0, and Rn 3.3 kPa.l^{-1}.s, Iaw 11.8, and Iti 2.7 Pa.l^{-1}.s^2, Cti 2.5 ml.kPa^{-1}, Iuaw 24 Pa.l^{-1}.s^2 and Cuaw 1.13 ml.kPa^{-1}, and Cg 0.05 ml.kPa^{-1}). The sensivity function shows some interesting features (Fig. 4.8, top): as the upper airway compartment of our model describes the low frequency behavior of Ztr, it may be

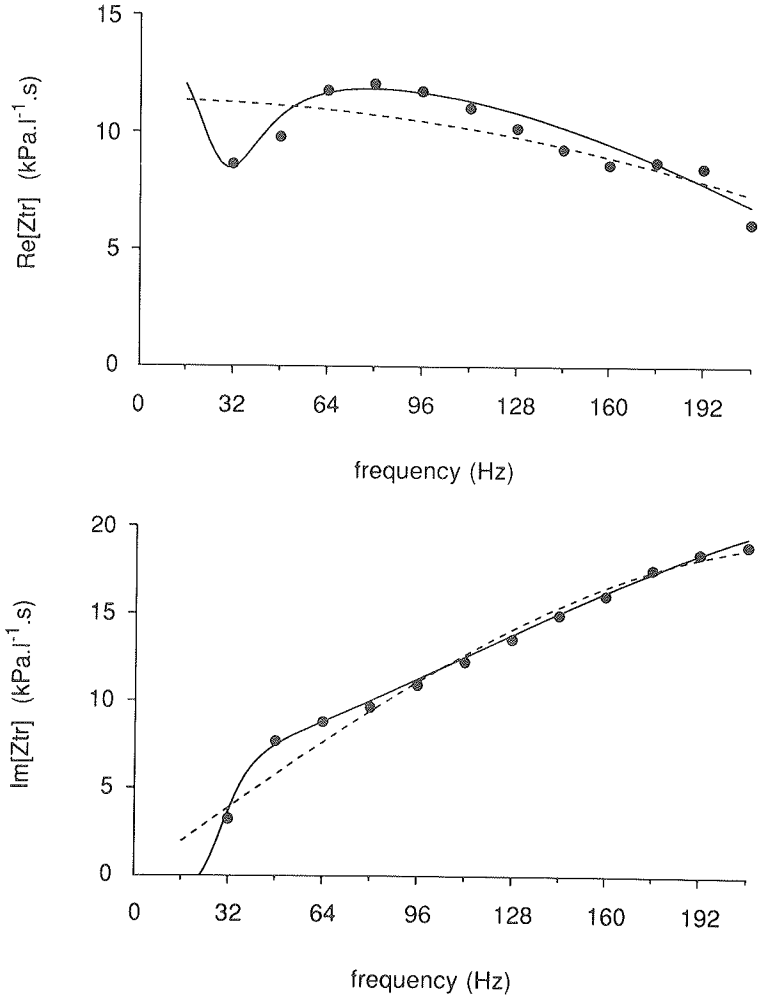

Figure 4.7. Example of experimental data (●) and the corresponding optimum responses of the DuBois' model (- - -) and the modified DuBois' model (——) for the real (Re, top) and imaginary part (Im, bottom) of Ztr.

expected that Ztr is sensitive to the upper airway coefficients in the low frequency range. It is interesting to note that the change in impedance by varying the upper airway coefficients is limited to a small part of the frequency range (16–64 Hz). At high frequencies the nose is no longer shunted because of the high (inertive) impedance of the upper airway shunt. The nose resistance is then added to the airway resistance, reducing the response of the nine-coefficient model to the response of the simpler six-coefficient model.

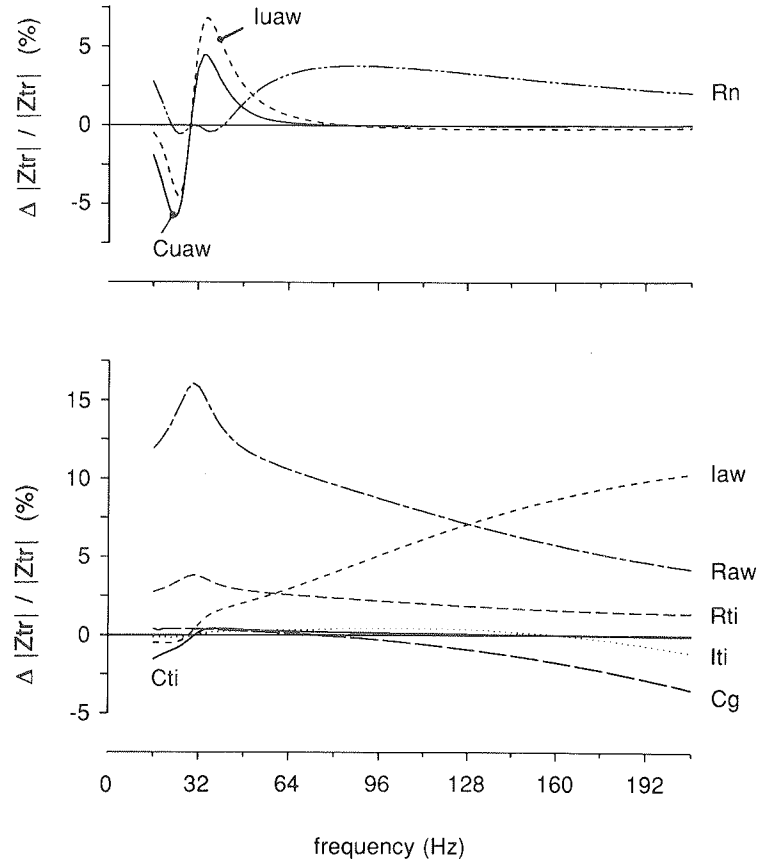

Figure 4.8. *Sensivity function of the modulus of Ztr of the modified DuBois' model. The relative change in |Ztr| is computed for a 20% increase in the value of the coefficients of the nose and upper airway compartment (top), and the airway, tissue, and alveolar gas compartment (bottom).*

The compressibility of the alveolar gas (Cg) determines the separation between the impedances of the airways and the tissues. This separation is established on the respiratory transfer impedance at high frequencies (Fig. 4.8, bottom). As the response of our extended model at high frequencies is equal to that of the six-coefficient model, it is not surprising that it shows the same two sets of solutions as the DuBois' model (24). In our results we have presented the solution with high Iaw values because the other solution provided unrealistically low values for Iaw (mean value 2.7 ± 0.8 $Pa.l^{-1}.s^2$). Based on the length and diameter of the airways in a cast of a rat lung (27), the calculated gas inertance for the trachea up to the tenth generation would already be 5.0 $Pa.l^{-1}.s^2$. As the trachea accounts for 70% of this value and our measurements include the airways up to the nose, an average Iaw of 11.8 $Pa.l^{-1}.s^2$ seems to be a realistic value (Table 4.1). We did not include an inertance of the nose in our modified DuBois' model because information on the nose impedance can only be obtained from the low frequencies, where the contribution of the inertia to the impedance is very small.

The sensivity function explains some of the variability of the parameter values found in this study: low CV values for Raw+Rn and Iaw (mean intraindividual CV 12% and 18%, respectively) compared to those of Rti and Iti (89% and 27%, respectively). As most of the respiratory resistance and inertance is located in the airways, the transfer impedance will be more sensitive to changes in Raw+Rn and Iaw than to changes in Rti or Iti. The tissue compliance influences Ztr only at the lowest frequency applied (Fig 8, bottom); extending the excitation signal to lower frequencies would improve the reliability of the estimate of Cti. The limited frequency range for estimating the upper airway coefficients may be part of the reason for the large variation in the estimated Iuaw and Cuaw values. Variation in the location and size of the dough collar probably add to the variation of these coefficients.

An indication of the goodness-of-fit of the model response to the measurement data is given by the $\sqrt{\chi^2}$. This index indicates that if the average measurement error would be 0.53 $kPa.l^{-1}.s$ (Table 4.1), the difference between model and data can be ascribed entirely to the statistical scattering of the data.

In order to be able to compare the goodness-of-fit of our model description of the impedance data with previous studies we calculated the relative residual distance D% ($= 100/n \Sigma (|Ztr_m - Ztr_o|)/|Ztr_o|$), (12, 24)) from our sets of coefficients. The mean relative distance between model response and measurement was 3.5 ± 1.5%. This value is comparable with the value obtained when optimizing DuBois' model to transfer impedance measurements in healthy man (24). It is, however, far better than

the value obtained by Jackson and Watson (12) for input impedance data of normal rats in the frequency range 20–90 Hz (12.3 ± 4.3%).

In our optimization procedure we made the assumption that the gas compressibility Cg was 0.05 ml.kPa^{-1}. To study the influence of Cg on the coefficients obtained we fitted the same model with an increase of Cg of 40%. As a result the separation between airway compartment and tissue compartment was slightly different. With a fixed value of Cg of 0.07 ml.kPa^{-1}, total airway resistance and airway inertance were increased by 5% and 7%, respectively. Tissue resistance and tissue inertance were correspondingly lower. Rrs, Irs, and Cti were virtually independent of Cg (differences less than 1%).

An alternative explanation for the occurrence of the local minimum of Re[Ztr] at low frequencies and the steep increase in slope of Im[Ztr] around 48 Hz is offered when the chest wall behaves nonhomogeneously. Nonhomogeneous behavior of the chest wall was found in man (6, 23) and in monkeys (28). Therefore, the data were also analyzed with a model where the rib cage and abdomen were modelled as two parallel compartments. Each compartment consisted of a series resistance, inertance and compliance. The model further consisted of the airway resistance (Raw) and inertance (Iaw), and the alveolar gas compressibility (Cg). The coefficients were estimated with a fixed value of 0.05 ml.kPa^{-1} for Cg. The model response succeeded in describing the low frequency behavior of Ztr. The average residual term ($\sqrt{\chi^2}$) was slightly but significantly higher than the value obtained with our modified DuBois' model (0.57 vs. 0.53 kPa.l^{-1}.s, $p < 0.05$; paired t-test). The estimated airway resistance and inertance were reproducible (10.2 ± 0.9 kPa.l^{-1}.s and 11.2 ± 1.5 Pa.l^{-1}.s^2, respectively). The rib cage compartment (the compartment that showed the lowest inertance) consisted of a high resistance (4.8 ± 5 kPa.l^{-1}.s), a low inertance (2.4 ± 0.8 Pa.l^{-1}.s^2) and a compliance of 1.4 ± 0.4 ml.kPa^{-1}. The abdomen compartment had an average resistance of 0.7 ± 0.7 kPa.l^{-1}.s, an inertance of 26.8 ± 24.0 Pa.l^{-1}.s^2 and almost the same compliance as the rib cage (1.4 ± 0.7 ml.kPa^{-1}). Especially the rib cage compliance and abdominal inertance and compliance showed considerable variation: rib cage compliance ranged from 0.4 to 2.9 ml.kPa^{-1}, the inertance of the abdomen ranged from 9.4 to 236 Pa.l^{-1}.s^2, and the abdominal compliance ranged from 0.1 to 5.4 ml.kPa^{-1}. This variability can hardly be ascribed to variation in measuring condition as was the case with the variation found for the upper airway wall coefficients of the modified DuBois' model (influence of the dough neck collar). Furthermore, the abdomen is expected to be more compliant than the rib cage. Therefore, we think that the frequency dependent behavior of Ztr at low

frequencies reflects the influence of the upper airway wall shunt. Our proposed model, however, needs further validation.

To our knowledge no data are available on the respiratory mechanical properties of conscious rats. Lung resistance values ranging from 9 to 50 kPa.l^{-1}.s were reported for anesthetized, tracheotomized or intubated rats during spontaneous breathing (3, 5, 13, 15, 22). Boyd et al. (2) measured Raw+Rn of anesthetized rats using DuBois' plethysmographic technique. Their values are almost four times as large as our average value for Raw+Rn. Jackson and Watson (12), using the oscillation technique in tracheotomized rats, found an average intrathoracic airway resistance which is comparable to our total airway resistance, i.e. resistance in intra- and extrathoracic airways. Although previously reported values for resistance were measured using a variety of techniques and were not always corrected for instrumental impedance, they are largely in excess of the total airway resistance including Rn in our study. Recent results of the effect of anesthesia on lung resistance may shed some light on this discrepancy. Skornik and Brain (25) studied the changes in total lung resistance (RL) in hamsters after administration of pentobarbital anesthesia. With a dose of 70 mg.kg^{-1} a maximum increase of 375% in RL was found 25 minutes after the onset of anesthesia. The effect of anesthesia on RL was time- and dose-dependent. The difference between our results and the results in anaesthetized rats is in good agreement with this range of increases.

Jackson and Watson (12) reported a value of 17.4 Pa.l^{-1}.s^2 for Iaw, which is 50% higher than our mean value for airway inertance. If the use of anesthesia influences the airway diameter, thus increasing Raw, an increase in Iaw is also expected since both Raw and Iaw are related to airway calibre. Although our estimates of tissue compliance showed a large variation, the mean value is two times larger than the respiratory compliance for anesthetized rats as reported by Jackson and Watson (12). Since small animals have very compliant chest walls (3), we think that this difference reflects differences in lung compliance. These differences are compatible with the decreases in Cdyn due to anesthesia (25).

In conclusion, our setup enables measurement of the total respiratory transfer impedance of conscious rats. With slight modifications it can be used for other small laboratory animals. The short-term variability in normal rats in repeated measurements was 10%. This result indicates that the respiratory mechanical properties of conscious rats can be followed in longitudinal studies. The setup has the potential advantage of on-line measurement of immediate responses to irritant or toxic gases

and drugs.

Our data were interpreted with the use of a variant of DuBois' model, including the resistance of the nose and the shunt impedance of the upper airway walls. The low residual distance between the model response and the experimental data indicates that the model provides a good description for the transfer impedance of normal rats. The impedance of our rats was lower than previously reported, probably because we used conscious instead of anesthetized rats.

References

1. BEVINGTON, PH.R. Data Reduction and Error Analysis for the Physical Sciences. New York: Mcgraw-Hill, 1969
2. BOYD, R.L., M.J. FISHER, AND M.J. JAEGER. Non-invasive lung function tests in rats with progressive papain-induced emphysema. Resp. Physiol. 40: 181-190, 1980.
3. CROSFILL, M.L., AND J.G. WIDDICOMBE. Physical characteristics of the chest and lungs and the work of breathing in different mammalian species. J. Physiol. 158: 1-14, 1961.
4. DARÓCZY, B., AND Z. HANTOS. Generation of optimum pseudorandom signals for respiratory impedance measurements. Int. J. Biomed. Comput. 25: 21-31, 1990.
5. DIAMOND, L., AND M. O'DONNELL. Pulmonary mechanics in normal rats. J. Appl. Physiol.: Respirat. Environ. Exercise Physiol.: 43: 942-948, 1977.
6. DUBOIS, A.B., A.W. BRODY, D.H. LEWIS, AND B.F. BURGESS, JR. Oscillation mechanics of lungs and chest in man. J. Appl. Physiol. 8: 587-594, 1956.
7. EYLES, J.G., R.L. PIMMEL, J.M. FULLTON, AND P.A. BROMBERG. Parameter estimates in a five-element respiratory mechanical model. IEEE Trans. Biomed. Eng. 29: 460-463, 1982.
8. FARRÉ, R., R. PESLIN, D. NAVAJAS, C. GALLINA, AND B. SUKI. Analysis of the dynamic characteristics of pressure transducers for studying respiratory mechanics at high frequencies. Med. & Biol. Eng. & Comput. 27: 531-537, 1989.
9. FRANKEN, H., J. CLÉMENT, AND K.P. VAN DE WOESTIJNE. Systematic and random errors in the determination of respiratory impedance by means of the forced oscillation technique: a theoretical study. IEEE Trans. Biomed. Eng. 30: 642-651, 1983.
10. HANTOS, Z., B. DARÓCZY, B. SUKI, AND S. NAGY. Low-frequency respiratory mechanical impedance in the rat. J. Appl. Physiol. 63: 36-43, 1987.

11. HIETT, D.M. Tests of ventilatory function for use in long-term animal studies. Br. J. Industr. Med. 31: 53-58, 1974.
12. JACKSON, A.C., AND J.W. WATSON. Oscillatory mechanics of the respiratory system in normal rats. Resp. Physiol. 48: 309-322, 1982.
13. JOHANSON, JR., W.G., AND A.K. PIERCE. A noninvasive technique for measurement of airway conductance in small animals. J. Appl. Physiol. 30: 146-150, 1971.
14. KEEFE, D.H. Acoustical wave propagation in cylindrical ducts: Transmission line parameter approximations for isothermal and nonisothermal boundary conditions. J. Acoust. Soc. Am. 75: 58-62, 1984.
15. KING, T.K.C. Mechanical properties of the lungs in the rat. J. Appl. Physiol. 21: 259-264, 1966.
16. LÁNDSÉR, F.J., J. NAGELS, M. DEMEDTS, L. BILLIET, AND K.P. VAN DE WOESTIJNE. A new method to determine frequency characteristics of the respiratory system. J. Appl. Physiol. 41: 101-106, 1976
17. LUTCHEN, K.R., AND A.C. JACKSON. Reliability of parameter estimates from models applied to respiratory impedance data. J. Appl. Physiol. 62: 403-413, 1987.
18. MEAD, J. Control of respiratory frequency. J. Appl. Physiol. 15: 325-336, 1960.
19. MICHAELSON, E.D., E.D. GRASSMAN, AND W.R. PETERS. Pulmonary mechanics by spectral analysis of forced random noise. J. Clin. Invest. 56: 1210-1230, 1975.
20. MILLER, III, T.K., AND R.L. PIMMEL. Standard errors on respiratory mechanical parameters obtained by forced random excitation. IEEE Trans. Biomed. Eng. 30: 826-832, 1983.
21. OOSTVEEN, E., R. PESLIN, C. GALLINA, AND A. ZWART. Flow and volume dependence of respiratory mechanical properties studied by forced oscillation. J. Appl. Physiol. 67: 2212-2218, 1989.
22. PALEČEK, F. Measurement of ventilatory mechanics in the rat. J. Appl. Physiol.: 27: 149-156, 1969.
23. PESLIN, R., C. DUVIVIER, AND C. GALLINA. Total respiratory input and transfer impedances in humans. J. Appl. Physiol. 59: 492-501, 1985.
24. PESLIN, R., J. PAPON, C. DUVIVIER, AND J. RICHALET. Frequency response of the chest: modeling and parameter estimation. J. Appl. Physiol. 39: 523-534, 1975.
25. SKORNIK, W.A., AND J.D. BRAIN. Breathing and lung mechanics in hamsters: effect of pentobarbital anesthesia. J. Appl. Physiol. 68: 2536-2541, 1990.
26. VINEGAR, A., E.E. SINNETT AND D.E. LEITH. Dynamic mechanisms determine functional residual capacity in mice, Mus Musculus. J. Appl. Physiol.: Respirat. Environ. Exercise Physiol.: 46: 867-871, 1979.

27. YEH, H.C., G.M. SCHUM, AND M.T. DUGGAN. Anatomic models of the tracheobronchial and pulmonary regions of the rat. Anat. Rec. 195: 483-492, 1979.
28. WEGNER, C.D., A.C. JACKSON, J.D. BERRY, AND J.R. GILLESPIE. Dynamic respiratory mechanics in monkeys measured by forced oscillations. Resp. Physiol. 55: 47-61, 1984.
29. ZWART, A., AND E. OOSTVEEN. The effect of cheek and neck shunt on transfer impedance in rat (Abstract). Eur. Resp. J. 3 [Suppl 10]: 65S, 1990.

Chapter 5

Effects of Pentobarbital and Halothane Anesthesia on the Respiratory Transfer Impedance of Rats

E. Oostveen and A. Zwart

Abstract

Total respiratory transfer impedance (Ztr) was measured from 16 to 208 Hz in normal rats, both during consciousness and during anesthesia with pentobarbital sodium or halothane. The Ztr data were obtained by applying pressure variations around the chest and measuring the flow response at the airway opening. Anesthesia induced a large increase in the real part of impedance and a decrease of the imaginary part at low frequency. During pentobarbital anesthesia, some rats exhibited substantial time-dependent changes in Ztr. The Ztr data obtained during anesthesia were analyzed with two different models incorporating parallel pathways in the lung. The first model accounted for mechanical inhomogeneity of the lung, and the second took into account the effects of intrathoracic airway wall compliance. The latter model provided the most realistic values of the coefficients. This model consisted of a central airway compartment and a peripheral airway compartment shunted by the airway wall compliance. Lung tissue and chest wall properties were represented by a single compartment. The analysis resulted in a mean value of the total airway resistance of 32 $kPa.l^{-1}.s$ and 25 $kPa.l^{-1}.s$ 20 minutes after injection of pentobarbital and induction of halothane anesthesia, respectively. The average pre-anesthetic value of the total airway resistance was 13 $kPa.l^{-1}.s$. During anesthesia, peripheral airway resistance was about 50% of total airway resistance. Airway wall compliance was about one-third of tissue compliance. As anesthesia induced large changes in respiratory impedance, the validity of lung function tests in anesthetized rats to evaluate the effects of toxic or pharmacological drugs should be questioned.

Introduction

Recently we have described a setup to measure the respiratory transfer impedance (Ztr) of conscious rats (chapter 4). The respiratory impedance was measured by applying pressure variations (frequency range 16 to 208 Hz) around the chest and measuring the flow response at the airway opening. Repeated measurements in the same animal showed that Ztr of young normal rats was reproducible (coefficient of variation about 10%).

To our knowledge, our study was the first that has reported on respiratory mechanics of unanesthetized rats. Our values of airway resistance, obtained by model analysis of the Ztr data, were low compared to previously reported values of airway or lung resistance including the nose as measured in anesthetized rats (1, 9, 11). Airway inertance was also low compared to the value reported by Jackson and Watson (8), who investigated tracheotomized rats with the forced oscillation technique. Our estimated tissue compliance was within the range of previously reported values of dynamic lung compliance (2, 6, 9, 17), but twice as large as the value reported by Jackson and Watson (8).

The discrepancy between our values and those of previous reports could be a direct consequence of the use of conscious rats in our study. Recently, Skornik and Brain (19) have demonstrated that anesthesia causes a dramatic increase in lung resistance and a reduction in dynamic compliance in hamsters and, therefore, questioned the value of measurements in anesthetized animals. In this connection, the purpose of our study was to determine to what extent anesthesia affects the respiratory mechanics of rats. To this end, we measured normal rats both during consciousness and during general anesthesia with two different anesthetic agents, pentobarbital sodium and halothane. For each drug, we followed the changes in Ztr and the changes in spontaneous ventilation as a function of time during the period of anesthesia.

Methods

Measurements

The technique to measure respiratory transfer impedance of rats has been described in detail elsewhere (chapter 4) and will be described only briefly here. The experimental setup consisted of a large body chamber (5 liters) with a small front chamber (100 ml) connected to it. The front chamber contained a wire-mesh screen with a resistance of about 5 $kPa.l^{-1}.s$. First, the rat was placed in a restraining tube,

where head and body were separated by means of a dough neck collar. Then, the restraining tube was placed in the body chamber so that the rat respired from the front chamber which was flushed with a bias flow (25 ml/s) to avoid rebreathing. By means of a loudspeaker mounted in the wall of the body chamber, pseudo-random noise pressure variations were applied to the chest wall. The excitation signal contained all harmonics of 16 Hz from 16 to 208 Hz. The peak-to-peak excitation pressure was limited to 0.2 kPa. The pressure at the body surface and at the airway opening corresponded to the pressure in the body chamber (Pbs) and in the front chamber (Pao), and were measured with identical pressure transducers (Validyne MP-15 (± 0.8 kPa)). After analogous low-pass filtering (fourth order, cutoff 250 Hz) the pressure signals were digitized for periods of 4 s at a sampling rate of 1024 Hz by the D/A-converter of a microcomputer (Tulip AT compact 2). The data were digitally high-pass filtered to reduce the components of spontaneous breathing. Data processing was performed according to Michaelson et al. (14). Fourier transform was performed on blocks of 512 data points with 50% overlap between blocks. The analysis also provided the coherence function which is an estimate of the amount of noise and/or non-linearity in the Pbs–Pao relationship. Data with a coherence value below 0.88 were discarded. The respiratory transfer impedance (Ztr) was calculated from:

$$Ztr = ((Pbs/Pao) - 1).Ze \qquad (1)$$

where Ze is the complex impedance of the front chamber (chapter 4). This yielded the real part or effective resistance (Re[Ztr]), and the imaginary part or reactance (Im[Ztr]) of the respiratory transfer impedance. The transfer impedance values obtained from five periods of 4 s were averaged. The corresponding data were collected within about one minute.

Calibration of the impedance of the front chamber

The impedance of the front chamber (Ze) was assessed by placing a calibration unit between the front and the body chamber. The calibration unit consisted of a tube (length 5.5 cm, ID 0.4 cm) with a wire-mesh screen (R 4.7 $kPa.l^{-1}.s$) placed at one of its ends. The resistance of the calibration unit was constant up to flows of 1 l/min. The impedance of the tube was calculated using the large tube approximation of Keefe (10). As Ztr of the calibration unit was known, Ze could be calculated from Eq. 1 by substituting the measured values of Pbs/Pao for the different frequencies.

Impedance Ze was also measured during flushing of the front chamber with a 2% halothane-in-air mixture (25 ml/s). During these measurements a small flow of room air (≈ 4 ml/s) was led through the calibration unit to insure that the calibration tube

contained room air and that its impedance was unaffected by halothane. It was verified that the total flow through the calibration unit (steady-state flow and flow due to the excitation pressure) did not exceed the linear range of the unit. Compared to room air, Ze during halothane administration had a slightly smaller imaginary part and showed a concomitant small fall in magnitude in the whole frequency range (|Ze| was reduced by about 1.5%).

Protocol

Pentobarbital anesthesia. After measurement of Ztr in the conscious state, the rat was injected with a fixed dose of pentobarbital sodium (Nembutal^R, 35 mg/kg ip). Before the rat had lost consciousness, it was placed in the restraining tube. The dough neck collar was adjusted and it was considered adequate when the time constant was larger than 10 s. The time constant of the leakage along the neck was measured by applying a small pressure step in the body box (injection or withdrawal of a small volume of air). The first Ztr measurement was started 10 or 20 min after the injection of the anesthetic. Next Ztr was measured every 5 minutes until the animal started to regain consciousness.

Halothane anesthesia. Ztr was measured in the conscious rat. To minimize struggling during the excitation stage, the rat was then tightly fixed in the restraining tube by compression at the back, and the bias flow flushing through the front chamber was switched from room air to a room air mixture containing halothane (Fluothane^R). After an initial concentration of 3% halothane in room air to induce anesthesia (about 1 min), the concentration was reduced to 2%. The rat was then freely repositioned in the tube and the dough collar was readjusted when necessary. The halothane concentration of the gas delivered to the front chamber was measured continuously throughout the measurements with a total carbon analyzer (Flame Ionization Detector). Administration of halothane was ended 30 min after the start of induction. The protocol of Ztr measurements was similar to that of the pentobarbital experiments. However, since the induction was faster, the first Ztr data were obtained at 5 or 10 minutes after the start of induction. Next Ztr was measured every 5 minutes. In most cases the measurements were continued until the animals had regained consciousness.

Nine conventional male Wistar rats (weighing 255 ± 18 (SD) g) were measured during pentobarbital anesthesia. From this group six animals were also used for measurements with halothane anesthesia. The interval between the experiments with pentobarbital and halothane anesthesia ranged from 3 to 8 days. The six rats, then,

weighed on average 284 ± 18 (SD) g. The animals were housed together in two cages, and were provided water and food ad libitum. The animals fasted during the night preceding the experiments.

Data on spontaneous breathing, frequency (f_{sp}) and tidal volume (V_T), were obtained from the recordings of the body box pressure signal. From these data minute volume was calculated ($\dot{V}_E = f_{sp} \times V_T$). The control values were the values measured during consciousness.

Statistics. Comparison of data was performed with the paired Student's t–test (0.05 significance level).

Results

Transfer impedance

Pentobarbital anesthesia. The duration of pentobarbital anesthesia was variable. Most animals started shivering between 55 and 75 minutes after injection; an indication that they were regaining or already had regained consciousness.

Anesthesia induced large changes in the transfer impedance of normal rats. At 20 minutes after injection (t=20), the real part of the transfer impedance (Re[Ztr]) had increased at all frequencies and the imaginary part (Im[Ztr]) had decreased in the low frequency range (Fig. 5.1). In all animals except one the resonant frequency (Im[Ztr] equals zero) shifted towards higher frequencies. The largest differences in Ztr were found at the lowest frequency measured: Re[Ztr] at 16 Hz increased on average by 140% and the negative value of Im[Ztr] decreased by 180%.

The real part further increased after t=20, and reached a maximum between t=25 and t=65. This maximum was found shortly before spontaneous respiration increased from its low(est) level found during deep anesthesia. As compared to Ztr at t=20, Re[Ztr] at the time of the maximum was increased at all frequencies, and Im[Ztr] tended to be lower at low frequency and was higher at high frequency (Fig. 5.1).

A change in the shape of the curves of Re[Ztr] and Im[Ztr] was observed during anesthesia as compared to the shape of the curves during consciousness. In general, Re[Ztr] of the conscious rat showed a local minimum in the low frequency range and Im[Ztr] showed a bend in the curve around 64 Hz. During anesthesia, however, Re[Ztr] decreased with increasing frequency and showed its highest value at the lowest frequency measured. Im[Ztr] increased almost curvilinearly with increasing

frequency. The shape of the mean curve of Re[Ztr] during pentobarbital anesthesia (Fig. 5.1) resembled the shape of the individual curves of eight animals. One rat showed a deviating shape for Re[Ztr]: after an initial decrease between 16 and 80 Hz, Re[Ztr] increased from 80 Hz to 160 Hz, followed by a plateau up to 192 Hz and a decrease from 192 to 208 Hz.

In some animals Ztr changed substantially as a function of time during the period of anesthesia. An indication of the change of Ztr as a function of time can be obtained from Table 5.1a. This table shows the relative change in impedance modulus ($|Ztr| = (Re[Ztr]^2 + Im[Ztr]^2)^{½}$) at 16 Hz at different points of time during anesthesia compared to the pre-anesthetic value. The impedance modulus takes into account both the increased Re[Ztr] and decreased Im[Ztr] at 16 Hz. This table also shows the variable onset of recovery.

Comparison of the last Ztr data to those obtained during consciousness showed that Re[Ztr] was still slightly elevated, but no significant differences were found for Im[Ztr]. The typical shapes of the curves of Re[Ztr] and Im[Ztr] as found during consciousness at low frequencies were restored. During the final Ztr measurements, $\dot{V}E$ had returned to 70% of its control value.

Halothane anesthesia. The changes in Ztr induced by halothane anesthesia were smaller than the changes induced by pentobarbital. Fig. 5.2 illustrates the average impedance obtained during consciousness, and at 10 and 30 min after induction of anesthesia with halothane. Ten minutes after the start of induction, Re[Ztr] had increased at low frequencies and slightly decreased at high frequencies as compared to Re[Ztr] during consciousness. Im[Ztr] was significantly lower between 16 and 64 Hz. Except for a small increase in Re[Ztr] at 208 Hz, no significant differences could be demonstrated between the Ztr data obtained t=10 and t=30.

The variation between animals is shown in Table 5.1b. This table further demonstrates that the effects of halothane anesthesia on Ztr are almost independent of time. Comparison of Table 5.1a and 5.1b further shows that the magnitude of the effects of the two anesthetics do not correlate; e.g. rat 2 shows a large increase with pentobarbital but a small increase with halothane, whereas rat 6 shows large effects with both anesthetic agents.

Ventilation

Spontaneous ventilation was largely reduced during general anesthesia. In Fig. 5.3 the changes in f_{SP}, V_T and $\dot{V}E$ are expressed as a percentage of their control values. During pentobarbital anesthesia (Fig. 5.3, left panels), the changes during the first 10

minutes after injection probably reflect the onset of sedation. During this period f_{sp}, VT and, as a consequence, $\dot{V}_E$ decreased to a low level which remained steady during the period in which all animals were sedated (t=10 to t=30). After 30 min some animals recovered while other rats remained sedated up to 70 min. This

Table 5.1. *Relative change in impedance modulus at 16 Hz during anesthesia*

a) Pentobarbital

Rat \ time (min)	10	20	30	40	50	60	70
#1	–	67	85	97	103	93	−12
#2	50	108	144	276	218	85	56
#3	147	166	194	120	39		
#5	82	100	98	−7	−11	−10	
#6	243	294	351	381	324	110	
#7	88	118	132	141	−3	37	23
#8	146	213	248	259	268	39	
#9	56	74	91	101	102	109	7
#10	64	107	117	119	106	−19	

b) Halothane

	Anesthesia			Recovery		
Rat \ time (min)	10	20	30	10	20	30
#1	88	83	77	80	50	
#2	33	23	33	54	0	16
#5	144	120	130	25		
#6	127	154	178	145		
#8	86	89	81	–		
#9	29	28	37	50	−18	

Differences (in percentage) of impedance modulus for the individual rats as a function of time after pentobarbital injection (a) and after the start of induction with halothane (b) relative to control (consciousness).

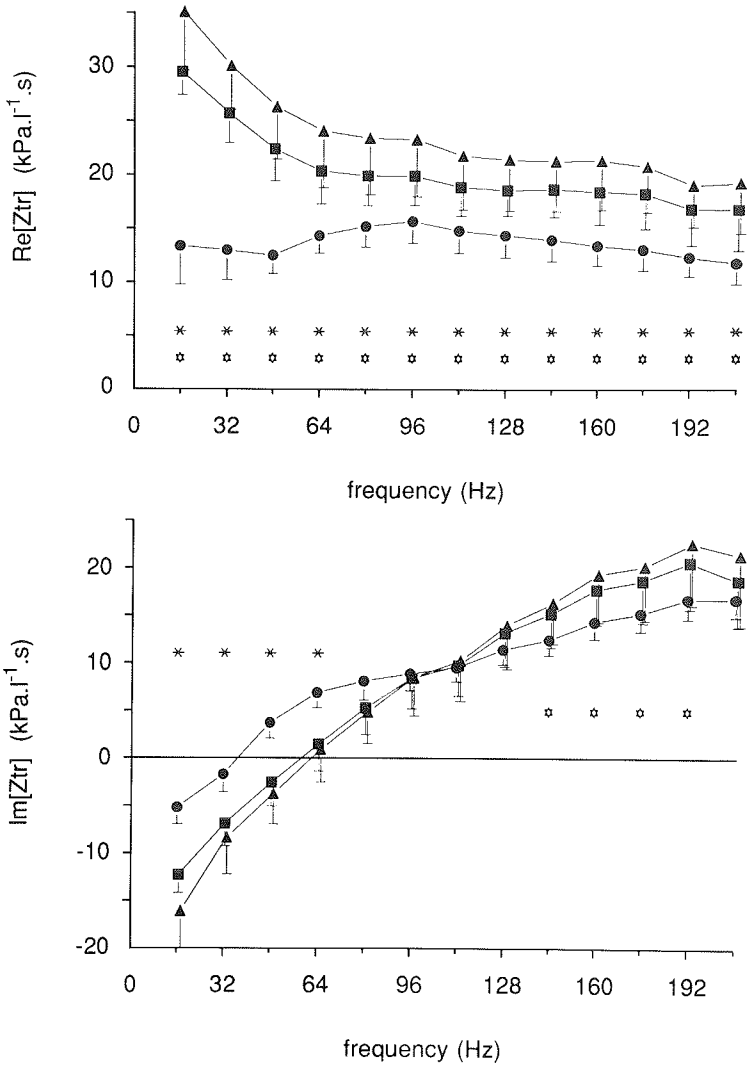

Figure 5.1. *Real (Re, top) and imaginary (Im, bottom) part of respiratory transfer impedance of rats during consciousness (●), 20 min after pentobarbital injection (■), and at the time when Re[Ztr] was maximum during anesthesia (▲). Means and SD of the group are shown. ✻ : paired t-test $p < 0.05$; comparison between conscious state and anesthetized state at t=20. ✡ : paired t-test $p < 0.05$; comparison between anesthetized state at t=20 and at the time of maximum impedance.*

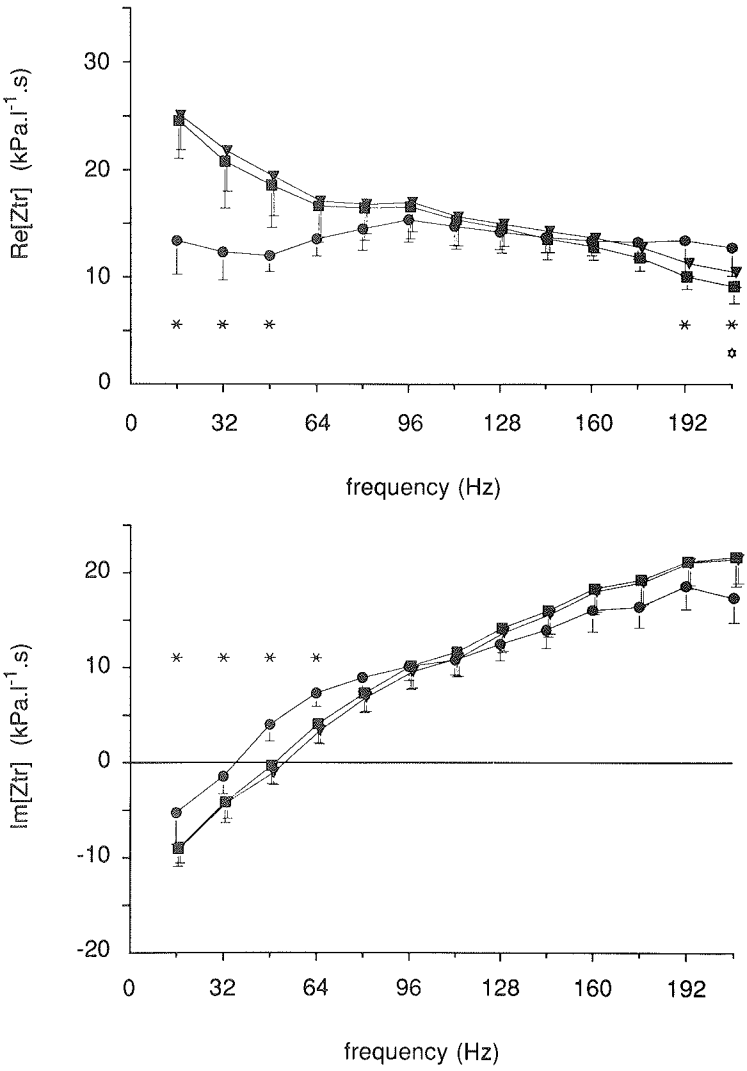

Figure 5.2. *Real (Re, top) and imaginary (Im, bottom) part of the respiratory transfer impedance of rats during consciousness (●), at 10 min (■), and 30 min (▲) after induction with halothane. Means and SD of the group are shown. ✻ : paired t-test $p < 0.05$; comparison between conscious state and anesthetized state at t=10. ✡ : paired t-test $p < 0.05$; comparison between anesthetized state at t=10 and t=30.*

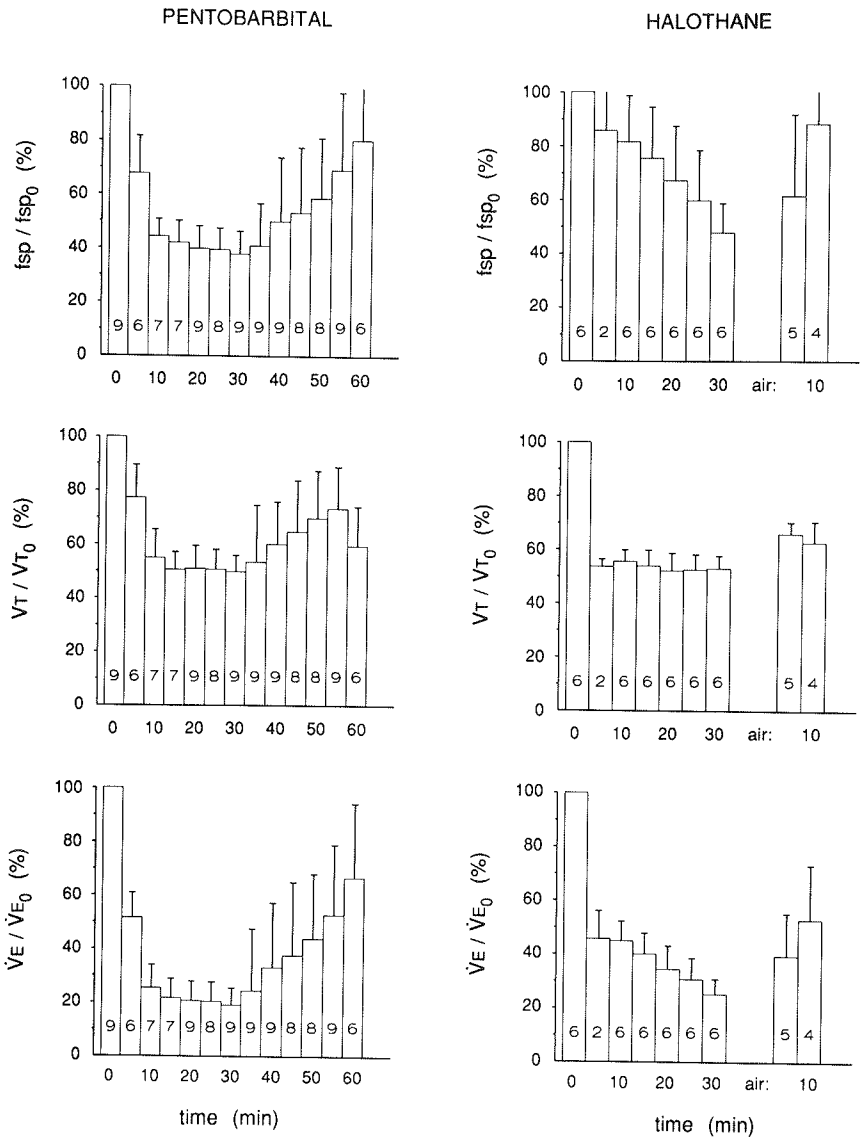

Figure 5.3. *Breathing frequency (f_{sp}, top), tidal volume (V_T, middle) and minute ventilation ($\dot{V}_E$, bottom) relative to their control values f_{sp_0}, V_{T_0} and $\dot{V}_{E_0}$, respectively. Pentobarbital anesthesia (left panels) and halothane anesthesia (right panels). Recovery as a function of time after cessation of halothane administration is also shown [about 5 min elapsed between t=30 (anesthesia) and t=0 (recovery)]. The number of rats contributing to each bar is indicated.*

variable onset of recovery is reflected in the increased SD found for t > 30. Recovery usually commenced with an increased and irregular breathing frequency.

Halothane anesthesia showed a different effect on spontaneous ventilation (Fig. 5.3, right panels). Immediately after induction, VT decreased to about 50% of its control value as was also found during pentobarbital anesthesia. Respiratory frequency, however, slowly decreased as a function of time. At t=30, the low breathing rate was reached which was found immediately after sedation of rats with pentobarbital. The rats awoke 5 to 25 minutes after cessation of the halothane administration.

Discussion

The aim of our study was to determine the effects of anesthesia on the respiratory impedance of normal rats. Our experimental setup enabled Ztr measurement during consciousness and during general anesthesia with the rat in the same prone position in the restraining tube. Both anesthetic agents used in our study are potent respiratory depressants (16). Indeed, they largely depressed respiratory rate, tidal volume, and hence minute ventilation. The anesthetized rats were not mechanically ventilated for two reasons. First, mechanical ventilation requires intubation or tracheotomy which excludes the possibility of comparison with consciousness. Second, the results obtained with our setup can be compared to those of other studies, since most of these have measured anesthetized rats during spontaneous breathing (1, 2, 5, 8, 9, 11, 17).

The very low $\dot{V}E$ during anesthesia (20% of the control value during pentobarbital anesthesia) seems to be too low to be sustained for long periods. The control values of the respiratory parameters, however, were high ($f_{sp} \approx 180$ breaths/min and, assuming adiabatic compression in the body box, $V_T \approx 2.0$ ml), probably as a result of stress due to restraining (20). During recovery $\dot{V}E$ returned to 70% of its control value and the Ztr data obtained in this period only slightly differed from those obtained during consciousness. Obviously, the rats tolerated the low ventilation.

General considerations

Both pentobarbital and halothane depress the Central Nervous System. Pentobarbital is known to be an anesthetic drug that shows large variations in duration of anesthesia for a fixed dose, and there are also differences between individuals in total dose needed for anesthesia. This was illustrated in our study by one rat which recovered from anesthesia within 15 min after injection and was excluded from the study. Nevertheless, pentobarbital is commonly used as a general anesthetic in small

animals because of the ease of administration. We used a fixed dose of 35 mg/kg, which is within the range of dosage reported in the literature to study the respiratory mechanical properties of rats [30 to 50 mg/kg (1, 6, 8, 12)].

Halothane is non-irritant to the respiratory tract and it does not increase bronchial secretions; however, it causes cardiovascular and respiratory depression, especially decreasing tidal volume. Initially the respiratory frequency may increase to compensate for the decreased tidal volume but, when anesthesia deepens, the respiratory rate will also decrease. These effects are consistent with our findings with halothane.

Changes in airway impedance will occur with inhalation anesthetics when the physical properties of the anesthetic gas mixture differ from those of air. The mixture of 2% halothane in air has a density 10% higher than that of air. The viscosity (not measured) is close to air because changes in Ze were small (section on calibration of Ze). Therefore, small increases in airway resistance and inertance may be expected during halothane anesthesia.

General anesthesia decreases end-expiratory lung volume in rodents (4). This is not a direct result of a change in relaxed lung volume. Rodents have very compliant chest walls and they control their end-expiratory lung volume during consciousness by interrupting expiration, i.e. inspiration is started before relaxed lung volume is reached. Vinegar et al. (21) have demonstrated that this reflex mechanism is lost in mice during barbiturate anesthesia, resulting in a reduction of end-expiratory lung volume.

For man, dogs and hamsters, a decreased dynamic lung compliance (Cdyn) and increased lung resistance [RL (resistance of airways+lung tissue)] during anesthesia have been reported (18, 19). The increase in RL probably reflects an increase in airway resistance due to a reduction of airway caliber. Airway caliber is affected by lung volume and by altered bronchomotor tone due to anesthesia. It may be expected that pentobarbital causes a larger decrease of airway caliber than halothane anesthesia since pentobarbital involves a release of histamine whereas halothane has been reported to prevent or reverse airway constriction (7). This is consistent with our findings that pentobarbital induced larger increases in Re[Ztr] than halothane.

In hamsters, Skornik and Brain (19) have demonstrated a time-dependent increase in RL during pentobarbital anesthesia, with an almost fourfold increase 25 min after injection. Cdyn showed a time-dependent decrease and reached its minimum value at about the same time that RL was maximal. In our study we also found large, time-dependent changes during pentobarbital anesthesia, but the maximum increase in Re[Ztr] was reached at a variable time between 25 and 65 min after injection. If the lung compliance is the major determinant of the respiratory compliance in rats, a

decreased lung compliance will result in an increased resonant frequency. Indeed, we found an increased resonant frequency in all rats except one, both during pentobarbital and halothane anesthesia.

Interpretation by model analysis

The curves of Ztr during anesthesia are different from those measured during consciousness (Fig. 5.1, 5.2). To describe the frequency-dependent fall of Re[Ztr] found during anesthesia, two different models were fitted to the data based on explanations for frequency dependence of resistance as proposed in the literature. In 1956, Otis et al. (15) described the behavior of mechanically inhomogeneous, parallel lung units. Assuming lung units with different resistive and elastic properties such that their RC products (time constants) are unequal, the lung will show uneven ventilation. Even when resistance and compliance of the individual lung units are frequency-independent, the effective resistance and compliance will decrease with increasing frequency. Mead (13) proposed an alternative explanation based on the observation that the airway walls are not completely rigid. Then, especially when peripheral airway resistance is large, the expansion of the more proximal airway walls may involve a second pathway (shunt) for the flow. This will result in a frequency-dependent fall in effective resistance since with increasing frequency the compliance of the airway walls presents a decreasing shunt impedance.

The two models which were used to describe the data are shown in Fig. 5.4. The model responses were fitted to the measured data by using a Marquardt least-square fit routine. This parameter estimation routine searches for the set of coefficients that minimizes the squared difference between the model response (Ztr,m) and the observed data (Ztr,o):

$$\chi^2 = \frac{1}{2n-a} \sum_{i=1}^{n} |Ztr,m - Ztr,o|^2$$

where n is the number of investigated frequencies and a is the number of model coefficients to be estimated. The Ztr curves of one animal (#5) obtained during pentobarbital anesthesia deviated from all other curves, and were, therefore, excluded from further analysis.

An electrical representation of an inhomogeneous lung is illustrated in Fig. 5.4A. The lung is represented by the central airways with a resistance (Rcaw) and inertance (Icaw), and two parallel peripheral lung units, each with an airway resistance, gas compressibility, and lung compliance (Rpaw1, Cg1, CL1 and Rpaw2, Cg2, CL2,

respectively). In this model, the following assumptions have been made in order to reduce the number of coefficients: chest wall compliance was not incorporated in the model, since the chest wall of the rat has been reported to be much more compliant than the lung (2, 4, 9, 12). Tissue resistance is small in conscious rats (chapter 4), so

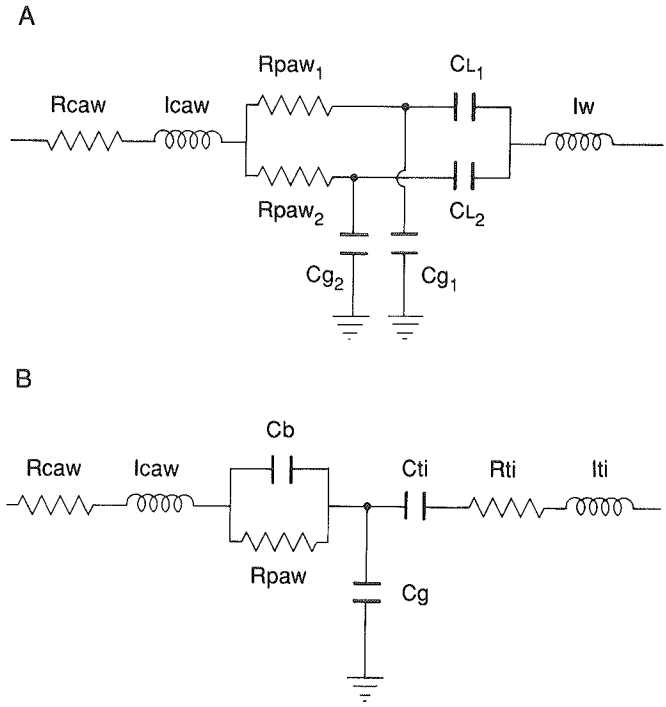

Figure 5.4. *Models including parallel pathways in the lung.*
A: inhomogeneity of peripheral lung. The model consists of the central airways, two peripheral lung compartments, and the chest wall.
B: model with airway wall compliance shunting the peripheral airways. The model further consist of the central airways, the alveolar gas compartment, and the tissue compartment.
Rcaw, Icaw, central airway resistance and inertance, respectively; Rpaw, peripheral airway resistance; Cg, alveolar gas compressibility; CL, lung compliance; Iw, chest wall inertance; Cti, Rti, Iti, tissue compliance, resistance, and inertance, respectively.

the chest wall was represented by only one coefficient: chest wall inertance (Iw). It was assumed that the two peripheral lung compartments had an equal volume, so the gas compressibilities Cg1 and Cg2 are the same. The model analysis was made with a fixed value for Cg1 and Cg2 (Cg1= Cg2= 0.02 ml.kPa^{-1}).

Analysis of the model response revealed that there were a variety of solutions for each measurement which fitted the data equally well. Therefore, we systematically analyzed all data with fixed values of Rpaw2 ranging from 0 to 20 kPa.l^{-1}.s with

Table 5.2. *Coefficients obtained with mechanically inhomogeneous lung.*

Rcaw kPa.l^{-1}.s	Icaw Pa.l^{-1}.s^2	Rpaw1 kPa.l^{-1}.s	CL1 ml.kPa^{-1}	Rpaw2 kPa.l^{-1}.s	CL2 ml.kPa^{-1}	Iw Pa.l^{-1}.s^2	$\sqrt{\chi^2}$ kPa.l^{-1}.s
Pentobarbital:							
16.9	18.7	26.6	1.10	0	0.29	2.5	0.66
(2.7)	(4.4)	(5.9)	(0.43)		(0.11)	(1.6)	(0.14)
9.1	18.0	31.3	1.23	10	0.17	2.7	0.66
(2.4)	(4.0)	(5.9)	(0.45)		(0.07)	(1.8)	(0.14)
3.8	17.6	35.3	1.27	20	0.12	2.7	0.66
(2.3)	(3.8)	(6.1)	(0.45)		(0.06)	(1.9)	(0.15)
Halothane:							
15.0	17.8	21.3	1.27	0	0.37	5.1	0.65
(1.5)	(2.8)	(7.0)	(0.23)		(0.19)	(1.6)	(0.16)
7.5	17.3	26.0	1.46	10	0.19	5.3	0.65
(1.9)	(2.4)	(6.4)	(0.28)		(0.12)	(1.6)	(0.16)
2.7	16.8	29.7	1.52	20	0.14	5.5	0.65
(2.3)	(2.1)	(6.5)	(0.30)		(0.09)	(1.8)	(0.16)

Rcaw, Icaw, resistance and inertance of central airways (including nose); Rpaw1, Rpaw2, CL1, CL2, peripheral airway resistance and lung compliance of compartment 1 and 2 (Fig. 5.4A); Iw, chest wall inertance. $\sqrt{\chi^2}$*, root of residual mean square difference between measured impedance and model response. Means and SDs are given for the group at 20 minutes after pentobarbital injection (n=8) and at 20 minutes after halothane induction (n=6).*

steps of 5 kPa.l^{-1}.s. Table 5.2 presents some of the results for the impedance data at t=20. Inertances were least affected by a different choice for the value of Rpaw2. With increasing value of Rpaw2, the value of the Rpaw1 increased and Rcaw decreased. Total lung compliance (CL1 + CL2) appeared to be independent of Rpaw2, but the most compliant lung compartment 1 further increased its compliance with increasing peripheral airway resistance, whereas the least compliant lung compartment 2 further decreased its compliance.

Independent of the solution, the time constant of lung compartment 1 was always larger than that of compartment 2 (30–47 ms and 0–3 ms, respectively). However, since both time constants are much smaller than the time period of spontaneous breathing, the lung will not show asynchronous ventilation. The two compartments had very different values for their compliance, such that, at a breathing rate of 1 Hz (as observed during anesthesia), the most compliant lung compartment 1 would receive 4 to 10 times more of the tidal volume than the stiffer lung compartment 2. Airway closure may have occurred during anesthesia, since the end-expiratory lung volume of the rat is probably not far from residual volume. However, when lung compartment 2 represents that part of the lung where airway closure has occurred, this lung compartment is expected to offer the highest resistance to flow. This is also expected when compartment 2 represents only a small part of the total lung. With our set of coefficients, lung compartment 2 was always the compartment that offered the lowest resistance to flow. Do these results depend on the assumptions of the model? We investigated the effects of introduction of peripheral airway inertance, chest wall resistance or chest wall compliance, and when using other values of Cg1 and Cg2 in the model analysis. The analysis was made on the mean Ztr curves at t=20 with a fixed value for Rpaw2 (10 kPa.l^{-1}.s). It appeared that extending the model or using other values for Cg did not reduce the CL1–CL2 ratio ($\geq$ 6) or the Rpaw1–Rpaw2 ratio ($\geq$ 2). Since there seems to be no physiological basis for this finding, we conclude that this model does not provide a realistic interpretation of the data obtained during anesthesia.

An alternative description of our data is a decrease in Re[Ztr] due to the distensibility of the intrathoracic airway walls (Fig. 5.4B). This model of the respiratory system, based on Mead's explanation for the frequency dependence of resistance and compliance, has recently been introduced by Ying et al. (22) to describe the impedance data of patients suffering from chronic obstructive pulmonary disease. The model consists of the central airways (resistance Rcaw, inertance Icaw) and the peripheral airways (resistance Rpaw) which are in parallel with the bronchial airway walls (compliance Cb). Lung tissue and chest wall properties are represented by a

single tissue compartment (compliance Cti, resistance Rti, inertance Iti). The alveolar gas volume is represented by its compressibility (Cg). This coefficient was fixed at a value of 0.04 ml.kPa^{-1}.

The results of the parameter estimation of this model are presented in Table 5.3. The mean value for the residual difference was slightly less than the value obtained with model A. Peripheral airway resistance was 45% (± 7%) of the total airway resistance during pentobarbital anesthesia, and 48% (± 7%) during halothane anesthesia. Especially for the pentobarbital data, the average Rti was very low. In some cases, however, Rti was substantial which explains the high SDs for Rti. Total airway resistance (Rpaw+Rcaw) accounted for 94% and 88% of total respiratory resistance (Rrs= Rcaw+Rpaw+Rti) during pentobarbital and halothane, respectively. Iti was only a small fraction of total respiratory inertance (< 20%). Tissue compliance was slightly lower for the pentobarbital data than for the halothane data. Bronchial compliance was about one-third of tissue compliance.

To investigate the effect of the introduced value of Cg on the obtained set of coefficients, the individual curves were also analyzed with a 20% decrease and increasein the value of Cg. The value of Cg hardly affected the estimates of Caw and Cti (changes less than 3%). The data obtained during pentobarbital anesthesia showed

Table 5.3. *Coefficients obtained with model featuring airway wall compliance.*

Rcaw kPa.l^{-1}.s	Icaw Pa.l^{-1}.s^2	Rpaw kPa.l^{-1}.s	Cb ml.kPa^{-1}	Cti ml.kPa^{-1}	Iti Pa.l^{-1}.s^2	Rti kPa.l^{-1}.s	$\sqrt{\chi^2}$ kPa.l^{-1}.s
Pentobarbital:							
17.0	17.9	14.6	0.46	1.41	1.9	1.8	0.59
(2.3)	(3.9)	(4.7)	(0.08)	(0.46)	(1.2)	(3.7)	(0.17)
Halothane:							
12.9	15.9	12.1	0.64	1.83	3.8	3.6	0.53
(1.4)	(1.1)	(3.5)	(0.26)	(0.19)	(0.7)	(3.4)	(0.12)

Rpaw, peripheral airway resistance; Cb, compliance of intrathoracic airway walls; Cti, Rti, Iti, tissue compliance, resistance and inertance, respectively. Other symbols as in Table 5.2. Means and SDs are given for the group at 20 minutes after pentobarbital injection (n=8) and at 20 minutes after halothane induction (n=6).

only small effects on the estimated airway resistances (Rcaw and Rpaw), Rrs, and inertances (Icaw and Irs) when other values of Cg were used (changes ≤ 2%). The data obtained during halothane aneshesia showed a larger influence of Cg, with the largest changes found for Rcaw and Icaw (−17% and −8%, respectively, when the value of Cg was 0.03 ml.kPa^{-1}). The change in total airway resistance (Rcaw+Rpaw), Irs, and Rrs, however, were much smaller (−7%, 2% and 2%, respectively).

Comparison with coefficients of Ztr during consciousness

The Ztr data obtained in conscious rats were analyzed with the model described in our previous report (chapter 4). This model is a variant of the model introduced by DuBois et al. (3). DuBois' model includes a tissue compartment (Rti, Iti, and Cti), an alveolar gas compartment (Cg), and an airway compartment (Raw, Iaw). To describe the local minimum of Re[Ztr] and the bump in the curve of Im[Ztr] around 64 Hz, the airway compartment of DuBois' model was extended with a compartment representing the nose and shunt impedance of the upper airway walls (chapter 4). The fact that these features of Ztr disappeared during anesthesia might indicate that the increased airway resistance completely obscured the nose resistance.

The Ztr data of the conscious rats were analyzed with a value of Cg of 0.05 ml.kPa^{-1}. Table 5.4 shows the average of the set of coefficients that best described the data obtained prior to pentobarbital anesthesia and prior to halothane anesthesia. Total airway resistance of this model is the sum of Raw and Rn. Compared to the conscious state, total airway resistance increased by 180 ± 70% and 105 ± 50% during pentobarbital and halothane anesthesia, respectively. Since the estimates of Rti were larger in the conscious rats than in the pentobarbital-anesthetized rats, the increase in total respiratory resistance (Rrs: sum of the resistances) was substantially lower: the increases in Rrs due to pentobarbital and halothane anesthesia were 110 ± 45% and 70% ± 20%, respectively. The average increase in airway inertance was 80 ± 60% during pentobarbital anesthesia and 50 ± 40% during halothane anesthesia. These results for Iaw indicate that during anesthesia the caliber of the central airways was also reduced. The variability in the estimated tissue compliance of conscious rats was large (Table 5.4). The Ztr data obtained during consciousness usually only showed one data point below the resonant frequency which determined the reliability of Cti (chapter 4).

Both the extended DuBois' model and the model featuring airway wall compliance provided a good description of the measured data (Tables 5.3, 5.4); the average differences between model response and measured data were 5% and 3% for Ztr obtained during consciousness and anesthesia, respectively.

Table 5.4. *Coefficients obtained with the modified DuBois' model for the data obtained in conscious rats.*

Raw + Rn kPa.l^{-1}.s	Iaw Pa.l^{-1}.s^2	Cti ml.kPa^{-1}	Iti Pa.l^{-1}.s^2	Rti kPa.l^{-1}.s	$\sqrt{\chi^2}$ kPa.l^{-1}.s
Before pentobarbital:					
12.5	10.5	2.37	1.1	4.0	0.70
(3.3)	(2.1)	(1.45)	(1.1)	(3.8)	(0.15)
Before halothane:					
12.6	11.5	2.69	0.5	4.2	0.69
(2.4)	(2.7)	(2.34)	(0.6)	(3.6)	(0.19)

Raw + Rn: total airway resistance. Other symbols as in Table 5.3. Means and SDs are given for the group during consciousness before pentobarbital injection (n=9) and before halothane induction (n=6).

Comparison with previous studies

Jackson and Watson (8) have measured respiratory input impedance of pentobarbital-anesthetized rats by forced oscillations (20–90 Hz). These authors have found a much lower value for the total airway resistance than we did (≈ 30% of our value), but the extrathoracic airways were excluded in their measurements by tracheotomy. Their estimates of total inertance and respiratory compliance were in the same range as our values, but the compliance of the intrathoracic airway walls was half the value we found. Both studies, however, show a large variation in this coefficient.

Our values for the total airway resistance were 32 and 25 kPa.l^{-1}.s during pentobarbital and halothane anesthesia, respectively (t=20). These values are close to previously reported values for RL including nasal resistance [30–44 kPa.l^{-1}.s (1, 9, 11)].

To summarize our findings, we observed that Ztr of normal rats (16–208 Hz) measured in the anesthetized state substantially differed from that measured in the conscious state. The real part of Ztr was increased and showed a negative frequency dependence, the imaginary part was lower at low frequencies. The magnitude of the

changes depended on the type of anesthetic agent. During pentobarbital anesthesia some rats exhibited large time-dependent changes in Ztr. By model analysis of the data, it was found that the increase in total respiratory resistance due to pentobarbital anesthesia ranged from 60 to 190%. Halothane anesthesia induced slightly lower increases in Rrs (range 50–100%). These results call in question the usefulness and validity of lung function measurements in anesthetized rats to evaluate the effects of toxic or pharmacological drugs.

References

1. BOYD, R.L., M.J. FISHER, AND M.J. JAEGER. Non-invasive lung function tests in rats with progressive papain-induced emphysema. Resp. Physiol. 40: 181–190, 1980.
2. DIAMOND, L., AND M. O'DONNELL. Pulmonary mechanics in normal rats. J. Appl. Physiol.: Respirat. Environ. Exercise Physiol. 43: 942–948, 1977.
3. DUBOIS, A.B., A.W. BRODY, D.H. LEWIS, AND B.F. BURGESS, JR. Oscillation mechanics of lungs and chest in man. J. Appl. Physiol. 8: 587–594, 1956.
4. GILLESPIE, J.R. Mechanisms that determine functional residual capacity in different mammalian species. Am. Rev. Respir. Dis. 128 (Suppl): S74–S77, 1983.
5. HARKEMA, J.R., J.L. MAUDERLY, AND F.F. HAHN. The effects of emphysema on oxygen toxicity in rats. Am. Rev. Respir. Dis. 126: 1058–1065, 1982.
6. HANTOS, Z., B. DARÓCZY, B. SUKI, AND S. NAGY. Low-frequency respiratory mechanical impedance in the rat. J. Appl. Physiol. 63: 36–43, 1987.
7. JACKSON, A.C., AND J.W. WATSON. Oscillatory mechanics of the respiratory system in normal rats. Resp. Physiol. 48: 309–322, 1982.
8. JOHANSON, W.G., AND A.K. PIERCE. A noninvasive technique for measurement of airway conductance in small animals. J. Appl. Physiol. 30: 146–150, 1971.
9. KEEFE, D.H. Acoustical wave propagation in cylindrical ducts: Transmission line parameter approximations for isothermal and nonisothermal boundary conditions. J. Acoust. Soc. Am. 75: 58–62, 1984.
10. KING, T.K.C. Mechanical properties of the lungs in the rat. J. Appl. Physiol. 21: 259–264, 1966.
11. LAI, Y.–L., AND J. HILDEBRANDT. Respiratory mechanics in the anesthetized rat. J. Appl. Physiol.: Respirat. Environ. Exercise Physiol.: 45: 255–260, 1978.
12. MEAD, J. Contribution of compliance of airways to frequency-dependent behavior of lungs. J. Appl. Physiol. 26: 670–673, 1969.
13. MICHAELSON, E.D., E.D. GRASSMAN, AND W.R. PETERS. Pulmonary mechanics

by spectral analysis of forced random noise. J. Clin. Invest. 56: 1210–1230, 1975.

14. OOSTVEEN, E., R. PESLIN, C. DUVIVIER, AND A. ZWART. Respiratory transfer impedance and derived mechanical properties of conscious rats (submitted).
15. OTIS, A.B., MCKERROW C.B., R.A. BARTLETT, J. MEAD, M.B. MCILROY, N.J. SILVERSTONE, AND E.P. RADFORD. Mechanical factors in distribution of pulmonary ventilation. J. Appl. Physiol. 8: 427–443, 1956.
16. PALEČEK, F. Measurement of ventilatory mechanics in the rat. J. Appl. Physiol.: 27: 149–156, 1969.
17. REHDER, K., AND H.M. MARSH. Respiratory mechanics during anesthesia and mechanical ventilation. In: *Handbook of Physiology. The respiratory system. Mechanics of breathing*. Bethesda, MD: Am. Physiol. Soc., 1986, sect. 3, vol. III, pt. 2, chapt 43, p 737–752.
18. SKORNIK, W.A., AND J.D. BRAIN. Breathing and lung mechanics in hamsters: effect of pentobarbital anesthesia. J. Appl. Physiol. 68: 2536–2541, 1990.
19. VINEGAR, A., E.E. SINNETT, AND D.E. LEITH. Dynamic mechanisms determine functional residual capacity in mice, Mus Musculus. J. Appl. Physiol.: Respirat. Environ. Exercise Physiol.: 46: 867–871, 1979.
20. YING, Y., R. PESLIN, C. DUVIVIER, G. GALLINA, AND J. FELICIO DA SILVA. Respiratory input and transfer mechanical impedances in patients with chronic obstructive pulmonary disease. Eur. Respir. J. 3: 1186–1192, 1990.

Samenvatting

Inleiding tot de studies

Bij de inademing ontstaat door contractie van de ademhalingsspieren een vergroting van de borstholte. Door de onderdruk, die hierdoor in de longen ontstaat, stroomt lucht de longen in. De grootte van de luchtstroom ("flow") hangt af van de mechanische eigenschappen van het ademhalingssysteem zoals de elasticiteit van het longweefsel en de luchtwegweerstand. Een niet-invasieve meetmethode om informatie over deze mechanische eigenschappen te verkrijgen is de methode van geforceerde oscillaties ("forced oscillations"). Deze methode bestaat uit het opleggen van uitwendige drukvariaties en het meten van de flow die daarvan het gevolg is.

Een mogelijke manier van meting is de volgende. De proefpersoon wordt tot aan de nek ingesloten in een zogenaamde lichaamskamer. Hij ademt buitenlucht via een mondstuk waaraan een flowmeter verbonden is. In de lichaamskamer worden met behulp van een luidspreker kleine drukvariaties opgewekt. De opgelegde drukvariaties resulteren in flowvariaties aan de mondzijde die onder meer afhankelijk zijn van de luchtwegweerstand en de elasticiteit van het longweefsel en van het borstkas- en buikweefsel. De flowrespons wordt verder beïnvloed door de weerstand die de weefsels bieden tegen vervorming. Als de drukvariaties snel wisselen, d.w.z. hoge frequenties bevatten, speelt bovendien de massatraagheid (inertia) van de lucht in de luchtwegen, de massatraagheid van het borstkas- en buikweefsel en de samendrukbaarheid van de lucht in de longen een rol bij de uiteindelijke grootte van de flow.

De mechanische grootheden van het ademhalingssysteem, die met geforceerde oscillaties worden gemeten, kunnen in drie basiselementen worden ingedeeld: de weerstand (R), de elasticiteit (vaak uitgedrukt in de inverse, de compliantie (C)) en de massatraagheid (ofwel inertia (I)). Door de druk-flow verhouding bij verschillende frequenties van drukoscillatie te bepalen kunnen de verschillende elementen onderscheiden worden. Daartoe wordt de luidspreker vaak met een 'random ruis' of 'pseudo-random ruis' signaal aangestuurd wat tot gevolg heeft dat langzame en snelle wisselingen door elkaar plaatsvinden, met andere woorden verschillende frequenties worden tegelijkertijd aangeboden. Zo kan men in een zeer korte tijd de druk-flow relatie ofwel de impedantie (Z) van het ademhalingssysteem als functie van de frequentie bepalen. De ademhalingsimpedantie Zrs wordt vaak beschreven door middel van wiskundige modellen, waarbij de modelparameters specifieke mechanische grootheden van het ademhalingssysteem voorstellen.

De aangeboden drukvariaties zijn klein (amplitude: 0.1 kPa ≈ 1 cm H_2O), zodat de normale ademhaling niet beïnvloed wordt. Tevens zijn de frequenties van de drukoscillaties een orde hoger dan de spontane ademhalingsfrequentie, zodat de oscillatie-signalen goed te scheiden zijn van die van de normale ademhaling.

Daar de drukoscillaties gesuperponeerd worden op de normale ademhaling en geen specifieke eisen gesteld worden aan de manier van ademhalen is longfunctiemeting door middel van geforceerde oscillaties niet-invasief en niet-belastend van karakter. De methode vereist weinig coöperatie van de proefpersoon of het proefdier en is daarom uiterst geschikt als longfunctiemeting bij kinderen, patiënten en dieren.

Als druk en flow aan verschillende zijden van het ademhalingssysteem gemeten worden, zoals in de hierboven beschreven situatie, wordt de gemeten druk-flow relatie de transfer impedantie genoemd (Ztr). De transfer impedantie van gezonde proefpersonen in het frequentiegebied 4 tot 30 Hz wordt goed beschreven door een 6-parameter model, het DuBois' model, waarin drie compartimenten onderscheiden worden. Het model bestaat uit een luchtwegcompartiment, met een weerstand (Raw) en inertia (Iaw), een weefselcompartiment met een weerstand (Rti), inertia (Iti) en compliantie (Cti) en een gascompartiment met een gassamendrukbaarheid (Cg) van de lucht in de longen. Als het longvolume bekend is, is de waarde van Cg bekend en kunnen de andere vijf parameters van het model geschat worden. Dit maakt het mogelijk om de mechanische eigenschappen van de luchtwegen en het weefsel in detail te bestuderen.

De impedantie van het ademhalingssysteem wordt meestal berekend door middeling van meetgegevens verkregen uit verschillende ademteugen. Sommige mechanische eigenschappen van het ademhalingssysteem zijn afhankelijk van de grootte van de flow en het longvolume en verschillen voor in- en uitademing. Ons eerste onderzoek bij mensen is verricht om meer inzicht te krijgen in de invloed van deze verschillende factoren. Dit is van belang bij de interpretatie van gegevens van verschillende personen of gegevens verkregen onder verschillende meetcondities.

Bij toepassing van de geforceerde oscillatie-techniek wordt de totale impedantie van het ademhalingssysteem gemeten. In de tweede studie is een toepassing van de geforceerde oscillatie-techniek onderzocht waarmee meer informatie verkregen kan worden over de mechanische eigenschappen van de luchtwegen. Hiertoe wordt de lucht, die langzaam ingeademd wordt, plotseling vervangen door een vreemd gas. Het vreemde gas zal eerst de lucht vervangen in de grote luchtwegen en later in de kleinere luchtwegen. Aangezien het vreemde gas andere fysische eigenschappen heeft dan lucht veranderen de lokale Raw en Iaw van die luchtwegen waar op dat moment het vreemde gas de lucht vervangt. Tijdens de hele inademing wordt de totale impedantie van het ademhalings-

systeem bepaald. De verandering van de totale impedantie, die optreedt als een klein volume vreemd gas is ingeademd, is het gevolg van veranderingen van Raw en Iaw in de grote luchtwegen. Veranderingen die laat optreedt, als een groot volume vreemd gas is ingeademd, duiden op veranderingen van Raw en Iaw in kleinere, dieper in de long gelegen luchtwegen. Het resultaat van de totale impedantiemeting verschaft dus informatie over de verdeling van luchtwegweerstand en -inertia in het luchtwegstelsel.

De oscillatie-techniek wordt bij mensen hoofdzakelijk niet-invasief tijdens spontane ademhaling toegepast. Bij kleine proefdieren wordt de techniek echter voornamelijk invasief toegepast onder algehele verdoving. Invasieve technieken vergroten in het algemeen het benodigde aantal dieren voor een experiment. Bovendien beïnvloedt verdoving de longfunctie en kan het toedienen van een verdovingsmiddel de werking van stoffen beïnvloeden die bijvoorbeeld voor farmacologische of toxicologische doeleinden onderzocht worden. Om nadelen en problemen te omzeilen is een meetmethode ontwikkeld om Ztr bij wakkere ratten te meten. De waarde van deze methode voor longfunctiemeting is geëvalueerd door een studie te verrichten naar de effecten van verdoving.

Samenvatting

De invloed van de flow, de fase van de ademhaling, en de grootte van het longvolume op de verschillende mechanische parameters is bepaald door Ztr (4-32 Hz) bij gezonde proefpersonen te meten tijdens ademmanoeuvres waarbij met een constante flow wordt in- of uitgeademd (hoofdstuk 2). De waarde van de mechanische parameters van het luchtwegstelsel en de weefsels zijn vervolgens voor elke manoeuvre afzonderlijk geschat door analyse van de Ztr-data met het DuBois' model. De studie laat zien dat Raw groter is tijdens de expiratie, toeneemt met toenemende flow en afneemt met toenemend longvolume. Deze resultaten zijn in overeenstemming met de resultaten gevonden met andere meetmethoden. Hiermee is tevens een validatie verkregen van de interpretatie van de parameters van het DuBois' model. Iaw neemt af met toenenemende flow, en varieert noch met het longvolume noch met de fase van de ademhaling. Weefselparameters vertonen verschillen tussen de verschillende ademmanoeuvres, die zeer waarschijnlijk samenhangen met de mate van spiercontractie nodig om een bepaalde manoeuvre uit te voeren.

De tweede studie bij mensen (hoofdstuk 3) is uitgevoerd om meer gedetailleerde informatie te verkrijgen over de lokalisatie van Raw en Iaw in de bronchiaalboom. Bij gezonde proefpersonen is Ztr gemeten bij 20 Hz terwijl de proefpersonen een inert gas inademen met andere fysische eigenschappen dan lucht. Elke periode van het 20 Hz

signaal is afzonderlijk geanalyseerd zodat Ztr als functie van de tijd en als functie van het geïnspireerde volume bekend is. De Ztr-data zijn vervolgens gecorrigeerd voor de weefselimpedantie (die niet verandert als gevolg van inademing van een vreemd gas), het longvolume en de impedantie van de meetopstelling. Hiermee wordt de totale Raw en Iaw als functie van het ingeademde volume vreemd gas verkregen. De resultaten laten zien dat de totale verandering van Iaw bij inademing van 500 ml vreemd gas te voorspellen is op grond van de verhouding van de dichtheden van het vreemde gas en die van lucht. De verandering van Raw en Iaw met het ingeademde volume vreemd gas geeft een indicatie van de globale verdeling van Raw en Iaw in het luchtwegstelsel. De resultaten bij gezonde proefpersonen laten zien, dat de verandering van Iaw met het volume ingeademde gas (het verdelingsprofiel van Iaw) niet varieert met het soort ingeademde inerte gas. Vergelijking van de verdelingsprofielen van Iaw en Raw toont dat Iaw meer in hogere luchtwegen gelokaliseerd is dan Raw. Het verdelingsprofiel van Raw vertoont veel meer fluctuaties dan dat van Iaw, waarschijnlijk vanwege fysiologische variatie van Raw in de tijd (variatie in de glottisopening) en vanwege het feit dat meetonnauwkeurigheid sterker doorwerkt bij de berekening van Raw. Ondanks de onnauwkeurigheid kunnen er echter systematische verschillen tussen personen waargenomen worden in de verdelingsprofielen van Raw. De proefpersoon met de grootste dichtheidsafhankelijkheid van Raw vertoont een verandering van Raw bij een kleiner geïnspireerd volume vreemd gas dan de proefpersoon met een grootste viscositeitsafhankelijkheid van Raw.

In hoofdstuk 4 wordt de meetopstelling beschreven waarmee Ztr van wakkere ratten in het frequentiegebied 16 tot 208 Hz bepaald kan worden. De rat wordt in een buis geplaatst. Met behulp van een deegkraag rondom de nek wordt een akoestische scheiding teweeg gebracht tussen kop en romp. De buis wordt vervolgens in een lichaamskamer geplaatst, waarbij de rat in een kleine voorkamer ademt. Drukvariaties in de lichaams- en voorkamer worden gemeten met identieke drukopnemers. Via een luidspreker in de lichaamskamer worden kleine drukvariaties aan het lichaam aangeboden. De resulterende (neus-)flow wordt afgeleid door de drukverschillen in de voorkamer te relateren aan de impedantie van de voorkamer. Op deze manier is Ztr van jonge, gezonde ratten gemeten. Herhaalde metingen bij dezelfde ratten laten zien dat de reproduceerbaarheid van de verkregen data bevredigend is (variatie $\approx$ 10%). De vorm van de impedantie-curven bij lage frequenties blijkt niet beschreven te kunnen worden met het DuBois' model maar wel door het luchtwegcompartiment van het DuBois' model uit te breiden met een neus-nek compartiment. Als een redelijke waarde voor het longvolume wordt gekozen, moet 85% van de gemeten weerstand toegeschreven worden aan de weerstand in het luchtwegstelsel inclusief de neus. De variatie in de geschatte waarde van de weefselcompliantie (Cti) is groter dan de variatie in andere parameters. De waarde van Cti komt

echter goed overeen met de waarde van de longcompliantie van de rat zoals gemeten door andere onderzoekers.

In een vervolgonderzoek (hoofdstuk 5) zijn de effecten onderzocht van anesthesie op de met geforceerde oscillaties gemeten mechanische eigenschappen van het ademhalingssysteem. Hiertoe is, na bepaling van Ztr in de wakkere toestand, Ztr gemeten van gezonde jonge ratten onder algehele narcose met pentobarbital of halothaan. Hoewel er systematische verschillen zijn tussen verdoving met pentobarbital en halothaan wat betreft de grootte en tijdsafhankelijkheid van de geïnduceerde veranderingen, geeft algehele anesthesie een twee- tot drievoudige toename van Raw en Iaw. Hiermee blijkt dat anesthesie een zeer grote invloed heeft op de mechanische eigenschappen van het ademhalingssysteem. Schattingen van mechanische parameters van het ademhalingssysteem uit meetresultaten verkregen onder anesthesie zijn dus niet representatief voor de mechanische eigenschappen onder normale omstandigheden.

Conclusies

Meting van de transfer impedantie bij gezonde mensen geeft de mogelijkheid tot scheiding van de impedantie van de luchtwegen van die van de weefsels. Hierdoor heeft Ztr-meting bijzondere toepassingsmogelijkheden voor fysiologisch onderzoek. Meting van de transfer impedantie van wakkere ratten geeft voornamelijk informatie over de mechanische eigenschappen van het luchtwegstelsel en het longweefsel. De impedantie van het ademhalingssysteem van wakkere ratten kan bovendien reproduceerbaar gemeten worden met de ontwikkelde methode. Hiermee ontstaat de mogelijkheid tot longitudinaal onderzoek bij deze proefdieren. Algehele anesthesie veroorzaakt een toename in de respiratoire weerstand en inertia en mogelijkerwijs tijdsafhankelijke variaties in de mechanische eigenschappen van het ademhalingssysteem.

Curriculum Vitae

Ellie Oostveen werd geboren op 25 juni 1960 in Snelrewaard. Na het behalen van het diploma Atheneum-B aan het St. Antoniuscollege te Gouda, werd in 1978 de studie biologie aangevangen aan de Rijksuniversiteit te Utrecht. Het kandidaatsexamen werd behaald in 1982. Haar doctoraalstudie bestond uit het hoofdvak mathematische biologie, waarbij onderzoek werd verricht naar de modellering van de O_2-opname en de ventilatie tijdens inspanning, en uit de nevenrichting medische en fysiologische fysica, waarbij onderzoek werd verricht naar de mogelijkheid tot kwantificering van de humane motoriek. Daarnaast werd een klein bijvak informatica gedaan en de eerstegraads onderwijsbevoegdheid in de biologie behaald. Tijdens de studie werden assistentschappen verricht bij de cursussen "Natuurkunde voor Biologen" en "Mathematische Biologie".

Aansluitend op het doctoraalexamen biologie (april 1986) werd zij voor drie maanden aangesteld als toegevoegd onderzoekster bij de Utrechtse vakgroep Medische en Fysiologische Fysica van de faculteit Natuur- en Sterrenkunde bij de werkgroep o.l.v. Prof. dr. ir. J.J. Denier van der Gon.

In augustus 1986 ving het onderzoek aan waarvan het huidige proefschrift het eindresultaat is. Haar aanstelling bij de Utrechtse vakgroep Medische Fysiologie en Sportgeneeskunde van de faculteit Geneeskunde werd bekostigd door TNO. Onderzoek naar niet-invasieve longfunctiemeting bij kleine proefdieren vond plaats bij de werkgroep ademhalingsfysiologie o.l.v. Prof. dr. S.C.M. Luijendijk van de vakgroep Medische Fysiologie en Sportgeneeskunde en bij de afdeling Inhalatie Toxicologie van TNO-Voeding in Zeist. Dit onderzoek stond onder directe begeleiding van Dr. A. Zwart (TNO-Voeding, Zeist). In 1988 en in 1989/1990 werd in totaal gedurende een jaar onderzoek verricht op het INSERM-instituut Unité 14 de Physiopathologie Respiratoire te Vandoeuvre-les-Nancy (Frankrijk). Daar werden onder meer de humane onderzoeken verricht onder leiding van Dr. R. Peslin. De Nederlandse organisatie voor Wetenschappelijk Onderzoek (NWO), TNO en INSERM hebben reissubsidies en salariëring verstrekt voor de twee periodes van onderzoek in Nancy.

Sinds augustus 1991 is zij werkzaam bij de afdeling Algemene Heelkunde van het Dijkzigt Ziekenhuis in Rotterdam. Zij verricht daar een door het Nederlands Astma Fonds gesubsidiëerd onderzoek naar de mogelijkheid tot longfunctie-monitoring met geforceerde oscillaties bij beademde patiënten.

Jere Mead, Dr. Ramon Farré, Dr. Bela Suki en Dr. Mar Rotger, veel dank verschuldigd voor de vele stimulerende wetenschappelijke discussies, de hulp bij mijn onderzoeken en de prettige tijd die ik in Nancy doorbracht.

Cher Dr. Peslin, j'y tiens à vous remercier profondement pour toutes les discussions stimulantes, pour l'aide et la possibilité de faire des recherches dans votre laboratoire à Nancy. J'éspère que notre collaboration pourra se continuer. Je suis trés honorée que vous serez membre du committé qui jugera de ma thèse. Cher Claude, merci pour tous tes efforts concernants les dispositifs de mesure, et aussi pour nos discussions serieuses et moins serieuses. Claudia, tu m'as aidée avec l'ordinateur et avec les recherches sur les rats. Je remercie aussi Bernadette Clement et Marie-Claude Rohrer pour leurs aide dans la préparation des articles.

Tot slot wil ik mijn ouders bedanken die mij in de gelegenheid stelden te studeren. Last but not least, bedank ik jou, Han, voor al je directe en indirecte steun.